UNIVERSITÀ DELLA CALABRIA

UNIVERSITA' DELLA CALABRIA

Dipartimento di Farmacia e Scienze della Salute e della Nutrizione

Dottorato di Ricerca in

Medicina Traslazionale

CICLO

XXIX

FoxO3a reactivation restores the sensitivity to the antiestrogen treatment in tamoxifen resistant breast cancer

Settore Scientifico Disciplinare

MED/06

Coordinatore: Ch.mo Prof. (Sebastiano Andò)

Firma _____

Supervisore/Tutor: Ch.mo Prof. (Diego Sisci)

Firma _____

Dottorando: Dott./ssa (Ada, Alice Donà)

Firma _____

ABSTRACT

Resistance to endocrine treatments is a major clinical challenge in the management of estrogen receptor alpha positive (ER+) breast cancers (BC). Although multiple mechanisms leading to endocrine resistance have been proposed, the poor outcome of this subgroup of BC patients demands additional studies. Here we show that the expression of FoxO3a transcription factor is strongly reduced in ER+ BC MCF-7 cells (wtMCF-7) that developed resistance to Tamoxifen (TamR). On the other hand, FoxO3a silencing (siF3a) was able to counteract Tam induced growth inhibition in wtMCF-7, demonstrating that FoxO3a is a mediator of cell response to Tam.

To analyze the role of FoxO3a in the acquisition of a Tam resistant phenotype, TamR clones bearing an active FoxO3a (F3aAAA), whose expression can be induced by Doxycycline (Dox) were developed. FoxO3a re-activation was able to re-establish the sensitivity of TamR cells to the antiestrogen, inhibiting proliferation and cell cycle progression, as well as restoring Tam dependent apoptotic response. For a closer look at the molecular mechanisms involved, an unbiased proteomics analysis on F3aAAA-inducible TamR cells was conducted, unveiling novel interesting and potential mediators of the anti-proliferative and pro-apoptotic activity of FoxO3a, all worthy of future investigations.

Kaplan-Meier (K-M) survival curves confirmed the relevance of FoxO3a also in a clinical setting, since high levels of the transcription factor strongly correlate to a positive response to tamoxifen therapy. Finally, to assess if FoxO3a reactivation is able to restore the sensitivity to Tam also *in vivo*, the widely used anti-epileptic drug (AED) Lamotrigine (LTG; Lamictal), which is able to induce FoxO3a expression in TamR cells leading to growth inhibition, was also tested on TamR deriving xenografts tumors, where it showed the same effects observed *in vitro*.

Altogether, our data indicate that FoxO3a could not only be considered a good prognostic factor in ER+ BC, predicting a positive response to endocrine therapy, but also a key target to be exploited in combination therapy. In this context, LTG might represent a valid candidate to be used as an adjuvant to Tam therapy in patients at risk.

INTRODUCTION

Breast cancer is the most common malignancy in women and represents one of the major causes of death worldwide, making up 21% of all new cancer diagnoses. Each year, almost 1.4 million women are diagnosed with breast cancer, and the disease will be responsible for 450 000 deaths [1]. Survival rates have been steadily extending over the past 50 years, primarily due to improvements in diagnosis and treatment.

The drivers of proliferation in breast cancer are also the phenotypic drug targets; hormone receptors (estrogen, progesterone and HER2 receptors) are commonly overexpressed. Early studies established that steroid hormones are of pivotal importance in directing the growth and development of breast tumours and endocrine treatments, by perturbing the steroid hormone environment of tumor cells, can promote extensive remissions in established tumors and furthermore provide significant patient survival benefits. More than 60% of human breast cancers are estrogen receptor α positive (ERα+) [2]. The presence of ERα is considered a good prognostic factor and correlates with a higher degree of differentiation of the tumour [3, 4] and increases disease-free survival [5]. The earliest approved therapy for the prevention and treatment of ERα+ breast cancer patients was Tamoxifen.

Tamoxifen is a triphenylethylene derivative pharmacologically classified as a *selective estrogen receptor modulator* (SERM) that acts as a partial antagonist (an agonist in the uterus but an antagonist in the breast), impairing ERα function by competing with 17β-estradiol (E2) for the binding to the receptor [6]. Binding of the primary human E2, to ERα seals the hydrophobic pocket by the helix-12 domain [7, 8] . ERα then translocates to the nucleus, binds to the estrogen response element (ERE), activates and drives the transcription of estrogen-dependent genes [9]. Tamoxifen is metabolized to 4-hydroxytamoxifen (4-OHT) [10, 11]; , which also binds to ERα. However, this leads to a different conformational change as compared to E2 and the hydrophobic pocket is not sealed by helix-12 [8]. Consequently, 4-OHT blocks ERα activation and reduces cell proliferation by activating apoptosis, and/or autophagy [12].

Thus, the effects of Tamoxifen in breast tissues result from its ability to bind to the ligand-binding domain of the ERα, thereby antagonizing the proliferative potential of estrogens [13, 14], which are responsible for cancer cell growth or proliferation [15]. Unfortunately, clinical application of all endocrine measures examined to date has revealed that their beneficial actions are limited and can eventually be counteracted by the capacity of breast cancer cells to ultimately circumvent the need for steroid hormones, allowing them to grow and progress despite such therapy.

In fact, with time, about 50% of patients with ERα+ breast cancer stop benefiting from Tamoxifen treatment and acquire resistance, leading to disease progression.

Thus, at presentation of breast cancer, current endocrine therapies are not effective in all patients (*de novo endocrine resistance*) and initially responsive tumors will invariably progress despite such treatments (*acquired resistance*) resulting in patients relapse and associated poorer survival [16]. The clinical existence of these phenomena, together with substantial experimental evidence, indicates that such a therapeutic approach based on using anti-hormones as single agents may be now regarded as somewhat simplistic. Indeed, an increasing body of data has revealed that the control of endocrine responsive and resistant breast cancer growth is in reality multi-faceted, comprising a complex network of interacting signal transduction pathways impinging on tumor proliferation and cell survival parameters [17, 18] . The identification of the pathways responsible for *de novo* and *acquired endocrine resistance* has thus been an important goal for many breast cancer researchers. It is self-evident that any accurate identification of factors indicative of endocrine resistance in advance of therapy would not only prevent unnecessary side effects in unresponsive patients, but would also significantly limit both the time lost during which the disease may progress unchecked by appropriate therapy, and the wastage of financial resources associated with ever escalating costs of drugs. Moreover, knowledge of the causative elements of *de novo* and *acquired endocrine resistance* might allow the development of new therapeutic agents and strategies to prevent either the evolution of these conditions or at least delay their appearance, hence severely compromising the disease process and enhancing patient survival.

The potential mechanisms underlying the evolution toward an antiestrogen resistant phenotype have been the object of extensive investigations, but the available data are not univocal. Some authors ascribed the acquisition of resistance to a loss or mutation of the ERα [19], other authors shown that breast cancer cells which lost sensitivity to anti-hormonal treatment, often retain an ERα+ phenotype with normal ERα functionality [20, 21]. In Tamoxifen resistant breast cancer, ERα has been reported to interact with deregulated growth factor pathways, facilitating the proliferation of resistant cells [22, 23] . The enhancement of growth factor signaling results in the increase of ERK1/2 phosphorylation [24] and in phosphatidylinositol 3-kinase (PI3K)/AKT cell survival pathway activation [25]. Furthermore, the PI3K-Akt signalling pathway has also been demonstrated to play a crucial role in the development of tamoxifen resistance [25-27]. AKT activation by phosphorylation (pAKT) regulates critical cellular activities such as growth, proliferation, differentiation, metabolism and survival as well as tumorigenesis [28]. Importantly, PI3K/AKT signaling is implicated in the pathogenesis of breast cancer. PI3K is activated in response to a variety of extracellular signals through a receptor tyrosine kinase (RTK) such as HER2, epidermal growth factor receptor (EGFR) or insulin-like growth factor 1 receptor (IGF1R). The serine/threonine kinase AKT is a downstream multifunctional kinase, which serves as the central mediator of the pathway [29]. pAKT promotes cellular survival via either direct inactivation by phosphorylation of multiple proapoptotic proteins or by inhibition of the Forkhead box transcription factors that results in decreased expression of proapoptotic proteins [30]. The characteristic attenuation of apoptosis by pAKT has been hypothesized as a major mechanism of resistance to cancer treatment [31]. Indeed, one of the downstream targets of AKT as well as of MAPK, currently attracting a great interest in hormone dependent breast cancer, is Forkhead box class O (FoxO)3a. The FoxO genes encode for the O-subfamily of proteins that belong to the larger family of winged-helix forkhead transcription factors which contains four members (FoxO1a, FoxO3a, FoxO4, and FoxO6), whose functions are negatively regulated by the insulin- PI3K/AKT signaling [32] and MAPK [33]. The expression and activity of FOXO factors are strongly controlled by post-translational modifications such as phosphorylation,

acetylation, methylation and ubiquitination [34]. A major mechanism of regulation of FOXOs consists of phosphorylation by AKT or SGK (serum and glucocorticoid-regulated kinase), on three residues (T32, S253 and S315 of FOXO3), following insulin or growth factor stimulation [30], leading to FOXO inactivation. Similarly, FoxO3a undergoes phosphorylation on residues (S294;S344;S425) [35] upon MAPK activation by growth factors. Indeed, these phosphorylations allow the binding of 14-3-3 proteins to FOXOs and their export from the nucleus to the cytoplasm (reviewed in [36]. Into the cytoplasm FOXOs are sequestrated and maintained in an inactive state, which can be rapidly reversed. In this condition FOXOs can also be ubiquitinated and degraded by proteasomes.

The mitogen-activated protein kinase (MAPK) cascades are evolutionary conserved, intracellular signal transduction pathways that respond to various extracellular stimuli and control a large number of fundamental cellular processes including growth, proliferation, differentiation, motility, stress response, survival and apoptosis [37, 38] . In mammalian cells, the major MAPK are extracellular signal-regulated protein kinase (ERK) [39], p38 MAP kinase [40], and c-Jun N-terminal kinase (JNK) [41, 42]. These MAP kinases are activated by the dual phosphorylations of neighbouring threonine and tyrosine residues in response to various extracellular stimuli [43, 44] . Specifically, p38 and JNK have been implicated in stress responsive signals leading to the initiation of adaptive events such as gene expression, differentiation, metabolism, and apoptosis [45]. ERKs are often activated by growth signals, such as epidermal growth factor (EGF) or platelet-derived growth factor [46]. Activation of ERK has been shown to phosphorylate FOXO proteins, resulting in nuclear exclusion and transcriptional repression. In addition to ERK, direct phosphorylation of FOXO by AKT results in its cytoplasmic retention and inactivation, causing the inhibition of the expression of FOXO-regulated genes, which control the cell cycle, cell death, cell metabolism and oxidative stress [47-49]. Moreover, active MAPK negatively regulates FOXO3 stability via an MDM2-mediated ubiquitin-proteasome pathway [50]. On the contrary, MAPKs signalling are potentially inhibited upon FOXO3

activation, in line with the observations in other studies [51]. This implies that FOXO3 activation results in an overall change in the wiring or activity of several signal transduction networks.

The mechanisms that direct FOXOs to degradation rather than sequestration might be related to the intensity of the signal that triggers nuclear export [34]. In absence of growth factors, FoxOs are mainly located within nuclei and regulate a set of target genes promoting cell cycle arrest, stress resistance, apoptosis, DNA damage repair and metabolism [52]. Increasing interest in FoxOs factors is emerging in the oncologic research field. In particular, in breast cancer, it has been proposed as a bona fide tumour suppressor [53]. In ERα+ breast cancer, several reports have suggested a functional interaction between ERα and FoxO members. E2 have been found to promote ERα binding to FoxO1a, FoxO3a, and FoxO4, which, in turn, regulate ERα-mediated transcription, showing either coactivator or corepressor functions on ERE sites [54, 55] . Noteworthy, a significant enrichment of Forkhead motifs within ERα binding regions was found at very high frequency [56], suggesting a role for FoxOs in determining ERα binding and function [57]. In line with this assumption, we have previously shown that in ERα+ breast cancer cells, nuclear (thus active) FoxO3a behaves as a repressor for ERα-mediated transcription by binding to Forkhead responsive elements on ERα target gene promoters, evidencing a protective role in ERα+ breast cancer [58]. On this basis seems to be important to understand the involvement of FoxO3a in the acquisition of the resistance of breast cancer cells to 4-OHT treatment. Moreover, a deeper knowledge of the molecular mechanisms involved in both 4-OHT resistance acquisition that in the inactivation and nuclear exclusion of FoxO3a will provide additional opportunities for the development of new therapeutic strategies that could increase nuclear FoxO3a content and function.

Here we suggest a possible role for an antiepileptic drugs Lamotrigine (LTG; Lamictal) [59] that have been found to exert anti-cancer activity [60, 61] . LTG has a strong antiproliferative activity on several types of breast cancer cells, including TamR cells, this effect is paralleled by a significant increase of FoxO3a expression and nuclearization. LTG behaves in a similar way also in vivo, where in TamR derived xenografts, induces a dramatic decrease of tumors mass.

MATERIALS AND METHODS

Cell culture, conditions, and treatments

The ER-positive human wild-type (wt) breast cancer epithelial cell line wtMCF-7 was maintained in monolayer culture in Dulbecco's modified Eagle's/Ham's F-12 medium (1:1) (DMEM/F-12), supplemented with 5% fetal bovine serum (FBS), 100 IU/ml penicillin, 100 ng/ml streptomycin, and 0.2 mM L-glutamine. For experimental purposes, cells were synchronized in phenol red-free and serum-free media (PRF-SFM) for 24 h and then, where opportune, switched to PRF-media containing 5% charcoal-treated FBS (PRF-CT) or 5% FBS, in presence or not of Tam (4-OHT) or EGF-1 (both from Sigma-Aldrich, Italy) depending on the experiment. All other media and reagents were purchased from ThermoFisher Scientific (Waltham, MA USA).

Selection Procedure of Tamoxifen resistant MCF-7 cells (TamR)

TamR cells were obtained after long-term cultivation of parent ERα (+) MCF-7 cell line (wtMCF-7) in Tam. wtMCF-7 cells were exposed to increasing concentrations of 4-OHT, starting from 10^{-9}M up to a final concentration of 10^{-6}M 4-OHT. Cells were refeed with fresh growth medium containing the drug every 2-3 days.

Generation of FoxO3a inducible stable clones

TamR/TetOn-AAA clones were generated using the Tet-On Gene Expression System (Clontech, Palo Alto, CA, USA). The Tet-On belongs to a high-level gene expression system that employs a regulator plasmid and a response plasmid to establish a double-stable Tet cell line.

The Tet-On system is a regulatory system that allows activation of gene expression by the addition of the effector substance tetracycline or one of its derivatives, e.g. Dox.

This control circuit was described as a rtTA dependent expression system, because a recombinant tetracycline controlled transcription factor, rtTA, interacts with a rtTA responsive promoter, Ptet, to drive expression of the gene under study. The effector, act at the level of DNA binding rtTA

transcription factors. So, rtTA requires tetracyclines for binding to tetO, and the subsequent fusion of the VP16 (herpes simplex virus protein) activation domain resulted in a reverse-tTA (rtTA) that binds Ptet and activates transcription exclusively in the presence of Dox.

To generate pTRE-F3aAAA inducible plasmid, the cDNA encoding the entire open reading frame of a constitutively active form of the human FoxO3a gene, where the three known AKT phosphorylation sites on FoxO3a have been mutated to alanine (F3aAAA), was excised as a 2kb BamHI-XbaI fragment from the plasmid 1319 pcDNA3 flag FKHRL1 AAA (Addgene, Cambridge, MA, USA, plasmid #10709). The fragment was sub-cloned into the pTRE-zeo vector, harboring a EGFP cassette and a Zeocin resistance gene to allow selection of stably transformed cells in the presence of zeocin. Restriction digestion and sequence analysis verified a correct cloning. The pTRE-F3aAAA plasmid allows the conditional expression of active FoxO3a under the control of a tetracycline-response element (TRE) in the presence of Doxycycline (Dox, Sigma Aldrich) and of a rTetR.

To obtain a stable TamR/TetOn-AAA cell line, TamR cells were first transfected with the regulator plasmid pTet-On, containing the Geneticin (G418, Invitrogen) resistance gene, and constitutively encoding rtTA proteins, using FuGENE® HD Transfection Reagent (Promega Italia s.r.l., MI-Italy) as a transfection reagent.

Several G418 resistant TamR/TetOn stable clones were isolated by single-cell cloning and selected by successful transient transfections with the pTRE-F3aAAA plasmid.

TamR/TetOn selected clones were pooled together and subjected to a second round of transfection with the pTRE-F3aAAA plasmid. G418- and Zeocin-resistant clones were isolated and screened by western blot (WB). TamR/TetOn-AAA clones with low background expression and high Dox-dependent (3 μg/ml) induction of FoxO3a protein were selected. In this cellular system, rtTA protein binds to TRE and activates FoxO3AAA transcription in response to Dox in a precise and dose-dependent manner.

Control cell lines (TamR/TetOn-V) were established by stably transfecting the pTRE backbone (vector only) without a cDNA insert.

Pools of TamR/TetOn-AAA and TamR/TetOn-V clones were collected and used in all experiments. Clones were maintained in monolayer culture in Dulbecco's modified Eagle's/Ham's F-12 medium (1:1) (DMEM/F-12), supplemented with 5% (FBS), 100 IU/ml penicillin, 100 ng/ml streptomycin, 0.2 mM L-glutamine, G418 (0.2 mg/ml) and Zeocin (0.1mg/ml).

siRNA-mediated RNA interference

Custom-synthesized siRNA-annealed duplexes (25 bp double- stranded RNA [dsRNA]) were used for effective depletion of FoxO3a (siF3a) transcripts. A scramble siRNA (siScramble) lacking identity with known gene targets was used as a negative control. 10^6 wtMCF-7 cells were seeded in 60mm Petri dishes in growing medium without antiobiotics. The day after cells were transfected with siF3a (150 pmol/dish) and siScramble (120pmol/dish), using Lipofectamine 2000 (all reagents were from ThermoFisher Scientific). Six hours after transfections, cells were synchronized in PRF-SFM for 24 h and then switched to 5% PRF-CT, in presence or absence of 1μM 4-OHT up to 72h, depending on the experiment.

Plasmids and transient transfections

For key experiments, results were confirmed by transiently over-expressing F3aAAA in TamR cells. 10^6 TamR cells were plated in 60mm plates and transfected in suspension in GM-PRF with 4μg/dish of the 1319 pcDNA3 flag FKHRL1 AAA (F3aAAA), encoding the constitutively active triple mutant of FoxO3a (provided by William Sellers, Addgene plasmid 10709), or the pcDNA3.1 vector (Invitrogen) as control. All the transfections were carried out using FuGENE® HD (DNA/ FuGENE ratio, 2:1). After 6 h, the medium was replaced with fresh PRF-SFM, shifted next day to PRF-CT and treated or not for 1, 2 and 3 days with 1μM 4-OHT.

RNA extraction, reverse transcription, and real-time (RT)-PCR

Total RNA was isolated using TRI-reagent (Ambion) and treated with DNase I (Life Technologies). Two micrograms of total RNA were reverse transcribed with the High-Capacity cDNA Reverse Transcription Kit (Applied Biosystems) according to the manufacturer's instructions. cDNA was diluted 1:3 in nucleasefree water, and 5 µl were analysed in triplicate by RT-PCR in a iCycler iQ Detection System (Bio-Rad) using SYBR green Universal PCR Master Mix (Bio-Rad) and the following pairs of primers: FoxO3a forward 5′- CAAACCCAGGGCGCTCTT-3′ and reverse 5′- CTCACTCAAG CCCATGTTGC T-3′ (221 bp). Negative controls contained water instead of first-strand cDNA. Each sample was normalized on its 18S rRNA content. The relative gene expression levels were normalized to a calibrator that was chosen to be the basal, untreated sample. The final results were expressed as n-fold differences in gene expression relative to 18S rRNA and the calibrator, calculated using the $\Delta\Delta C_T$ method as follows: n-fold = $2^{-(\Delta C_T \text{ sample} - \Delta C_T \text{ calibrator})}$, where the ΔC_T values of the sample and calibrator were determined by subtracting the average C_T value of the 18S rRNA reference gene from the average C_T value of the different genes analysed.

Western blotting (WB) assay

Proteins were extracted using a lysis buffer containing 50 mM Hepes (pH 7,5), 150 mM NaCl, 1,5mM $MgCl_2$, 1mM EGTA, 1mM Glycerine, 1% Triton X-100 plus inhibitors (0.1 mM Na_3VO_4, 1% PMSF and 20 mg/ml aprotinin). Where opportune, after the collection of cytoplasmic proteins, intact nuclei were lysed with nuclear buffer containing 20 mM HEPES (pH 8), 0.1 mM EDTA, 5 mM $MgCl_2$, 0.5 M NaCl, 20% glycerol, 1% NP-40, plus inhibitors (as above). The protein content was determined using Bradford dye reagent (Bio-Rad). Lysates were separated on an 11% polyacrylamide denaturing gel, transferred to nitrocellulose membranes: proteins of interest were detected with specific polyclonal (p) or monoclonal (m) antibodies (Abs), recognized by HRP (Horse Radish Peroxidase)-coupled secondary Abs, and developed using the Clarity Western ECL Substrate Detection System (BIO-RAD). The following Abs were employed: anti-FoxO3a (75D8), p-FoxO3a (Ser253) (#13129), p-FoxO3a (Ser294) #5538, Her2/ErbB2 (D8F12) XP® (#4290), p44/42 MAPK (ERK1/2) #9102,

Phospho-p44/42 MAPK (Erk1/2) (Thr202/Tyr204) #9101 (all from Cell Signalling, The Netherlands, EU). Anti-phospho-erbB2/Her2 (Tyr1248) (06-229) was purchased from Millipore (Vimodrone, MI-Italy). AKT 1/2/3 (H136) sc-8312 p-AKT 1/2/3 (Ser473) sc-7985 and β-Actin (AC-15) sc-69879, GAPDH (FL-335) sc-25778 all from Santa Cruz Biotechnology, Inc. (Heidelberg, Germany). Images were acquired by using an Epson Perfection scanner (Epson).

Proliferation assay

To perform growth curves, 10^5 cells/well were plated in triplicates in 12-well plates in GM-PRF. After 16h, cells were shifted in PRF-SFM for 24h (day zero) to synchronize the cells in the same cell cycle phase, thus avoiding growth differences among cells. Following starvation cells were shifted in PRF-CT and treated or not with Dox (3μg/ml) for 1, 2, and 3 days. Cells were harvested by trypsinization, incubated in a 0.5% trypan blue solution for 10 min at room temperature. Trypan blue negative cells were counted through a Countess II FL Automated Cell Counter (Life Technologies, Italy). Tam (1μM) treatment was refreshed every day to maintain constant levels in the medium.

Immunostaining

wtMCF-7 and TamR cells were seeded in growing medium on coverslips. The day after, cells were fixed with 3% paraformaldehyde and permeabilized with 0.2% Triton X-100. Non-specific sites were blocked with bovine serum albumin (BSA) (3% for 30 min). The blocked samples were incubated for 1 h with FoxO3a (75D8) antibody (2 μg/ml), washed with phosphate-buffered saline (PBS) (Invitrogen) and incubated with fluorescein-conjugated goat anti-rabbit IgG (Sigma-Aldrich) secondary antibody. 4',6-Diamidino-2-phenylindole (DAPI, Sigma-Aldrich, Italy) was used to counterstain the nuclei. FoxO3a subcellular localization and DAPI nuclear staining were examined under a microscope connected to an Olympus camera system dp50. Captures were taken at x400 magnification using ViewFinder™ 7.4.3 Software. The optical densities of stained FoxO3a proteins were analyzed by ImageJ software (NIH, USA).

TUNEL assay

Apoptosis was determined by enzymatic labeling of DNA strand breaks using a Dead End Fluorometric TUNEL System (Promega, Italy) according to the manufacturer's instructions. This system measures the fragmented DNA of apoptotic cells by catalytically incorporating fluorescein-12-dUDP at 3'-OH DNA ends, forming polymeric tail, by means of the recombinant enzyme Terminal Doxynucleotidyl Transferase (rTdT).

$3x10^5$ cells were seeded on coverslips in 35 mm Petri dishes and then treated as described for growth experiments. After 72 hours of incubation, coverslips were mounted on slides using Fluoromount mounting medium (Sigma-Aldrich, Italy) and observed under a fluorescence microscope (Olympus BX51, Olympus Italia srl, Milan, Italy). DAPI was used to counterstain the nuclei. Apoptotic cells were photographed at 10x magnification using ViewFinder™ 7.4.3 Software, through an Olympus camera system dp50 and then counted using Image J software (NIH, USA).

Transmission electron microscopy (TEM)

TEM was conducted as previously described [62]. Cells were seeded on coverslips in 60 mm Petri dishes and then treated as described for growth experiments for 48 and 72 hours. At indicated time points, cells were fixed in 3% glutaraldehyde (Sigma- Aldrich, Milan-Italy) solution in 0.1 M phosphate buffer (pH. 7.4) for 2h. Then the samples were post-fixed in osmium tetroxide (3%), dehydrated in graded acetone, and embedded in Araldite (Sigma-Aldrich, Milan-Italy). Ultrathin sections were collected on copper grids and contrasted using both lead citrate and uranyl acetate. The grids were examined in a "Zeiss EM 10" electron microscope.

Cell Cycle Analysis

For cell cycle distribution analysis 10^6 cells were seeded on coverslips in 60 mm Petri dishes and then treated as described for growth experiments for 24 and 48 hours. Cells were then harvested by trypsinization, resuspended in 0.5 ml of propidium iodide solution and processed as already described

[63]**.** The DNA content was measured using a FACScan flow cytometer (Becton Dickinson, Mountain View, CA, USA) and the data acquired using BD CellQuest™ Pro Analysis software. Cell cycle profiles were determined using ModFit LT™ (by Verity Software House).

Label-free semi-quantitative proteomics analysis

Cell lysates were prepared for trypsin digestion by sequential reduction of disulphide bonds with TCEP and alkylation with MMTS. Then, the peptides were extracted and prepared for LC-MS/MS. All LC-MS/MS analyses were performed on an LTQ Orbitrap XL mass spectrometer (Thermo Scientific, San Jose, CA) coupled to an Ultimate 3000 RSLCnano system (Thermo Scientific, formerly Dionex, The Netherlands). Xcalibur raw data files acquired on the LTQ-Orbitrap XL were directly imported into Progenesis LCMS software (Waters Corp) for peak detection and alignment. Data were analysed using the Mascot search engine. Five technical replicates were analysed for each sample type [64].

Ingenuity pathway analyses

Pathway and function analyses were generated using Ingenuity Pathway Analysis (IPA) (Ingenuity systems, http://www.ingenuity.com), which assists with proteomics data interpretation via grouping differentially expressed genes or proteins into known functions and pathways. Pathways with a z score >1.5 were considered as significantly activated, and pathways with a z score <-1.5 were considered as significantly inhibited.

***In vivo* studies**

Female 45-day-old athymic nude mice (nu/nu Swiss; Harlan Laboratories, Milan, Italy) were maintained in a sterile environment. At day 0, estradiol pellets (0.72 mg per pellet, 90-day release; Innovative Research of America, Sarasota, FL, USA) were subcutaneously implanted into the

intrascapular region of the mice. The next day, exponentially growing TamR cells (5.0 $x10^6$ per mouse) were inoculated subcutaneously in 0.1 ml of Matrigel (BD Biosciences, Bedford, MA).

When the tumors reached average ~ 0.2 cm^3 (i.e. in about 4 weeks), mice were randomly allocated to estrogen withdrawal plus tamoxifen [n = 5 mice per group; estradiol pellets were removed and tamoxifen pellets (5 mg per pellet, 90-day release) were given to each mouse into the intrascapular region]. After two weeks, mice were divided into two groups, according to treatments administered by intraperitoneal (i.p.) injection for 28 days. The first group of mice (n = 5) was treated daily with 100 µl of vehicle (0.9% NaCl with 0.1% albumin and 0.1% Tween-20), (Sigma-Aldrich, Milan, Italy), the second group of mice (n = 5) was treated daily with 100 µl LTG (20 mg/kg/die). Lamotrigine was dissolved in DMSO at 10 mg/ml, and, before administration, an appropriate volume of resuspension vehicle was added.

TamR derived xenograft tumor growth was monitored twice a week by caliper measurements, along two orthogonal axes: length (L) and width (W). Tumor volumes (in cubic centimeters) were estimated as described [65]. At day 28, animals were sacrificed following the standard protocols and tumors were dissected from the neighboring connective tissue. Specimens of tumors were frozen in nitrogen and stored at - 80°C; the remaining tumor tissues of each sample were fixed in 4 % formalin and embedded in paraffin for the histologic analyses. Animal care, death, and experiments were done in accordance to the principle of the 3Rs and to the institutional guidelines and regulations at the University of Calabria, Italy. The project was approved by the local ethical committee.

Histological Analysis

Formalin-fixed, paraffin-embedded sections of tumour xenografts were cut at 5 µm and allowed to air dry. Deparaffinized, rehydrated sections were stained for 6 min with haematoxylin (Bio-Optica, Milan, Italy), washed in running tap water, and counterstained with eosin Y (Bio-Optica, Milan, Italy). Sections were, then, dehydrated, cleared with xylene, and mounted with resinous mounting medium. The epithelial nature of the tumors was verified by immunostaining (Vectastain Elite ABC

HRP Kit, VECTOR Laboratories, CA, USA) with mouse monoclonal antibody directed against human cytokeratin 18 (Santa Cruz Biotechnology, Milan, Italy), and nuclei were counterstained with hematoxylin. Tumour sections were immune-labelled with FoxO3a (Cell Signaling Technology, Inc) and Ki67 (Santa Cruz Biotechnology, Milan, Italy) which served as a proliferation markers. For negative controls, nonimmune horse serum (included in the Vectastain Elite ABC HRP Kit) was used in place of the primary antibody.

Statistical analysis

All data were expressed as the mean ± standard deviations (SD) of at least three independent experiments. Statistical significances were evaluated using Student's t test.

RESULTS

FoxO3a expression is downregulated in TamR BCC

In order to assess the role of FoxO3a in the acquisition of antiestrogen resistance, we developed a Tam resistant MCF-7 clone (TamR), by chronic exposure of ER+ BC MCF-7 cells (wtMCF-7) to 4-hydroxytamoxifen (4-OHT), as described in *Materials and Methods*. The acquired resistance to the antiestrogen was checked on a scheduled basis by the lack of any inhibitory effect on the proliferation of TamR compared to the parental cell line (**Fig.1A** and **B**).

FoxO3a expression and subcellular localization was compared in the two cell lines. A significant decrease of both FoxO3a mRNA (**Fig.1C**) and protein expression, associated to a dramatic reduction of its nuclear localization (**Fig.1D**), was observed in TamR cells with respect to wtMCF-7. FoxO3a nuclear exclusion (thus inactivation) was confirmed by immunostaining of endogenous FoxO3a, which showed how the nuclear accumulation of the transcription factor observed in wtMCF-7, was almost completely lost in TamR cells (**Fig. 1E**).

The molecular mechanism underlying FoxO3a downregulation in Tam resistant cells is currently under investigation in our laboratory. Nevertheless, a potential explanation might reside in the hyperactive growth factor signaling observed in Tam resistant cells, which results in the increase of

ERK1/2 phosphorylation [24] and in phosphatidylinositol 3-kinase (PI3-K)/Akt cell survival pathway activation [25]. Indeed, ERK1/2 MAP kinases is hyperphosphorylated in TamR cells, compared to wtMCF-7, under EGF-1 stimulation, resulting in FoxO3a hyperphosphorylation on the MAPK target Ser294 residue, which presumably leads to FoxO3a degradation through the MDM2-mediated ubiquitin-proteasome pathway [50] (ongoing experiments). On the contrary, the pro-survival AKT pathway is more active in wtMCF-7 than in TamR and this is reflected in a lower FoxO3a phosphorylation on the AKT target Ser253 residue (Fig.1F).

In addition, an unbiased proteomics analysis conducted on TamR cells and parental wtMCF-7 cells (Fiorillo M. *et al.*, Oncotarget, *in press*) revealed a decreased expression in E2F-1 (~ -1.2 fold *vs* wt) and p53 (~ -0.5 fold *vs* wt), both reported as upstream transcriptional regulators of FoxO3a [66]. The role of these two proteins in mediating the transcriptional inhibition of FoxO3a in TamR is also under investigation in our laboratory.

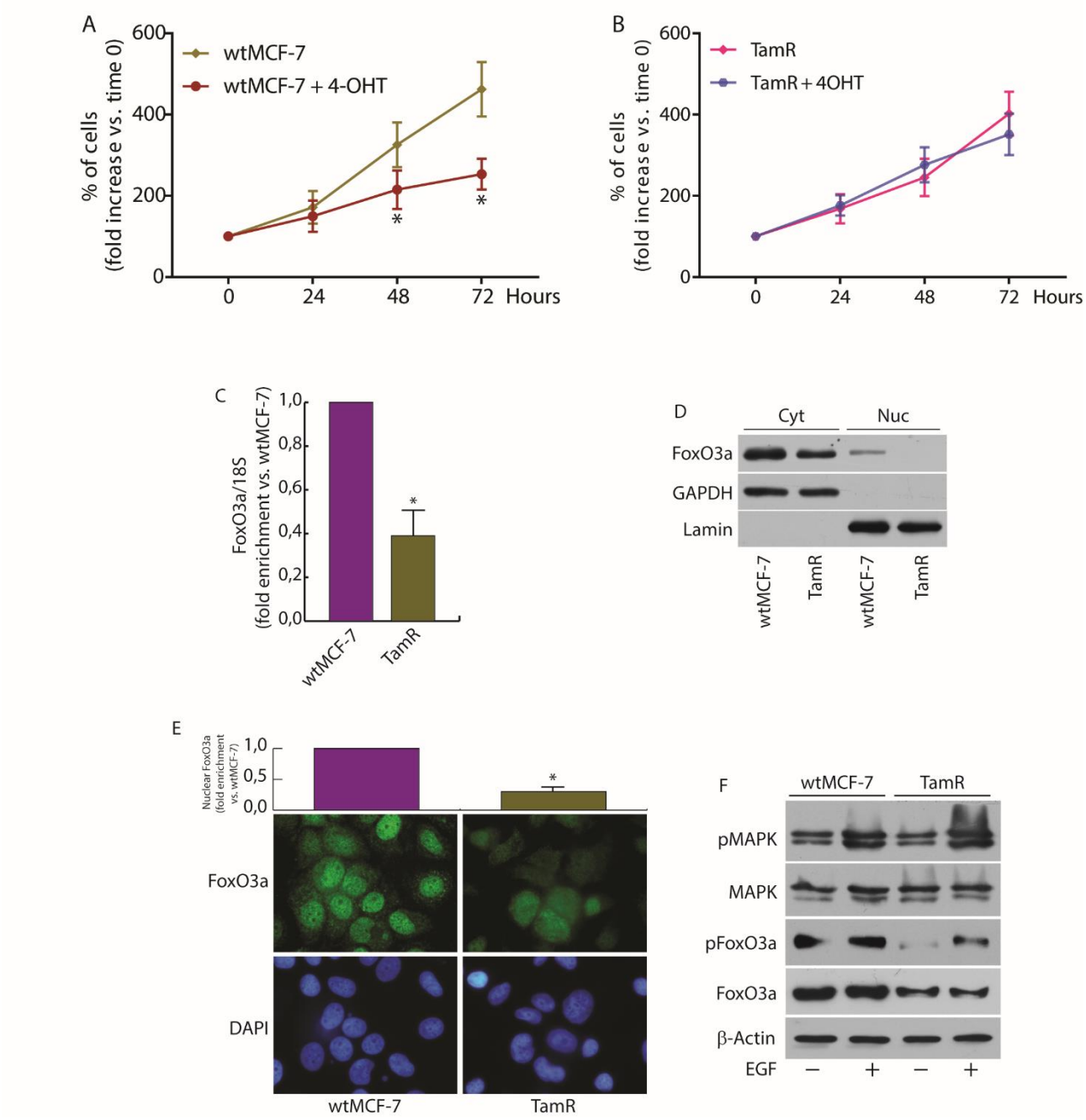

Figure 1. FoxO3a is down-regulated in TamR breast cancer cells

wtMCF-7 (A) and TamR (B) cells were treated or not with 4-OHT 1μM for 24, 48 and 72 hours, and processed as described in *Materials and Methods*. Data are reported as percentage of cell increase over time 0. Results are the mean ± s.d. of at least three independent experiments. *, $P < 0.05$ vs. untreated. C) FoxO3a transcripts were analysed by real-time PCR in wtMCF-7 and TamR cells cultured in growing medium. Each sample was normalized *vs* its 18S rRNA content and presented as fold enrichment versus wtMCF-7. Results represent the mean ± s.d. of 3 independent experiment. *, $P < 0.01$ vs. untreated D) A duplicate set of growing wtMCF-7 and TamR cells was lysed and cytoplasmic and nuclear protein extracts were subjected to WB (30 μg/lane) to evaluate the subcellular localization of FoxO3a. GAPDH (cytosolic marker) and Lamin B (nuclear marker) were used as loading controls and to assess the subcellular protein fractionation. E) Immunostaining of FoxO3a expression and localization (green) in wtMCF-7 and TamR growing cells; nuclear integrity was visualized by DAPI (blue). F) Comparison in signal transduction pathway in wtMCF-7 and TamR cells. Cells were seeded in 60mm dishes, starved in PRF-SFM for 16h and then treated or not with 10ng/ml EGF-1 for 15 min. Protein expression were analyzed by WB using indicated antibodies.

Re-expression of FoxO3a in TamR cells restores the sensitivity to the antiestrogen

To investigate if FoxO3a re-expression could restore the sensitivity of TamR cells to the treatment, we developed two Tet-On based inducible clones of TamR (see *Materials and Methods*), which we will refer to as TamR/TetOn-AAA, i.e. a tetracycline inducible clone expressing the constitutively active triple mutant of FoxO3a (FoxO3aAAA), and the relative control TamR/TetOn-V (containing the empty vector in place of the FoxO3aAAA).

As expected, FoxO3aAAA (F3aAAA) induction by Doxycycline (Dox) inhibited cell growth and restored the sensitivity to 4-OHT treatment only in TamR/TetOn-AAA but not in TamR/TetOn-V cells (**Fig.2A** and **B** and data not shown). Interestingly, FoxO3a silencing (siF3a), by reproducing the FoxO3a status in TamR cells, was able to counteract 4-OHT induced growth arrest in wtMCF-7 (**Fig. 2E** and **F**).

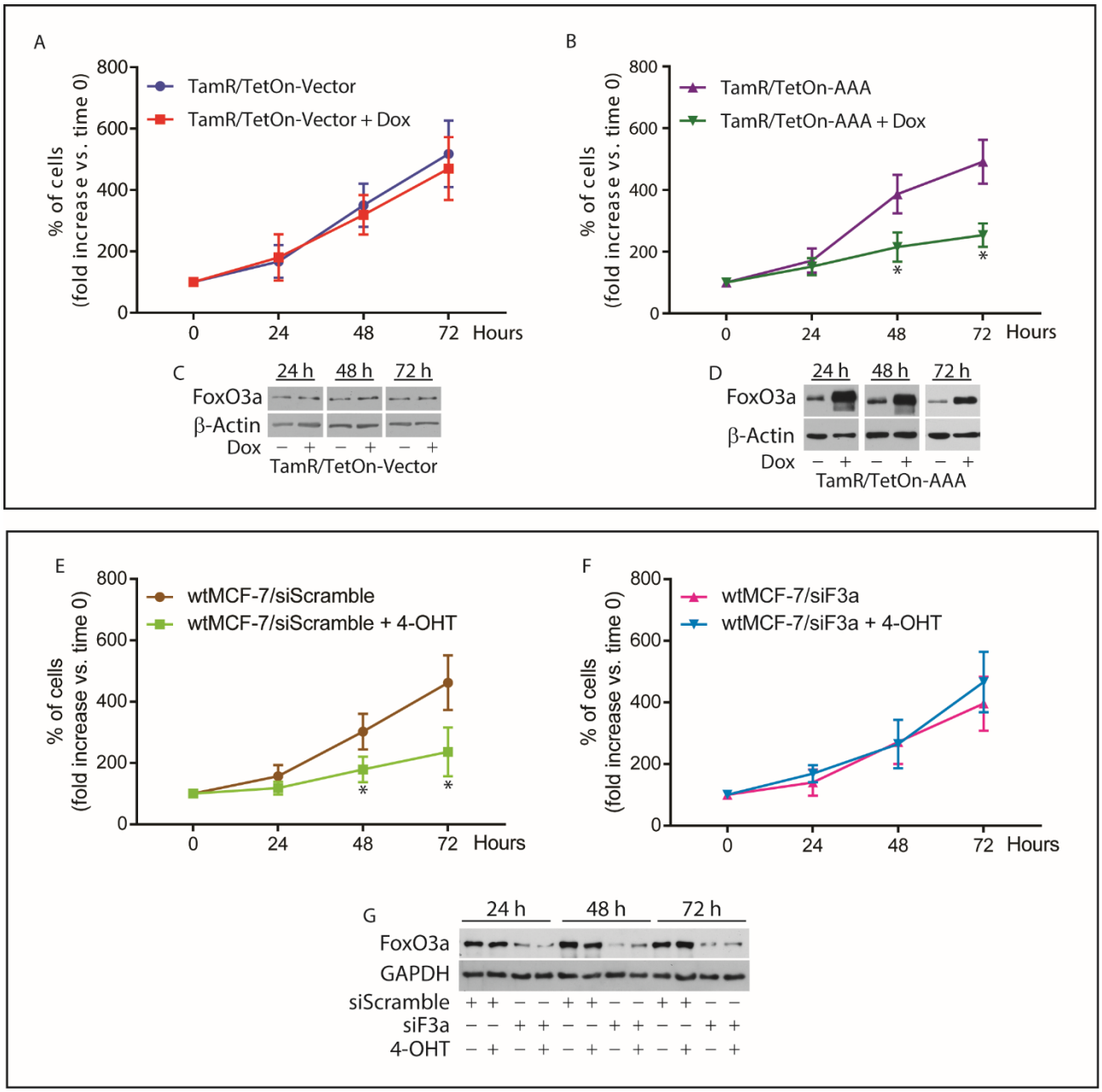

Figure. 2. FoxO3a restores the sensitivity of Tam resistant BCC to tamoxifen

TamR/TetOn-V (A) and TamR/TetOn-AAA (B) cells were serum starved for 24 h and then switched to 5% PRF-CT plus 1μM Tam and treated or not up to 72 h with Dox (3μg/ml). wtMCF-7 cells were transfected with E) a siRNA for FoxO3a (siF3a) or a F) Scramble siRNA (siScramble) as control. After 6 h, cells were serum starved for 16 h and then shifted to 5% PRF-CT +/- Tam (1μM) up to 72 h. Tam treatment was renewed every day. Cells were then harvested by trypsinization and counted using trypan blue dye exclusion assay. Data represent the mean±SD of three independent experiments. *$p<0.05$ vs. relative treated cells. The error bars indicate SD.

Duplicate experiments were subjected to WB analysis to assess FoxO3a expression in Dox treated TamR/TetOn-V and TamR/TetOn-AAA clones (C and D), and in wtMCF-7 FoxO3a silenced cells (G). β-Actin and GAPDH were used as loading controls.

Cell cycle distribution of TamR/TetOn-AAA clones was analyzed through flow cytometry in presence or absence of Dox for 72h. A significant inhibition of cell cycle progression was observed in F3aAAA over-expressing (Dox treated) cells compared to control (Dox untreated) cells, as a result of a relevant increase in the percentage of cells in the G1 phase and the concomitant decrease in the S-phase population (**Fig. 3A** and **B**). No relevant change in the G1 and S phase was observed in Dox treated TamR/TetOn-V cells, confirming that the effect is not due to Dox treatment, but, indeed, to FoxO3a overexpression (data not shown).

Cell cycle distribution was also conducted on wtMCF-7 silenced or not for FoxO3a, in presence or absence of 4-OHT for 72 hours. As expected, 4-OHT caused a substantial increase in G1 phase if compared to control (siScramble) cells, dramatically lowering the S phase, indicating a block in G1/S transition. Although the relatively short time of exposure to 4-OHT, a small amount of apoptotic cells (0.03%) was already detectable. Surprisingly, siF3a was able to counteract the antiestrogen effect, restoring the transition from G1 to S phase (**Fig. 3D** and **E**).

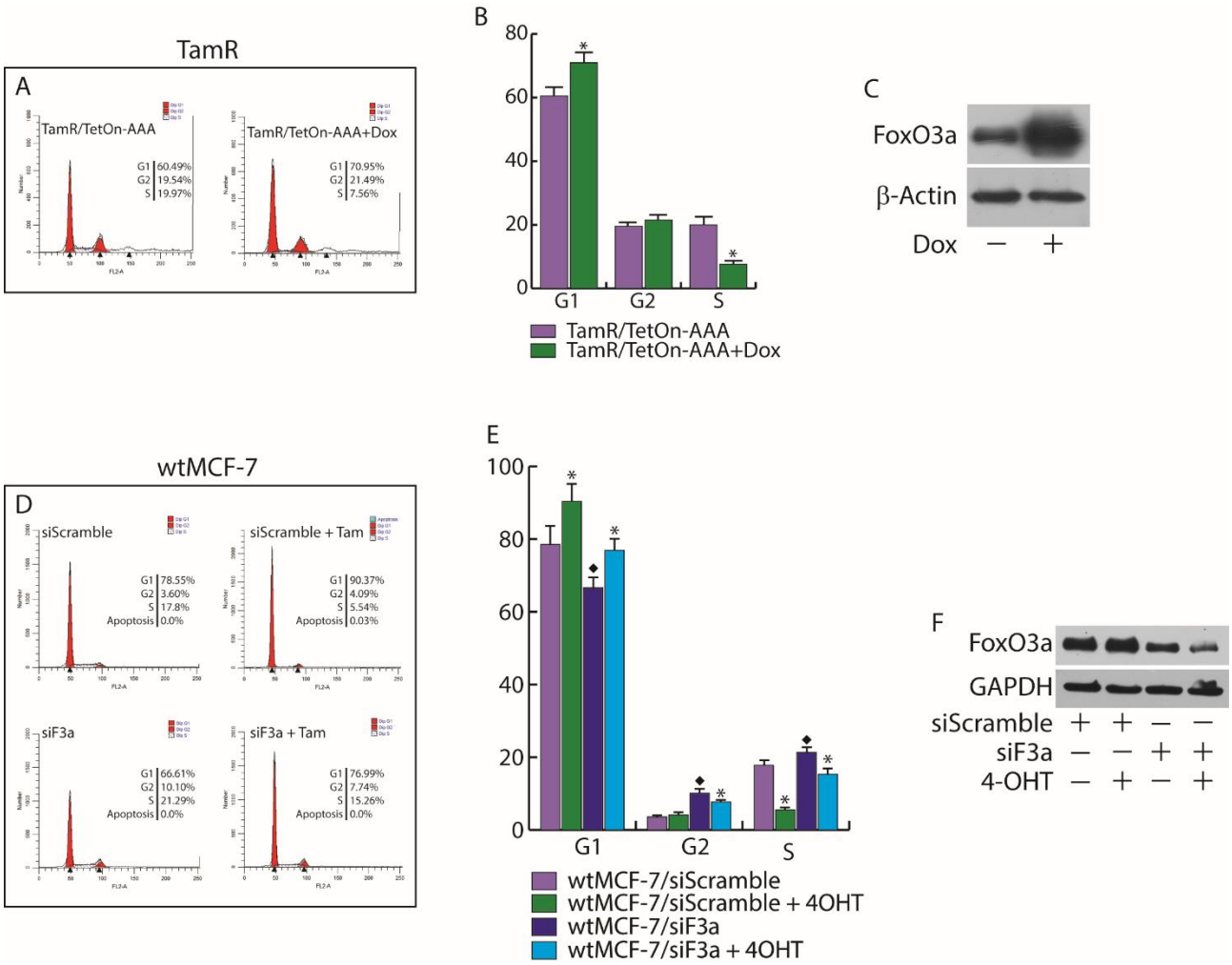

Figure. 3. Effect of FoxO3a on cell cycle distribution in wtMCF-7 and Tam resistant cells

A-B) TamR/TetOn-AAA cells were treated or not with Dox (3µg/ml) and D-E) wtMCF-7 cells were silenced for FoxO3a as already described in presence or absence of Tam. After 72 h cells were subjected to cell cycle analysis (see *Materials and Methods*). The percentage of cells in the G0/G1, S, and G2/M phases of the cell cycle are reported. Results are expressed as mean ± SD from three independent experiments. *, $p<0.05$ vs. relative untreated control, ◆, $p<0.05$ vs. untreated siScramble.

Duplicate experiments were subjected to WB analysis to assess FoxO3a expression in Dox treated TamR/TetOn-AAA clones (C), and in wtMCF-7 FoxO3a silenced cells (F). β-Actin and GAPDH were used as loading controls.

FoxO3a restores the apoptotic response to Tam in TamR cells

In line with these results, the Dox-induced over-expression of F3aAAA was able to restore the normal sensitivity to the antiestrogen treatment, by triggering the apoptotic pathway in TamR/TetOn-AAA cells (**Fig. 4** and data not shown), while FoxO3a silencing in wtMCF-7 rescued the cells from 4-OHT dependent apoptosis (data not shown).

The ultrastructural effects of the F3aAAA over-expression in TamR/TetOn-AAA cells and those of FoxO3a silencing in wtMCF-7 cells have been assessed by TEM analysis. Most of the Dox-treated TamR/TetOn-AAA cells (~ 80%), over-expressing F3aAAA, showed clear signs of injury characterized by rarefaction of the nuclear chromatin and cytoplasm, with formation of electron-dense bodies, vacuoles and lipid droplets, while 90% of Dox-treated TamR/TetOn-V cells appeared normal, with complete cell organelles, and well-distributed chromatin, mitochondria and bundles of tonofilaments (**Fig. 4A**). Moreover, a consistently greater amount of apoptotic cells were found in the surnatants collected from TamR/TetOn-AAA cells compared to controls (data not shown).

TUNEL assay confirmed this result, with Dox treated TamR/TetOn-AAA showing a much higher level of apoptosis compared to Dox treated TamR/TetOn-V (Fig. **4B**).

On the other hand, FoxO3a silencing in 4-OHT-treated wtMCF-7 cells resulted in a significant reduction of cell damage (95% of intact cells) respect to 4-OHT-treated siScramble samples (75% of intact cells), maintaining the morphology of control, non-treated, cells (siScramble and siF3a samples, both showing ~ 90% of intact cells), with well-preserved cellular elements. A small percentage of apoptotic cells were only found in 4-OHT treated controls (data not shown). TUNEL assay gave similar results (data not shown).

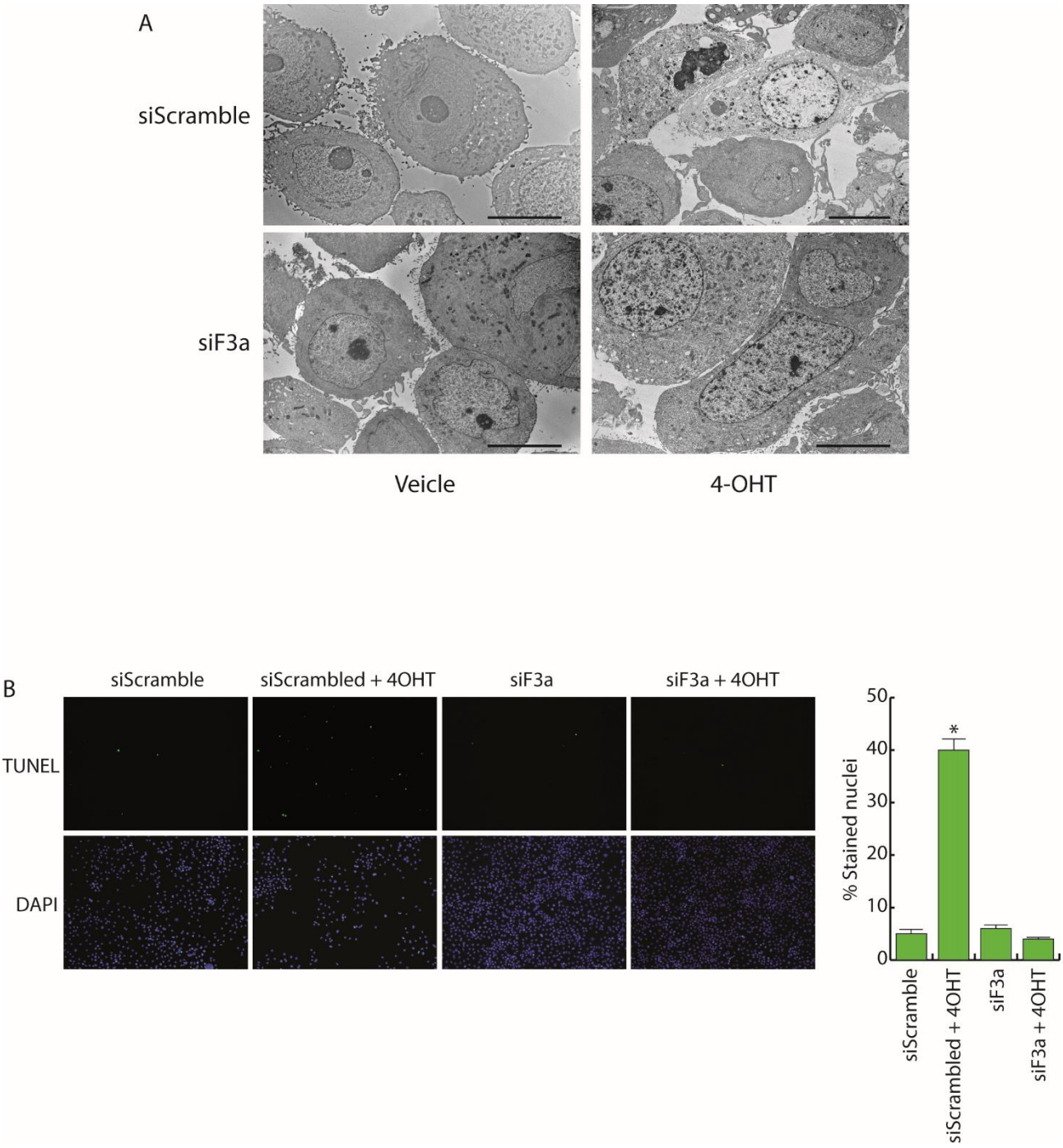

Figure 4. FoxO3a reactivates apoptosis in Tam resistant cells

A) TamR/TetOn-V and TamR/TetOn-AAA cells were treated with Dox (3μg/ml) for 72 h and processed for TEM analysis. Scale bars: 10 μm. Original magnification: x1200. B) TamR/TetOn-V and TamR/TetOn-AAA cells were treated as in (A) and processed for TUNEL assay. DAPI was used to counterstain the nuclei. Apoptotic cells were photographed at 10x magnification and then counted using Image J software. Graph on the right represent the corresponding apoptotic index (% apoptotic cells/total cell number in the field).

Proteomic analysis of TamR cells expressing active FoxO3a: the impact on several proteins controlling G1/S cell cycle phase, apoptosis and growth factor signals

To analyze the molecular mechanisms through which FoxO3a re-expression can restore the response to the antiestrogen, TamR/TetOn-V and TamR/TetOn-AAA cells were next subjected to unbiased proteomics analysis [67]. Among all proteins affected by FoxO3a re-expression in TamR cells, we selected all the modified proteins involved in the regulation of cell cycle, apoptosis and growth factors signals. The results confirm the block of cell cycle in G1/S phase indicating that it may be due to the decrease of several cell cycle regulators such as cyclin D1 and cyclin D3, of CDK4, and CDK2 and an increase in $p21^{Waf1}$ and $p27^{Kip1}$ cyclin dependent kinase inhibitors that are involved in G1/S phase transition and RB1. The reduced mitosis is also underlined by the increased expression of CDC16 and CDC27, components of the anaphase promoting complex/cyclosome, and by the reduced expression of PLK1 and by the increase in 14-3-3σ expression (Table 1).

Table 1. Some cell cycle controlling proteins regulated modified by nuclear FoxO3a expression in TamR cells (fold change versus vector).

	Symbol	Description	ID	Fold Change
Cell Cycle	CCNB1	*Cyclin B1*	E9PC90	-16,9929
	CCND1	*Cyclin D1*	Q6FI00	-16,8071
	CCND3	*Cyclin D3*	P30281	-4,51636
	CDKN1A	*Cyclin Dependent Kinase Inhibitor 1A (P21, Cip1)*	Q59ED0	3,456563
	CDKN1B	*Cyclin Dependent Kinase Inhibitor 1B (P27, Kip1)*	Q96TE0	8,027846
	CDC16	*Cell Division Cycle 16*	A0A024RDZ2	5,934377
	CDC27	*Cell Division Cycle 27*	B4DL80	9,51735
	CDK2	*Cyclin Dependent Kinase 2*	P24941	-114,1328
	CDK4	*Cyclin Dependent Kinase 4*	A0A024RBB6	-79,5918
	CDK6	*Cyclin Dependent Kinase 6*	Q00534	-16,4662
	PLK1	*Polo Like Kinase 1*	B2R841	-14,5685
	RB1	*Retinoblastoma 1*	Q59HH0	Infinity
	SFN	*Stratifin (14-3-3σ)*	P31947	Infinity

Alterations in cell cycle regulation are paralleled by an increase in the expression of pro-apoptotic genes such as AIFM1, BAD, BCLAF1, Caspase 2, 6, 7, and 9, DIABLO and PARP1 indicating restoration of the apoptotic events in response to 4-OHT treatment (Table 2).

Table 2. Some Pro-apoptotic proteins up-regulated by nuclear FoxO3a expression in TamR cells (fold change versus vector).

	Symbol	Description	ID	Fold Change
Apoptosis	AIFM1	*Apoptosis inducing factor, mitochondria associated 1*	O95831	14,924
	BAD	*BCL2 associated agonist of cell death*	A0A024R562	4,126
	BCLAF1	*BCL2 Associated Transcription Factor 1*	B7Z8J9	1058,722
	CASP2	*Caspase 2*	P42575	10,106
	CASP6	*Caspase 6*	P55212	14,237
	CASP7	*Caspase 7*	P55210	14,997
	CASP8	*Caspase 8*	B5BU46	Infinity
	DIABLO	*Diablo IAP-binding mitochondrial protein*	Q9NR28	24,874
	PARP1	*Poly(ADP-ribose) polymerase 1*	A0A024R3T8	Infinity

Consistent with cell growth inhibition and with apoptotic induction, unbiased proteomic analysis revealed a down-regulation of several proteins involved in growth factor signaling (Table 3).

Table 3. Some Growth factors signaling proteins down-regulated by nuclear FoxO3a expression in TamR cells (fold change versus vector).

	Symbol	Description	ID	Fold Change
GF signaling	AKT1	*AKT serine/threonine kinase 1*	P31749	-14,180
	AKT2	*AKT serine/threonine kinase 2*	P31751	-441,405
	AKT3	*AKT serine/threonine kinase 3*	Q9Y243	-16,161
	IRS1	*insulin receptor substrate 1*	A0A024R49	-10000,000
	MTOR	*mechanistic target of rapamycin*	P42345	-10000,000
	PIK3C3	*phosphatidylinositol 3-kinase catalytic subunit type 3*	B4DPV9	-40,509
	PIK3C2A	*phosphatidylinositol-4-phosphate 3-kinase catalytic subunit type 2 alpha*	L7RRS0	-14,866
	PIK3CB	*phosphatidylinositol-4,5-bisphosphate 3-kinase catalytic subunit beta*	P42338	-10000,000
	RAF1	*Raf-1 proto-oncogene, serine/threonine kinase*	P04049	-10000,000
	SHC1	*SHC adaptor protein 1*	H0Y539	-10000,000

Nuclear FoxO3a down regulates three Akt family members and several PI3K catalytic subunit. In addition, other important proteins involved in growth factor pathways, such as IRS1, SHC1 and RAF1, resulted markedly reduced. Altogether, proteomic analysis indicates that nuclear FoxO3a restores the sensitivity to 4-OHT by switching off the hyperactivation of Growth factor signals.

In silico validation of the clinical relevance of FoxO3a in human ER+ BC patients

To assess the possible clinical relevance of FoxO3a in the response to endocrine treatment and in the acquisition of tamoxifen resistance, we questioned if its levels (in terms of mRNA) might be indicative of the potential outcome of ER+ human BC patients cohorts, with long-term follow-up (more than 5 years). The Kaplan-Meier (K-M) relapse-free survival (RFS) curve (**Fig. 5A**) demonstrated a poorer prognosis for Luminal A subtype BC patients expressing low level of FoxO3a mRNA (log-rank test, p=0.0095). The relevance of FoxO3a mRNA expression was also evident by evaluating the overall survival in the Luminal A subtype cohort (**Fig. 5B**) (log-rank test, p=0.043). Anyway, we have to consider this result as indicative due to the small number of patients. Interestingly, in a small part of the luminal A subtype cohort (n. 30) treated with 4-OHT (**Fig. 5C**), the K-M curve reported a high probability of RFS in the group expressing high FoxO3a levels (log-rank test, p=0.0086). Even in this case, the results are only indicative due to the small number of patients. We were not able to evaluate the overall survival in the luminal A subtype cohort treated with 4-OHT since only 19 samples were found.

Finally, since low levels of FoxO3a mRNA were associated with disease progression in patients that received endocrine therapy (**Fig. 5D**), this may probably be indicative of a clinical association with endocrine therapy-resistance. Thus, low levels of FoxO3a could be used to identify high-risk ER+ BC patients that might benefit from potential adjuvant treatments that are able to increase FoxO3a expression, restoring the sensitivity to 4-OHT therapy.

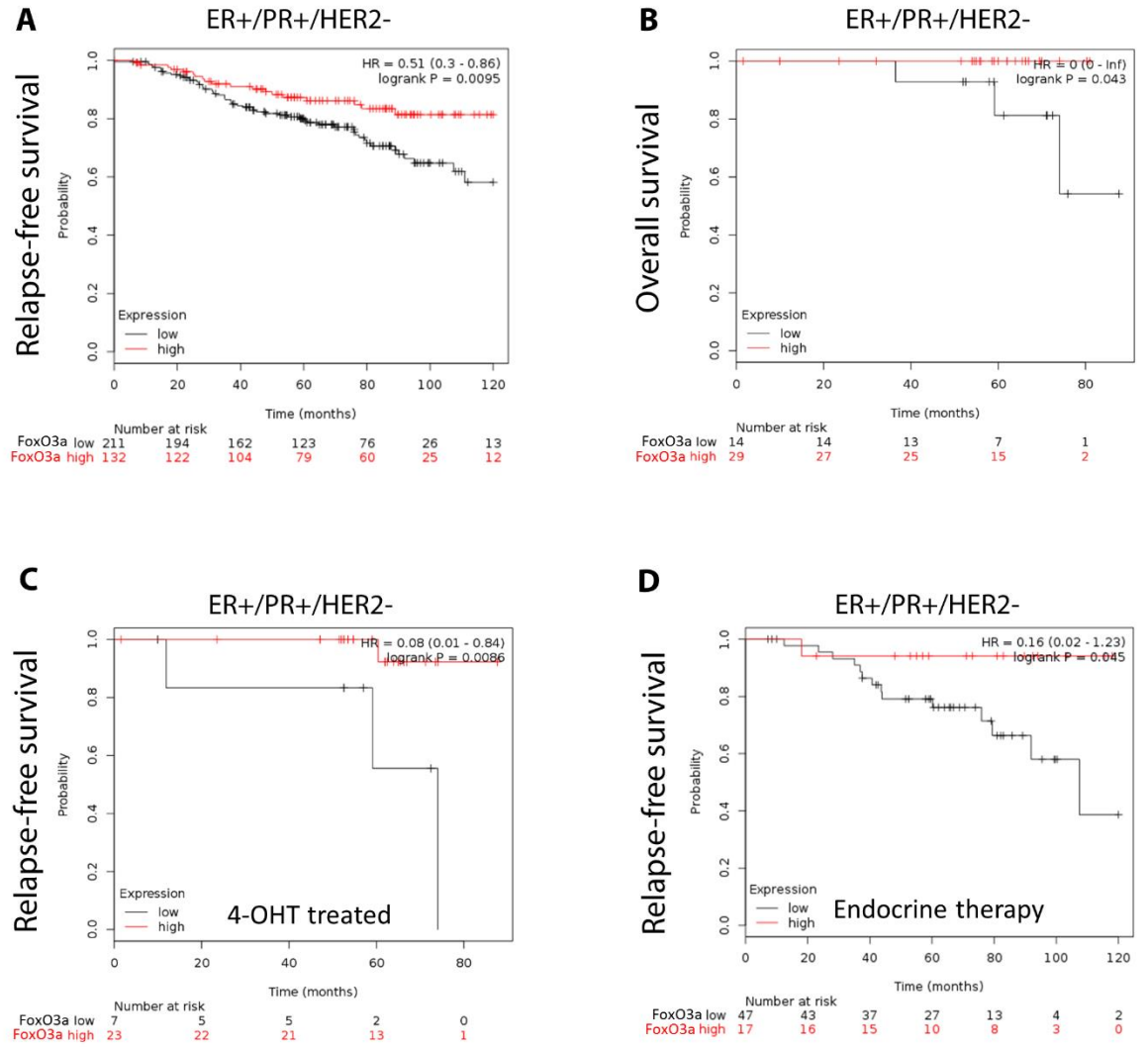

Figure 5. The relapse-free and overall survival of patients according to FoxO3a expression.
All graphs are calculated using microarray data from luminal A subtype cohorts of 343 patients (relapse-free survival, panel A), 43 patients (overall survival, panel B), 30 patients (relapse-free survival 4-OHT treated, panel C), and 64 patients (relapse-free survival endocrine therapy, panel D) determined using an online survival analysis tool. Kaplan-Meier correlations are plotted for high (above median, in red) and low (below median, in black) FoxO3a gene expression. Biased and outlier array data were excluded from the analysis. Hazard-ratios were calculated, at the best auto-selected cut-off, and p-values were calculated using the logrank test and plotted in R. K-M curves were also generated online using the K-M-plotter (as high-resolution TIFF files), using univariate analysis: http://kmplot.com/analysis/index.php?p = service&cancer = breast. This allowed us to directly perform in silico validation of the clinical relevance of FoxO3a in human BC patients. The most updated version of the database was used for all analyses.

The antiepileptic drug Lamotrigine restores the sensitivity to Tam treatment through FoxO3a re-expression in tamoxifen resistant xenografts: perspective on an off-label use

Ongoing studies in our laboratory suggest that a promising pharmacological candidate for such an adjuvant therapy in patients who result refractory to the antiestrogen treatment is lamotrigine (LTG), a well-known AED which is able to increase FoxO3a expression in BCC (manuscript in preparation). Thus, in order to evaluate if LTG causes FoxO3a induction also *in vivo* and, consequently, if it is able to restore the sensitivity to the anti-hormonal therapy, the effects of LTG on the development of TamR derived breast carcinomas, was evaluated in mice models. To this aim, female nude mice, bearing TamR cells-derived tumor xenografts into the intrascapular region, were treated with LTG (20 mg/kg/die) on the basis of our *in vitro* results (manuscript in preparation) and on pertinent literature [68]. Mice well tolerated all *in vivo* procedures, since no changes in body weight (data not shown), in motor function or in food and water consumption was observed. In addition, no significant difference in the mean weights or histologic features of the major organs (liver, lung, spleen, and kidney) after sacrifice was observed between vehicle-treated mice and those that received LTG treatment. On the other hand, a significant reduction in tumor volume (~ 50%) was observed in mice administered with 20 mg/ml LTG (**Fig. 6A** and **B**).

To distinguish the xenograft from the mouse tissue, immunohistochemistry was performed on xenograft sections with hematoxylin and eosin which revealed that xenografts were primarily composed of tumor epithelial cells, as also confirmed by immunostaining for the human epithelial cell marker cytokeratin 18 (Cyt18) (**Fig. 6C**).

The antiproliferative effect mediated by LTG was confirmed by reduced expressions of the proliferation marker Ki-67 in LTG treated xenografts compared to those deriving from control mice (**Fig. 6D**). These results are congruent with the strong increase in FoxO3a expression observed both in tissue sections and in protein extracts from LTG treated tumors respect to control tumors (**Fig. 6D** and **E**). Moreover, Cyclin D1 downregulation associated to FoxO3a upregulation perfectly fits with other authors' observations [69] and with our proteomics results. Notably, the immunohistochemical

analysis of LTG samples clearly shows a markedly nuclear localization of FoxO3a (**Fig. 6D**), which is consistent with an antiproliferative effect. Taken together, these results indicate that LTG might represent a useful therapeutic tool to be exploited as an adjuvant treatment in patients who failed to respond to the antiestrogen regimen.

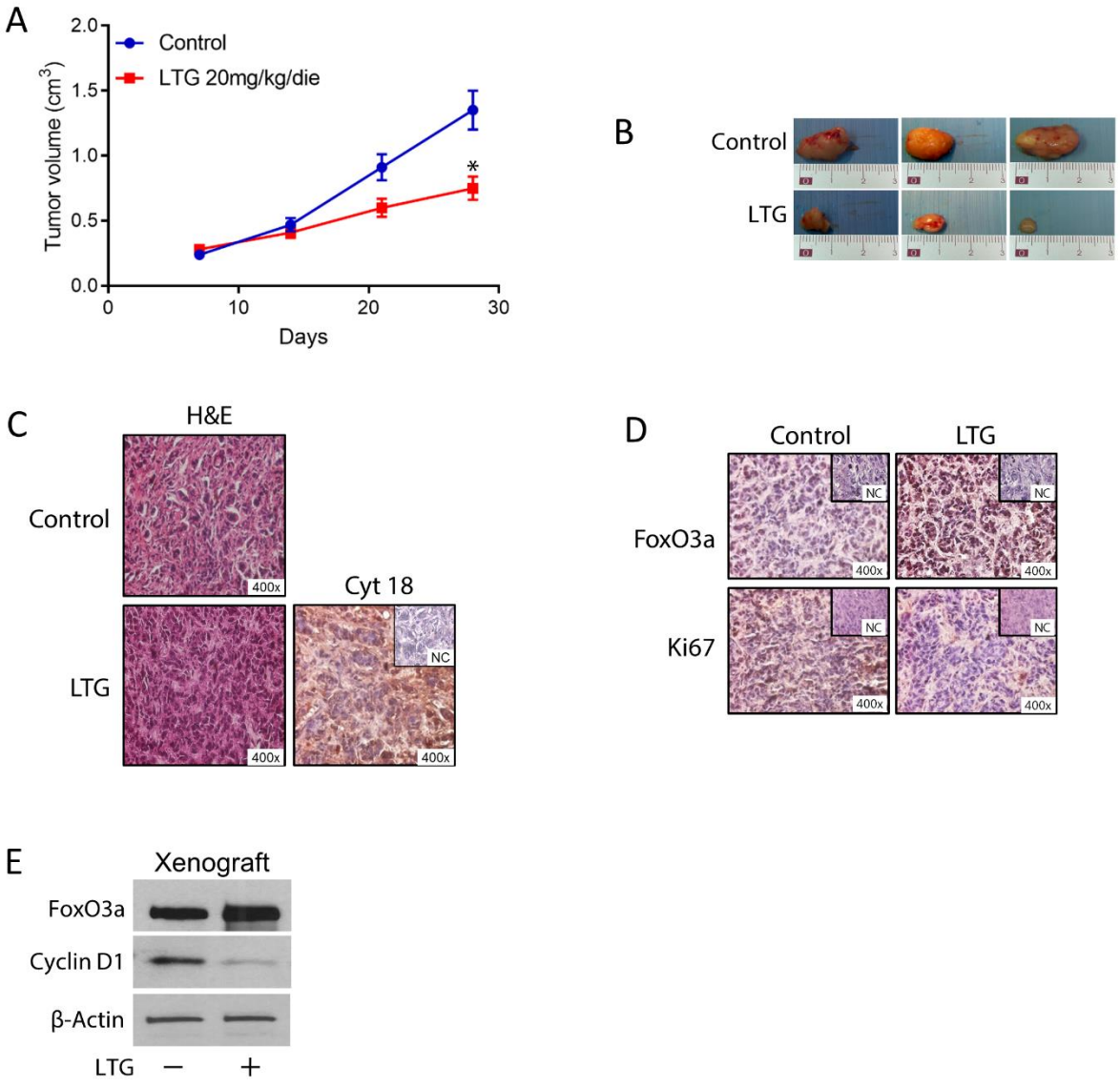

Figure 6. Lamotrigine induces FoxO3a in vivo and inhibits the growth of TamR derived tumor xenografts.
A) Xenografts were established with TamR cells in female mice implanted with E2 and, successively, Tam pellets (see *Materials and Methods* for details). One group was treated with 20 mg/kg/day LTG (*n = 5*) and a second group with vehicle alone (*n = 5*). Tumor mass was measured at indicated time points with a caliper. *, P < 0.05, treated versus control group. B) Representative images of explanted tumors at day 28. Scale bar, 0.3 cm. C) Representative tumor sections from mice at 28 days were formalin fixed, paraffin embedded, sectioned, and stained with hematoxylin and eosin Y (H&E) or incubated with antibodies directed against the epithelial marker cytokeratin 18 (Cyt 18). D) Immunostaing were also performed for the proliferation marker Ki67 and for FoxO3a. The insets in C) and D) are representative images of negative control sections, where the primary antibody was replaced by nonimmune serum. E) FoxO3a and CyclinD1expression was assessed in protein extracts from xenografts excised from control mice and LTG treated mice. β-actin was used as loading control.

DISCUSSION

Approximately 70% of BCs do express ER and are subjected to endocrine-based therapies (selective ER modifiers, e.g. tamoxifen, selective ER down-regulators, e.g., fulvestrant, and aromatase inhibitors, e.g., letrozole, anastrozole and excemestane), but the development of endocrine resistance is highly common and it still remains an unsolved problem. Thus, elucidating the molecular mechanisms leading to hormone insensitivity of BC is important to improve the efficacy of endocrine therapy.

To this aim, we addressed our studies on the involvement of tumor suppressor FoxO3a in the acquisition of resistance to tamoxifen in BC. Indeed, several data from our and other's laboratories, established the existence of a functional interaction between FoxOs and ER in BCC (reviewed in [70]). In particular, FoxO3a seems to have a protective role in ER+ breast tumors [55, 71, 72], therefore, it is reasonable to suppose that FoxO3a deregulation could favor the acquisition of a phenotype resistant to treatments targeting ER, such as tamoxifen.

In line with this assumption, here we report that ER+ cells chronically exposed to Tam (TamR cells) show a strong decrease in FoxO3a mRNA and protein expression and in its nuclear localization, if compared to parental, Tam sensitive, cell lines. Notably, the phenomenon was not peculiar to a specific cell line (i.e. MCF-7), but it was observed in other BCC (e.g. ZR-75, data not shown).

The mechanism underlying FoxO3a downregulation in TamR cells does not seem to directly depend on the estrogen/antiestrogen action, nor on epigenetic modifications of FoxO3a regulatory regions that might have been caused by long-term Tam exposure [73] (data not shown).

Two additional mechanisms are currently under investigation in our laboratory: i) the involvement of FoxO3a transcriptional regulators p53 and E2F-1 (reviewed in [66]), whose levels are decreased in TamR cells compared to parental cells, and ii) post-translational modifications of FoxO3a, which results hyper-phosphorylated by hyperactive ERK1/2 MAPK in TamR cells, leading to FoxO3a degradation through the MDM2-mediated ubiquitin-proteasome pathway [50]. These results will be included in a forthcoming article.

Instead, here we questioned if FoxO3a re-activation might restore the sensitivity to Tam in TamR cells. Indeed, the over-expression of constitutively active FoxO3a (F3aAAA) in TamR cells was able to re-establish the anti-proliferative effect of the antiestrogen (**Fig. 2A** and **B**), by triggering the apoptotic pathway, as confirmed by TUNEL (**Fig. 4B**) and Annexin V (data not shown) assays, as well as by TEM observations (**Fig. 4A**).

Oddly, proteomics results and WB analysis did not reveal any significant change in the levels of the pro-apoptotic factors Bim and Fas-L, whose expression is notoriously regulated by FoxO3a [74], in F3aAAA overexpressing clones compared to relative controls. Neither we were able to obtain the induction of these two proteins in cells transiently expressing F3aAAA (see *Materials and Methods*), nor their downregulation in parental cells silenced for FoxO3a. However other pro-apoptotic proteins like BAD, PARP, TP53I3 (Tumor Protein P53 Inducible Protein 3) and several caspases were upregulated, some of these even ∞ folds (Tables 1-3). Since none of these other apoptotic markers have ever been reported as FoxO3a target genes, these novel findings will be further investigated.

In addition, although FoxO3a seems to be involved in the regulation of autophagy [75] proteomics analysis, nor our TEM observations revealed any significant alteration in mediators of the autophagy response (e.g. p67, Ulk1, PI3K class III, AMBRA, UVRAG, Beclin1, Atg5, LC3 II and LC3B) in F3aAAA expressing TamR cells (data not shown).

The increased apoptosis is paralleled by a down regulation of several cell cycle controlling proteins (**Table1**) such as Cyclin D1, Cyclin D3, CDK4, and CDK6 all involved in the transition from G1 to S phase of the cycle, and CDK2 that drives the entrance in S phase of the cycle. Moreover, the blockage of cell cycle is ensured by the down regulation of Cyclin B1 involved in the G2 phase and PLK1 (Polo Like kinase 1) involved in the M phase. In addition, nuclear FoxO3a increases the expression of CDC16, CDC27 (both components of the anaphase-promoting complex), and $p21^{Cip1}$, $p27^{Kip1}$, RB1 and SFN, all inhibitors of the transition from the G1 to the S phase of cell cycle. Interestingly, proteomic analysis revealed a deeper involvement of FoxO3a in the modulation of cell cycle regulating proteins (Reviewed in [76]). Here we reported that active FoxO3a modifies the

expression of additional cell cycle regulators, at least in TamR breast cancer cells, such as CDC16, CDC27, CDK2, CDK4, CDK6 and SFN that have never been described before and that require a deeper study in the future. The ability of nuclear FoxO3a to restore the sensitivity of breast cancer cell to the hormonal treatment is, additionally, highlighted by the down regulation of several proteins involved in the signaling pathways activated by growth factors. Proteomic analysis revealed a down regulation of several components of the PI3K/AKT pathway, the major inhibitor of FoxO3a activity (**Table 3**). In addition, the majority of the growth factor signals are down-regulated since both adaptor proteins such as IRS1 and SHC1, and transductional factors such as RAF1 are markedly down regulated in FoxO3AAA expressing TamR breast cancer cells.

FoxO3a involvement in mediating the cellular response to Tam treatment was confirmed by the inhibition of apoptosis and the increased cell proliferation observed in FoxO3a-silenced wtMCF-7 cells, particularly in Tam treated samples (an accurate analysis of the mechanism through which FoxO3a mediates the antiproliferative effect of Tam in wtMCF-7 is ongoing). Indeed, low FoxO3a expression stemming from FoxO3a silencing, reflects somehow the FoxO3a downregulation observed in TamR cells, thus mimicking the behavior of a resistant phenotype.

In agreement with these findings, the K-M survival curves of a population of breast cancer patients subjected to Tam therapy suggest that high levels of FoxO3a strongly correlate with a positive response to the tamoxifen treatment and, consequently, with a long-term relapse free survival. Thus, FoxO3a expression might not only be considered a general favorable prognostic marker in breast cancer [71, 77], but might also be predictive of the potential efficacy of the antiestrogen therapy. Nevertheless, it cannot be excluded that the low levels of FoxO3a observed in ER+ BC patients might be, at least for the subgroup receiving tamoxifen therapy, a consequence of the gradual acquisition of a Tam resistant phenotype (**Fig. 4**).

Our results confirm the need of developing anti-cancer therapies exploiting FoxO3a in BC patients with acquired resistance to Tam treatment. Indeed, FoxO3a reactivation could represent an adjuvant to Tam therapy by restoring the sensitivity to the antiestrogen.

Several drugs have been reported to increase FoxO3a activity and promote apoptosis by targeting the growth factors, PI3k/PTEN, Akt and MAPK pathways in breast cancer cell lines. Moreover two clinical trials (one using a combination of the pure antiestrogen fulvestrant with a PI3k inhibitor and the other using reparaxin, an IL-8 receptor antagonist) aimed to assess, among the other endpoints, FoxO3a status, just ended [78].

Here we add a new molecule to the list of FoxO3a activating drugs, showing how the well-known AED Lamotrigine (LTG; Lamictal) [59], widely used in the clinic, has a strong anti-proliferative activity on xenografts tumors deriving from TamR cells. The restored response to Tam treatment was paralleled by a significant increased expression and mainly nuclear localization of FoxO3a *in vivo*.

Taken together, our results show that: 1) FoxO3a is hyper-phosphorylated, thus inactivated, by hyper-active growth factors signaling in TamR cells; 2) FoxO3a re-expression is able to overcome tamoxifen resistance; 3) low levels of FoxO3a are predictive of the failure of the antiestrogen therapy; 4) the AED LTG might represent a good candidate for adjuvant endocrine therapy in patients refractory to Tam treatment.

Reference

1. Siegel, R., et al., *Cancer statistics, 2011: the impact of eliminating socioeconomic and racial disparities on premature cancer deaths.* CA Cancer J Clin, 2011. **61**(4): p. 212-36.
2. Keen, J.C. and N.E. Davidson, *The biology of breast carcinoma.* Cancer, 2003. **97**(3 Suppl): p. 825-33.
3. McCarty, K.S., Jr., et al., *Correlation of estrogen and progesterone receptors with histologic differentiation in mammary carcinoma.* Cancer, 1980. **46**(12 Suppl): p. 2851-8.
4. Mossler, J.A., K.S. McCarty, Jr., and W.W. Johnston, *The correlation of cytologic grade and steroid receptor content in effusions of metastatic breast carcinoma.* Acta Cytol, 1981. **25**(6): p. 653-8.
5. Osborne, C.K., *Steroid hormone receptors in breast cancer management.* Breast Cancer Res Treat, 1998. **51**(3): p. 227-38.
6. Banerjee, S., et al., *17alpha-estradiol-induced VEGF-A expression in rat pituitary tumor cells is mediated through ER independent but PI3K-Akt dependent signaling pathway.* Biochem Biophys Res Commun, 2003. **300**(1): p. 209-15.
7. Brzozowski, A.M., et al., *Molecular basis of agonism and antagonism in the oestrogen receptor.* Nature, 1997. **389**(6652): p. 753-8.
8. Shiau, A.K., et al., *The structural basis of estrogen receptor/coactivator recognition and the antagonism of this interaction by tamoxifen.* Cell, 1998. **95**(7): p. 927-37.
9. Kushner, P.J., et al., *Estrogen receptor pathways to AP-1.* J Steroid Biochem Mol Biol, 2000. **74**(5): p. 311-7.
10. Jordan, V.C., et al., *A monohydroxylated metabolite of tamoxifen with potent antioestrogenic activity.* J Endocrinol, 1977. **75**(2): p. 305-16.
11. Allen, K.E., E.R. Clark, and V.C. Jordan, *Evidence for the metabolic activation of non-steroidal antioestrogens: a study of structure-activity relationships.* Br J Pharmacol, 1980. **71**(1): p. 83-91.
12. Clarke, R., J.J. Tyson, and J.M. Dixon, *Endocrine resistance in breast cancer--An overview and update.* Mol Cell Endocrinol, 2015. **418 Pt 3**: p. 220-34.

13. Ali, S. and R.C. Coombes, *Endocrine-responsive breast cancer and strategies for combating resistance.* Nat Rev Cancer, 2002. **2**(2): p. 101-12.

14. Elkak, A.E. and K. Mokbel, *Pure antiestrogens and breast cancer.* Curr Med Res Opin, 2001. **17**(4): p. 282-9.

15. Chang, X.Z., et al., *Identification of the functional role of peroxiredoxin 6 in the progression of breast cancer.* Breast Cancer Res, 2007. **9**(6): p. R76.

16. Robertson, J.F., *Current role of endocrine therapy in the management of breast cancer.* Breast Cancer, 2002. **9**(4): p. 276-81.

17. Nicholson, R.I. and J.M. Gee, *Oestrogen and growth factor cross-talk and endocrine insensitivity and acquired resistance in breast cancer.* Br J Cancer, 2000. **82**(3): p. 501-13.

18. Nicholson, R.I., et al., *Modulation of epidermal growth factor receptor in endocrine-resistant, estrogen-receptor-positive breast cancer.* Ann N Y Acad Sci, 2002. **963**: p. 104-15.

19. Ring, A. and M. Dowsett, *Mechanisms of tamoxifen resistance.* Endocr Relat Cancer, 2004. **11**(4): p. 643-58.

20. Brunner, N., et al., *MCF7/LCC2: a 4-hydroxytamoxifen resistant human breast cancer variant that retains sensitivity to the steroidal antiestrogen ICI 182,780.* Cancer Res, 1993. **53**(14): p. 3229-32.

21. Johnston, S.R., et al., *Changes in estrogen receptor, progesterone receptor, and pS2 expression in tamoxifen-resistant human breast cancer.* Cancer Res, 1995. **55**(15): p. 3331-8.

22. Nicholson, R.I., et al., *Growth factor signalling in endocrine and anti-growth factor resistant breast cancer.* Rev Endocr Metab Disord, 2007. **8**(3): p. 241-53.

23. Musgrove, E.A. and R.L. Sutherland, *Biological determinants of endocrine resistance in breast cancer.* Nat Rev Cancer, 2009. **9**(9): p. 631-43.

24. Gee, J.M., et al., *Phosphorylation of ERK1/2 mitogen-activated protein kinase is associated with poor response to anti-hormonal therapy and decreased patient survival in clinical breast cancer.* Int J Cancer, 2001. **95**(4): p. 247-54.

25. Campbell, R.A., et al., *Phosphatidylinositol 3-kinase/AKT-mediated activation of estrogen receptor alpha: a new model for anti-estrogen resistance.* J Biol Chem, 2001. **276**(13): p. 9817-24.

26. Faridi, J., et al., *Expression of constitutively active Akt-3 in MCF-7 breast cancer cells reverses the estrogen and tamoxifen responsivity of these cells in vivo.* Clin Cancer Res, 2003. **9**(8): p. 2933-9.

27. DeGraffenried, L.A., et al., *Eicosapentaenoic acid restores tamoxifen sensitivity in breast cancer cells with high Akt activity.* Ann Oncol, 2003. **14**(7): p. 1051-6.

28. Kandel, E.S. and N. Hay, *The regulation and activities of the multifunctional serine/threonine kinase Akt/PKB.* Exp Cell Res, 1999. **253**(1): p. 210-29.

29. Franke, T.F., et al., *Direct regulation of the Akt proto-oncogene product by phosphatidylinositol-3,4-bisphosphate.* Science, 1997. **275**(5300): p. 665-8.

30. Brunet, A., et al., *Akt promotes cell survival by phosphorylating and inhibiting a Forkhead transcription factor.* Cell, 1999. **96**(6): p. 857-68.

31. Osborne, C.K., et al., *Estrogen receptor: current understanding of its activation and modulation.* Clin Cancer Res, 2001. **7**(12 Suppl): p. 4338s-4342s; discussion 4411s-4412s.

32. Greer, E.L. and A. Brunet, *FOXO transcription factors in ageing and cancer.* Acta Physiol (Oxf), 2008. **192**(1): p. 19-28.

33. Wang, X., W.R. Chen, and D. Xing, *A pathway from JNK through decreased ERK and Akt activities for FOXO3a nuclear translocation in response to UV irradiation.* J Cell Physiol, 2012. **227**(3): p. 1168-78.

34. Calnan, D.R. and A. Brunet, *The FoxO code.* Oncogene, 2008. **27**(16): p. 2276-88.

35. Coomans de Brachene, A. and J.B. Demoulin, *FOXO transcription factors in cancer development and therapy.* Cell Mol Life Sci, 2016. **73**(6): p. 1159-72.

36. Van Der Heide, L.P., M.F. Hoekman, and M.P. Smidt, *The ins and outs of FoxO shuttling: mechanisms of FoxO translocation and transcriptional regulation.* Biochem J, 2004. **380**(Pt 2): p. 297-309.

37. Shaul, Y.D. and R. Seger, *The MEK/ERK cascade: from signaling specificity to diverse functions.* Biochim Biophys Acta, 2007. **1773**(8): p. 1213-26.

38. Pimienta, G. and J. Pascual, *Canonical and alternative MAPK signaling.* Cell Cycle, 2007. **6**(21): p. 2628-32.

39. Schaeffer, H.J. and M.J. Weber, *Mitogen-activated protein kinases: specific messages from ubiquitous messengers.* Mol Cell Biol, 1999. **19**(4): p. 2435-44.

40. Han, J. and R.J. Ulevitch, *Emerging targets for anti-inflammatory therapy.* Nat Cell Biol, 1999. **1**(2): p. E39-40.

41. Davis, R.J., *Signal transduction by the JNK group of MAP kinases.* Cell, 2000. **103**(2): p. 239-52.

42. Robinson, M.J. and M.H. Cobb, *Mitogen-activated protein kinase pathways.* Curr Opin Cell Biol, 1997. **9**(2): p. 180-6.

43. Woessmann, W., Y.H. Meng, and N.F. Mivechi, *An essential role for mitogen-activated protein kinases, ERKs, in preventing heat-induced cell death.* J Cell Biochem, 1999. **74**(4): p. 648-62.

44. Kyriakis, J.M. and J. Avruch, *Sounding the alarm: protein kinase cascades activated by stress and inflammation.* J Biol Chem, 1996. **271**(40): p. 24313-6.

45. Ono, K. and J. Han, *The p38 signal transduction pathway: activation and function.* Cell Signal, 2000. **12**(1): p. 1-13.

46. Lubinus, M., et al., *Independent effects of platelet-derived growth factor isoforms on mitogen-activated protein kinase activation and mitogenesis in human dermal fibroblasts.* J Biol Chem, 1994. **269**(13): p. 9822-5.

47. Cappellini, A., et al., *The phosphoinositide 3-kinase/Akt pathway regulates cell cycle progression of HL60 human leukemia cells through cytoplasmic relocalization of the cyclin-dependent kinase inhibitor p27(Kip1) and control of cyclin D1 expression.* Leukemia, 2003. **17**(11): p. 2157-67.

48. Uddin, S., et al., *Role of phosphatidylinositol 3'-kinase/AKT pathway in diffuse large B-cell lymphoma survival.* Blood, 2006. **108**(13): p. 4178-86.

49. Stahl, M., et al., *The forkhead transcription factor FoxO regulates transcription of p27Kip1 and Bim in response to IL-2.* J Immunol, 2002. **168**(10): p. 5024-31.

50. Yang, J.Y., et al., *ERK promotes tumorigenesis by inhibiting FOXO3a via MDM2-mediated degradation.* Nat Cell Biol, 2008. **10**(2): p. 138-48.

51. van den Heuvel, A.P., A. Schulze, and B.M. Burgering, *Direct control of caveolin-1 expression by FOXO transcription factors.* Biochem J, 2005. **385**(Pt 3): p. 795-802.

52. Yang, J.Y. and M.C. Hung, *Deciphering the role of forkhead transcription factors in cancer therapy.* Curr Drug Targets, 2011. **12**(9): p. 1284-90.

53. Paik, J.H., et al., *FoxOs are lineage-restricted redundant tumor suppressors and regulate endothelial cell homeostasis.* Cell, 2007. **128**(2): p. 309-23.

54. Zhao, H.H., et al., *Forkhead homologue in rhabdomyosarcoma functions as a bifunctional nuclear receptor-interacting protein with both coactivator and corepressor functions.* J Biol Chem, 2001. **276**(30): p. 27907-12.

55. Zou, Y., et al., *Forkhead box transcription factor FOXO3a suppresses estrogen-dependent breast cancer cell proliferation and tumorigenesis.* Breast Cancer Res, 2008. **10**(1): p. R21.

56. Lin, C.Y., et al., *Whole-genome cartography of estrogen receptor alpha binding sites.* PLoS Genet, 2007. **3**(6): p. e87.

57. Carroll, J.S., et al., *Chromosome-wide mapping of estrogen receptor binding reveals long-range regulation requiring the forkhead protein FoxA1.* Cell, 2005. **122**(1): p. 33-43.

58. Morelli, C., et al., *Akt2 inhibition enables the forkhead transcription factor FoxO3a to have a repressive role in estrogen receptor alpha transcriptional activity in breast cancer cells.* Mol Cell Biol, 2010. **30**(3): p. 857-70.

59. Brodie, M.J., *Lamotrigine.* Lancet, 1992. **339**(8806): p. 1397-400.

60. Cinatl, J., Jr., et al., *Sodium valproate inhibits in vivo growth of human neuroblastoma cells.* Anticancer Drugs, 1997. **8**(10): p. 958-63.

61. Gottlicher, M., et al., *Valproic acid defines a novel class of HDAC inhibitors inducing differentiation of transformed cells.* EMBO J, 2001. **20**(24): p. 6969-78.

62. Morelli, C., et al., *PEG-templated mesoporous silica nanoparticles exclusively target cancer cells.* Nanoscale, 2011. **3**(8): p. 3198-207.

63. Catalano, S., et al., *Evidence that leptin through STAT and CREB signaling enhances cyclin D1 expression and promotes human endometrial cancer proliferation.* J Cell Physiol, 2009. **218**(3): p. 490-500.

64. Lamb, R., et al., *Doxycycline down-regulates DNA-PK and radiosensitizes tumor initiating cells: Implications for more effective radiation therapy.* Oncotarget, 2015. **6**(16): p. 14005-25.

65. Mauro, L., et al., *Evidences that estrogen receptor alpha interferes with adiponectin effects on breast cancer cell growth.* Cell Cycle, 2014. **13**(4): p. 553-64.

66. Klotz, L.O., et al., *Redox regulation of FoxO transcription factors.* Redox Biol, 2015. **6**: p. 51-72.

67. Peiris-Pages, M., et al., *Proteomic identification of prognostic tumour biomarkers, using chemotherapy-induced cancer-associated fibroblasts.* Aging (Albany NY), 2015. **7**(10): p. 816-38.

68. Nakanishi, H., et al., *Impact of P-glycoprotein and breast cancer resistance protein on the brain distribution of antiepileptic drugs in knockout mouse models.* Eur J Pharmacol, 2013. **710**(1-3): p. 20-8.

69. Schmidt, M., et al., *Cell cycle inhibition by FoxO forkhead transcription factors involves downregulation of cyclin D.* Mol Cell Biol, 2002. **22**(22): p. 7842-52.

70. Bullock, M., *FOXO factors and breast cancer: outfoxing endocrine resistance.* Endocr Relat Cancer, 2016. **23**(2): p. R113-30.

71. Habashy, H.O., et al., *FOXO3a nuclear localisation is associated with good prognosis in luminal-like breast cancer.* Breast Cancer Res Treat, 2011. **129**(1): p. 11-21.

72. Sisci, D., et al., *The estrogen receptor alpha is the key regulator of the bifunctional role of FoxO3a transcription factor in breast cancer motility and invasiveness.* Cell Cycle, 2013. **12**(21): p. 3405-20.

73. Stone, A., et al., *Tamoxifen-induced epigenetic silencing of oestrogen-regulated genes in anti-hormone resistant breast cancer.* PLoS One, 2012. **7**(7): p. e40466.

74. Burgering, B.M. and R.H. Medema, *Decisions on life and death: FOXO Forkhead transcription factors are in command when PKB/Akt is off duty.* J Leukoc Biol, 2003. **73**(6): p. 689-701.

75. Chiacchiera, F. and C. Simone, *The AMPK-FoxO3A axis as a target for cancer treatment.* Cell Cycle, 2010. **9**(6): p. 1091-6.

76. Zhang, X., et al., *Akt, FoxO and regulation of apoptosis.* Biochim Biophys Acta, 2011. **1813**(11): p. 1978-86.

77. Jiang, Y., et al., *Foxo3a expression is a prognostic marker in breast cancer.* PLoS One, 2013. **8**(8): p. e70746.

78. Taylor, S., et al., *Evaluating the evidence for targeting FOXO3a in breast cancer: a systematic review.* Cancer Cell Int, 2015. **15**(1): p. 1.

AL Magnifico Rettore
Università della Calabria

Presentazione al Collegio dei docenti della Dott.ssa Ada Donà per il conseguimento del titolo di "Dottore di Ricerca in Medicina Traslazionale"

Durante il primo anno di Dottorato la Dott.ssa Donà ha acquisito una elevata abilità nell'utilizzo di tecniche di biologia molecolare per valutare l'attività e l'espressione di proteine coinvolte nella regolazione di vie di trasduzione di segnali che gestiscono alcune delle funzioni cellulari coinvolte nella promozione e progressione dei tumori.

Il progetto di ricerca dalla Dott.ssa **Donà** si prefiggeva di valutare il ruolo del fattore di trascrizione FoxO3a nel ripristinare la sensibilità al trattamento con farmaci anti ormonali delle cellule ci carcinoma mammario resistenti al trattamento farmacologico. In particolare la ricerca ha evidenziato come un incremento dell'espressione di FoxO3a nucleare ristabilisce la sensibilità al Tamoxifene ripristinando le vie apoptotiche e la morte cellulare (lavoro in preparazione). Inoltre sono stati valutati i cambiamenti metabolici indotti dalla resistenza al trattamento con tamoxifene e la capacità di FoxO3a di riprogrammare le funzioni metaboliche cellulari ripristinando un fenotipo cellulare meno aggressivo (lavoro in preparazione). La dottoressa Donà ha, inoltre, partecipato alla realizzazione di vettori d'espressione inducibili da utilizzare in cellule di carcinoma mammario da impiantare in animali da laboratorio per valutare in vivo le osservazioni prodotte in vitro, mostrando grande interesse e capacità. La Dott.ssa Donà ha mostrato un'elevata capacità sia nell'analizzare i dati ottenuti che nella programmazione e gestione del proprio lavoro, approfondendo le sue conoscenze teoriche mediante costante studio della letteratura corrente.

Durante il suo percorso formativo, la Dott.ssa Donà ha partecipato alla relazione di tre progetti. 1) La valutazione dell'espressione del micro RNA 21 (miR-21) in cellule di carcinoma mammario in risposta alla stimolazione con androgeni (Casaburi I. et al 2016). Lo studio ha prodotto interessanti risultati che hanno evidenziato un ruolo protettivo degli androgeni sulla progressione tumorale. Infatti, l'esposizione agli androgeni, quali il testosterone o suoi metaboliti non aromatizzabili, riduce drasticamente l'espressione di miR-21 riducendo la sopravvivenza delle cellule di carcinoma mammario. 2) La caratterizzazione del profilo metabolico di due linee cellulari di carcinoma mammario evidenziando il ruolo protettivo e farmacologico del bergaptene, molecola derivante dal bergamotto, nell'indurre una riprogrammazione metabolica delle sesse cellule (Santoro M. et al 2016). 3) Il ruolo protettivo del recettore B per il progesterone nella induzione e progressione del tumore al seno. Lo studio ha evidenziato alcuni meccanismi molecolari che

portano all'attivazione delle vie di senescenza/autofagia attraverso la regolazione della trascrizione di geni cardine nella regolazione di tali funzioni quali beclin-1 e Bcl-2 (De Amicis F. et al 2016).

La Dott.ssa Donà ha partecipato regolarmente alle attività e ai seminari organizzati nell'ambito del Dottorato. Durante i tre anni di dottorato, la Dott.ssa Donà, ha dimostrato entusiasmo e notevole attitudine alla ricerca. Dotata di spirito critico nella elaborazione e nella interpretazione dei risultati sperimentali, ha acquisito ottima padronanza delle metodologie di biologia molecolare utilizzate.
Il contributo scientifico è dimostrato dai seguenti lavori pubblicati su riviste internazionali:

1. Casaburi I, Cesario MG, Donà A, Rizza P, Aquila S, Avena P, Lanzino M, Pellegrino M, Vivacqua A, Tucci P, Morelli C, Andò S, Sisci D. Androgens downregulate miR-21 expression in breast cancer cells underlining the protective role of androgen receptor. Oncotarget. 2016 Mar 15;7(11):12651-61. doi: 10.18632/oncotarget.7207.
2. De Amicis F, Guido C, Santoro M, Giordano F, Donà A, Rizza P, Pellegrino M, Perrotta I, Bonofiglio D, Sisci D, Panno ML, Tramontano D, Aquila S, Andò S. Ligand activated progesterone receptor B drives autophagy-senescence transition through a Beclin-1/Bcl-2 dependent mechanism in human breast cancer cells. Oncotarget. 2016 Sep 6;7(36):57955-57969. doi: 10.18632/oncotarget.10799.
3. Santoro M, Guido C, De Amicis F, Sisci D, Cione E, Vincenza D, Donà A, Panno ML, Aquila S. Bergapten induces metabolic reprogramming in breast cancer cells. Oncol Rep. 2016 Jan;35(1):568-76. doi: 10.3892/or.2015.4327.

Pertanto si esprime parere estremamente positivo sull'attività scientifica della Dott.ssa Ada Donà.

Rende, 22-05-2017

Docente Tutor
Prof. Diego Sisci

Research Paper

Ligand activated progesterone receptor B drives autophagy-senescence transition through a Beclin-1/Bcl-2 dependent mechanism in human breast cancer cells

Francesca De Amicis[1,2], Carmela Guido[1,2], Marta Santoro[1], Francesca Giordano[2], Ada Donà[1,2], Pietro Rizza[2], Michele Pellegrino[2], Ida Perrotta[3], Daniela Bonofiglio[1,2], Diego Sisci[1,2], Maria Luisa Panno[2], Donatella Tramontano[4], Saveria Aquila[1,2,*], Sebastiano Andò[1,2,*]

[1]Centro Sanitario, University of Calabria, Rende, Italy

[2]Department of Pharmacy, Health Science and Nutrition, University of Calabria, Rende, Italy

[3]DiBEST University of Calabria, Rende, Italy

[4]Department of Molecular Medicine and Medical Biotechnologies, University of Naples "Federico II", Naples, Italy

[*]Joint senior authors

Correspondence to: *Francesca De Amicis,* ***email:*** *francesca.deamicis@unical.it*
Sebastiano Andò, ***email:*** *sebastiano.ando@unical.it*

Keywords: *progesterone, Bcl-2, cell cycle arrest, pRb, p16*

Received: *February 03, 2016* ***Accepted:*** *July 09, 2016* ***Published:*** *July 23, 2016*

ABSTRACT

Loss of progesterone-receptors (PR) expression is associated with breast cancer progression. Herein we provide evidence that OHPg/PR-B through Beclin-1 evoke autophagy-senescence transition, in breast cancer cells. Specifically, OHPg increases Beclin-1 expression through a transcriptional mechanism due to the occupancy of Beclin-1 promoter by PR-B, together with the transcriptional coactivator SRC-2. This complex binds at a canonical half progesterone responsive element, which is fundamental for OHPg effects, as shown by site-directed mutagenesis. Beside, OHPg *via* non-genomic action rapidly activates JNK, which phosphorylates Bcl-2, producing the functional release from Beclin-1 interaction. This is not linked to an efficient autophagic flux, since p62 levels, marker of degradation *via* lysosomes, were not reduced after sustained OHPg stimulus. Instead, the cell cycle inhibitor p27 was induced, together with an irreversible G1 arrest, hallmark of cellular senescence. Specifically the increase of senescence-associated β-galactosidase activity was blocked by Bcl-2 siRNA but also by Beclin-1 siRNA. Collectively these findings support the importance of PR-B expression in breast cancer cells, thus targeting PR-B may be a useful strategy to provide additional approaches to existing therapies for breast cancer patients.

INTRODUCTION

Estrogen (ER) and Progesterone Receptors (PR) and their ligands, known factors involved in breast cancer initiation and progression, are able to determine a dynamic bio-molecular context correlated with breast tumor heterogeneity [1, 2]. This is the major problem which critically influences the response of patients to therapy [3].

Progesterone receptors action in mediating progesterone effects is highly context dependent and heavily influenced by post-translational modifications [4] as well as cofactor availability [5]. Several independent *in vitro* studies have demonstrated the inhibitory action of progesterone on breast cancer cell growth [6-8] and in agreement with these findings in a very recent paper we report that hydroxyprogesterone (OHPg), *via* PR-B isoform, leads to a reduced cell survival due to autophagy induction [9] through PTEN up-regulation.

Autophagy, is a genetically regulated mechanism responsible for the turnover of cellular proteins and

damaged organelles which exhibits a complex control, crucially depending on mTOR, through the switch of several signal pathways, such as LKB1/AMPK, MEM/ERK and PI3K/Akt [10]. The activation of the process can be oncogenic by contributing to tumor cell survival [11], besides the data from autophagy defective Beclin-1 knockout mice also suggest a tumor suppressive activity [12, 13].

Beclin-1, the master regulator, interacts with PI3KIII during autophagosomal membrane engulfing of damaged cytoplasmic organelles and long-lived proteins [14]. The function of Beclin-1 is, in part, defined by its interaction with the anti-apoptotic gene products, Bcl-2 and Bcl-xL [15]. The dissociation of Beclin-1 from Bcl-2 is critical for autophagy induction [16] and is regulated by many proteins and signal pathways. Specifically JNK1 or ERK1/2-mediated phosphorylation of Bcl-2 or DAPK-mediated phosphorylation of Beclin-1 [17-18].

Recent acquisitions suggest that autophagy may serve as a switch to shift the cell fate to senescence, providing a protective mechanism against the tumorigenic factors [13, 19-21]. Progestins activate nuclear PR-B leading to robust induction of cell cycle mediators of senescence in ovarian cancer cells [22].

Herein, in the aim of further explore OHPg/PR-B protective effects in breast cancer we investigate how PR-B prolonged activation, driving autophagy through Beclin-1, may influence cell cycle control by intercepting a signalling pathway responsible for autophagy-senescence transition.

RESULTS

OHPg increases Beclin-1 through a genomic mechanism

Beclin-1 is a component of the class IIIPI3 kinase complex which is required for autophagy activation by various stimuli [23, 24]. Stemming from our data indicating that 10 nM OHPg *via* PR-B [9] increases protein and mRNA levels of Beclin-1 in T47-D and MCF-7 cells (Figure 1A-1C), we next investigated the effects of OHPg/PR-B on Beclin-1 gene transcription. To this aim we performed transient transfection studies by using the 5' flanking region of Beclin-1 expression vector and two different deleted constructs (Figure 2A, *left panel*) [23]. 10 nM OHPg significantly increased the activity of the construct p(-644) in MCF-7 cells, as depicted in Figure 2A (*right panel)* and co-treatment with RU-486 (RU), a synthetic steroid with anti-progesterone receptor activity [25], counteracted this effect. None noticeable effect was observed in MCF-7 as well as in T47-D cells upon OHPg in the presence of p(-277) and p(-58) constructs, therefore the region between -644 bp to -277 bp holds important regulatory elements implicated in OHPg-mediated up-regulation of Beclin-1 promoter activity.

For instance, sequence analysis identified a canonical half progesterone responsive element (1/2PRE) located from -512 bp to -507 bp. To investigate the potential role of this specific site we performed site-directed mutagenesis and we changed 3 bp of the 1/2PRE to ensure that the altered binding site would not be recognizable by the PR. Transient transfections were performed in MCF-7 cells using multiple independent clones containing the desiderated mutation. We found that the activity of construct mut(-644) carrying the mutation in the 1/2PRE site, was unaffected by OHPg stimulus (Figure 2B). These results indicate that the 1/2PRE element is required for induction of Beclin-1 promoter activity by OHPg.

To prove PR-B specific involvement we used PR-negative MDA-MB-231 co-transfected with expression plasmids encoding either PR-B, PR-A or PR mutated in the DNA binding domain (mDBD) (Figure 2C). PR-B isoform expression itself was able to significantly increase the activity of Beclin-1 promoter which was further enhanced by OHPg treatment. Instead, ectopic expression of PR-A isoform or mDBD did not exert significant modulatory effects. Altogether, these data strongly indicate that PR-B *via* 1/2PRE represents a fundamental activator of Beclin-1 transcription by OHPg.

To investigate PR-B recruitment to the Beclin-1 gene promoter, we performed ChIP assays. MCF-7 cells were exposed for 6h to either control vehicle or 10 nM OHPg, after which chromatin was cross-linked with formaldehyde, and protein-DNA complexes were immunoprecipitated with antibodies directed against PR. The qPCR primers used encompass the 1/2PRE site we identified within the Beclin-1 promoter (Figure 3A). Results obtained after OHPg treatment demonstrate an enhanced recruitment of PR and RNA polymerase II to the Beclin-1 promoter and a reduction of HDAC1 indicating that the chromatin is in a more permissive environment for Beclin-1 gene transcription. Among the different PR coactivators previously described [26], some authors report that SRC-2 is critical for progesterone dependent function in breast morphogenesis [27]. We found that SRC-2 was present at the Beclin-1 promoter encompassing the half-PRE site, in a ligand-dependent manner, in contrast SRC-1 was absent (data not shown). All the above described effects were reversed by PR-B siRNA (Figure 3B). As a control, we did not see recruitment to an unrelated Beclin-1 promoter region located upstream of the 1/2PRE site (data not shown). Similar results were obtained in T47-D cells (Figure 3C).

Next to demonstrate that Beclin-1 levels determined by OHPg stimulus, could mediate autophagy initiation [9], we performed siRNA studies. Accordingly with our previous data, OHPg treatment induced the accumulation of autophagic vacuoles in MCF-7 cells after 24h (Figure 4C, 4D, 4E) compared with vehicle treated cells (Figure 4A, 4B) as monitored by transmission electron microscopy (TEM)

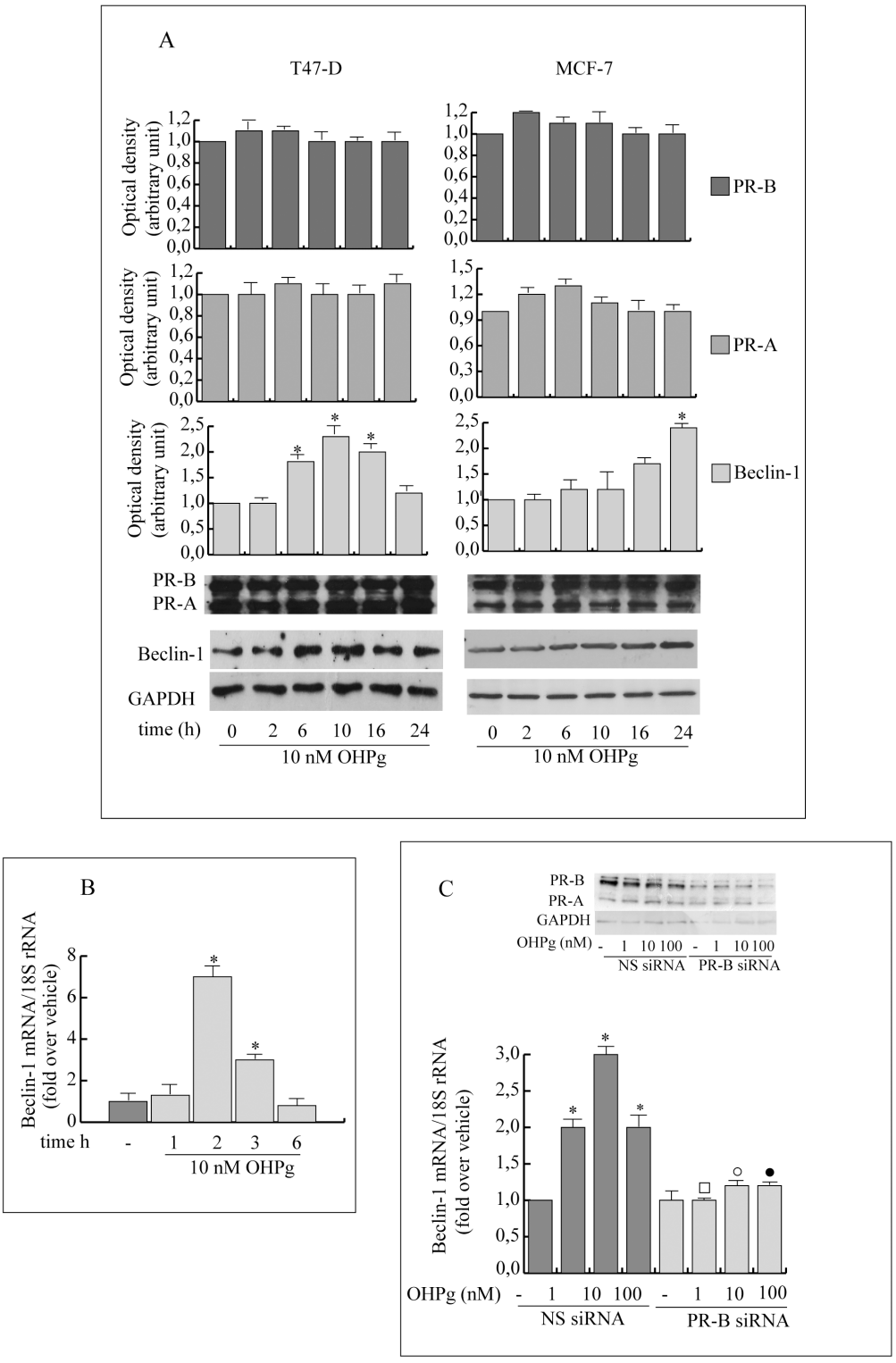

Figure 1: OHPg through PR-B up-regulates Beclin-1 protein and mRNA levels in breast cancer cells. A. Western blotting analysis of Beclin-1, PR-A and PR-B. T47-D and MCF-7 breast cancer cells treated with 10 nM OHPg at different times as indicated. GAPDH was used as loading control. Autoradiograph shows the results of one representative experiment out of three. **B.** Real-time PCR assay of Beclin-1 mRNA expression in T47-D cells treated at different times as indicated. **C.** Real-time PCR assay of Beclin-1 mRNA expression in MCF-7 cells transfected with non specific (NS)- or targeted against PR-B siRNA treated with vehicle (-) or OHPg for 24h as indicated. 18S rRNA was determined as control. Columns are the mean of three independent experiments each in triplicate; bars, SD; * $p \leq 0.05$ vs vehicle treated cells; ▪ $p \leq 0.05$ vs. 1 nM OHPg; ○ $p \leq 0.05$ vs. 10 nM OHPg ● $p \leq 0.05$ vs 100 nM OHPg. In the insert, Western blotting analysis of PR-B expression in MCF-7 cells in the same experimental conditions. GAPDH was used as loading control.

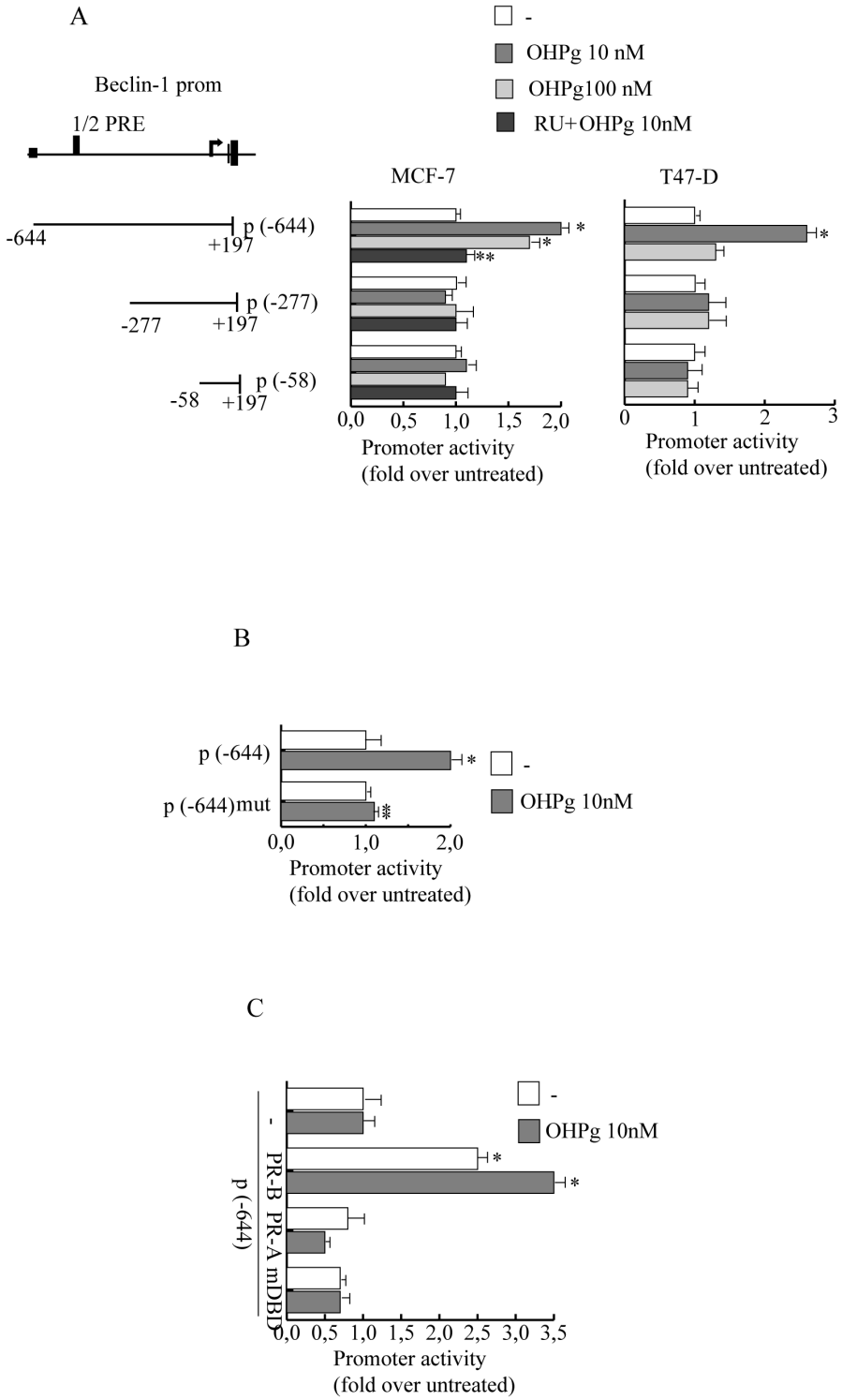

Figure 2: OHPg transactivates Beclin-1 promoter gene in breast cancer cells. A. left panel. Schematic representation of deletion fragments of the Beclin-1 gene promoter. Right panel. Constructs depicted were transiently transfected in MCF-7 and T47-D cells, treated with vehicle (−) or OHPg or 1μM RU 486 +10 nM OHPg as indicated. Columns are mean of three independent experiments and expressed as fold change over untreated, which was assumed to be 1; bars SD; * p ≤0.05 vs vehicle. ** p ≤0.05 vs OHPg 10 nM **B.** Site-directed mutagenesis of the 1/2PRE site. p(-644) and p(-644) mut promoter constructs were transfected into MCF-7 cells, and activity was assessed in the absence or presence of 10 nM OHPg. After 24 h, cells were harvested and luciferase activities were determined; bars SD; * p ≤0.05 vs vehicle. ** p ≤0.05 vs p(-644) 10 nM OHPg. **C.** MDA-MB231 cells were co-transfected with the Beclin-1 promoter construct p(-644) and PR-B or PR-A or mDBD expression vector, and then treated for 24 h with vehicle (-) or 10nM OHPg; bars, SD; * p ≤0.05 vs vehicle.

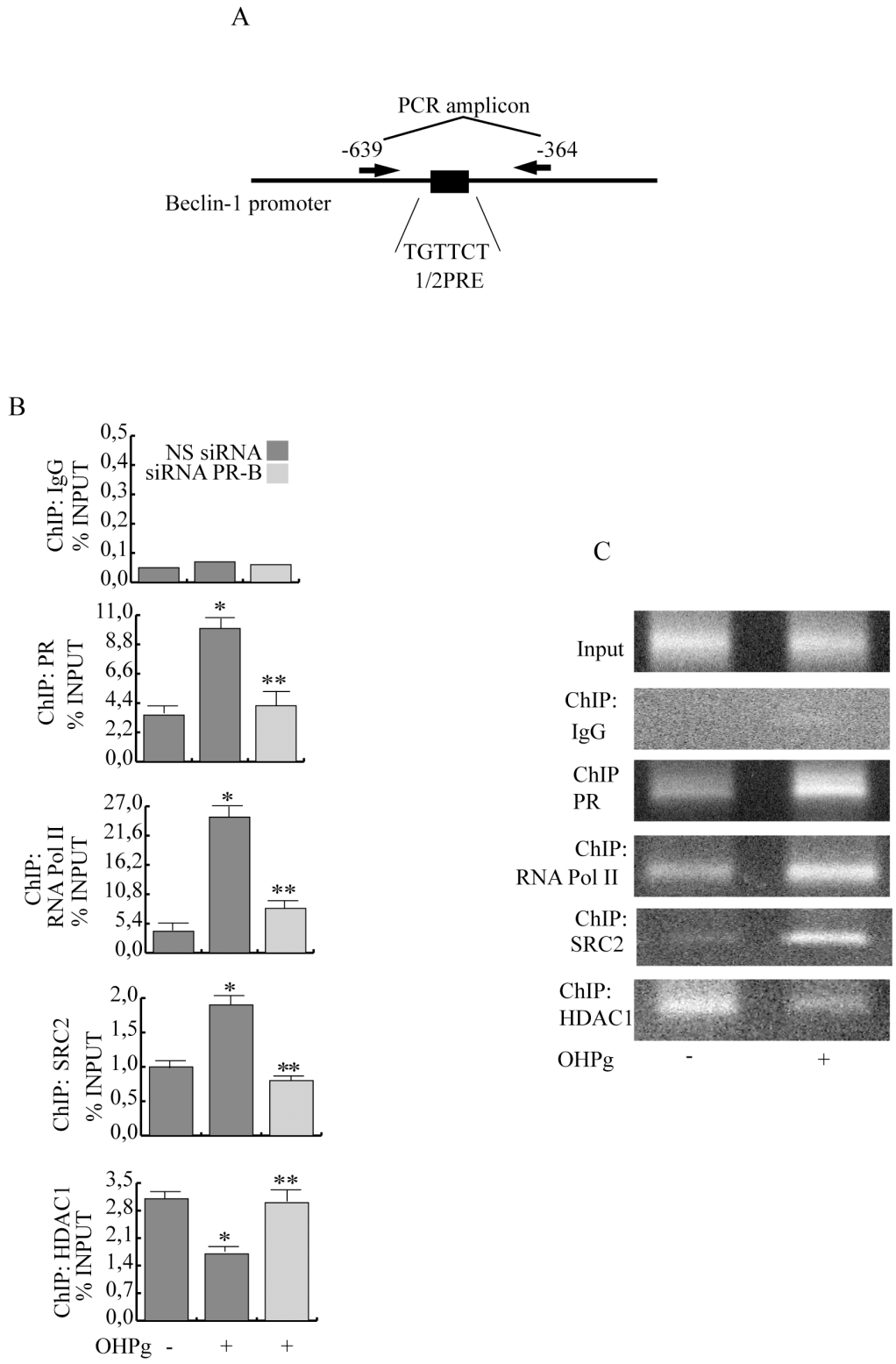

Figure 3: Ligand-activated PR-B binds the Beclin-1 gene promoter together with SRC-2 coactivator. A. Schematic representation of Beclin-1 promoter region containing the 1/2PRE site. **B.** ChIP-qPCR. MCF-7 cells transfected with non specific (NS) or targeted against PR-B siRNA treated with vehicle (−) or 10 nM OHPg. ChIP-qPCR was performed using primers as depicted in (A) and antibodies are used as indicated. IgG was used as control. Columns are the mean of three independent experiments. bars, SD; * $p \leq 0.05$ vs vehicle. ** $p \leq 0.05$ vs 10 nM OHPg. **C.** ChIP assay. T47-D treated with vehicle (−) or 10 nM OHPg. DNA Input, loading control. PCR was performed using primers as depicted in (A) antibodies are used as indicated. IgG was used as control. Images are representative of three independent experiments.

and the specific silencing of Beclin-1 greatly attenuated the effect produced by OHPg (Figure 4F, 4G, 4H).

OHPg reduces Beclin-1/Bcl-2 interaction through a JNK-mediated rapid and sustained phosphorylation of Bcl-2

Beclin-1 specific function in autophagy is inhibited by its interaction with Bcl-2 which dissociates once phosphorylated [17, 18]. Thus we investigated the effect of OHPg/PR-B on Beclin-1/Bcl-2 complex formation in T47-D and MCF-7 cells (Figure 5A, 5B). As shown by our IP studies, Bcl-2 associated with Beclin-1 in untreated cells. Worthy of note, this association decreased upon 24h of OHPg stimulation and specific silencing of PR-B abrogated this effect. IgG controls were performed (data not shown). Beside we observed that Bcl-2 was rapidly and sustained iper-phosphorylated after OHPg exposure in both cell types (Figure 5C).

C-jun N-terminal protein kinase (JNK) and the MAPK family members phosphorylate Bcl-2 at multiple sites [17, 28] thus we first evaluated whether JNK could be activated by OHPg (Figure 5D). A sustained increase of p-JNK was detected starting from 10' in treated cells

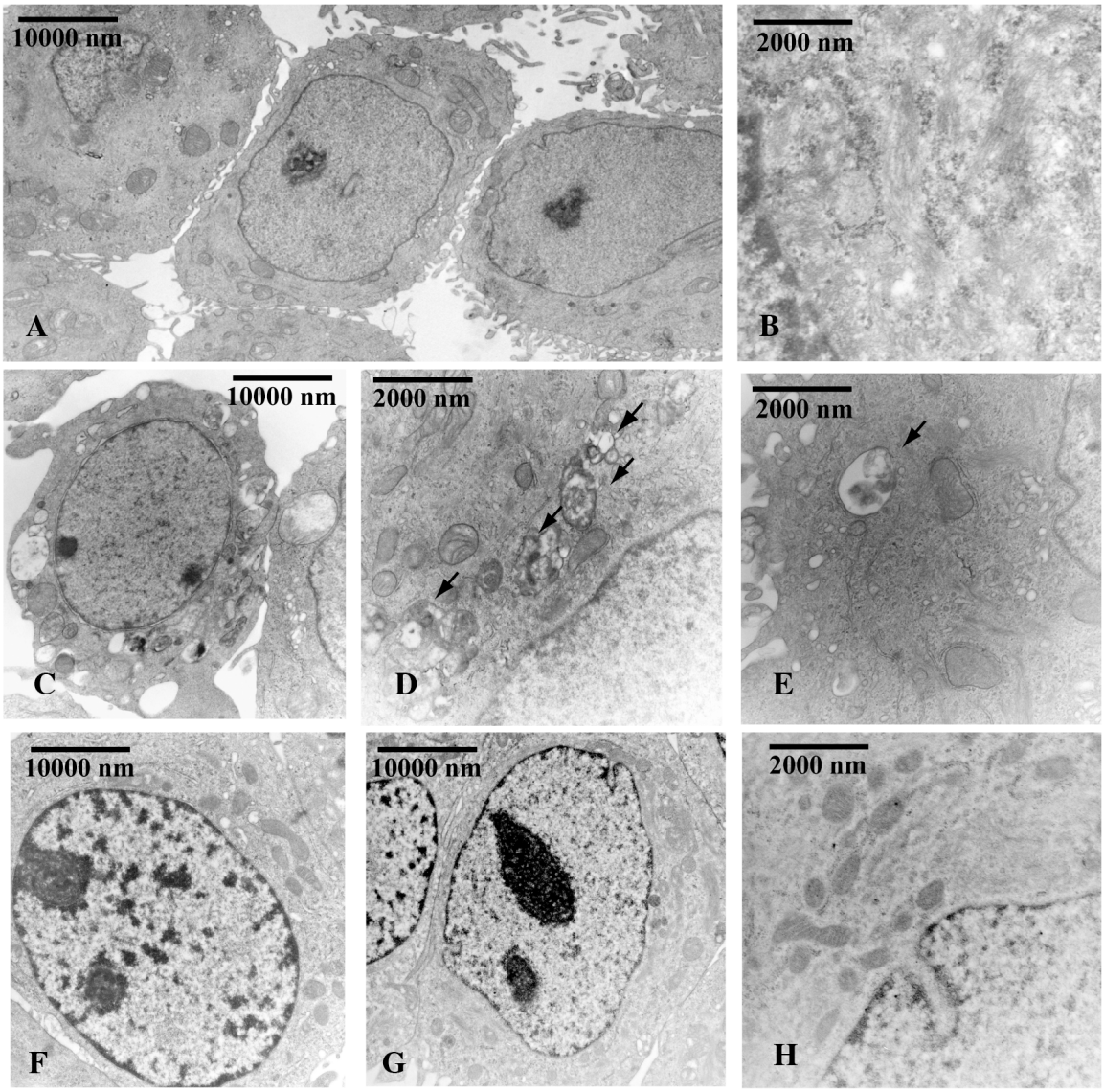

Figure 4: Beclin-1 is involved in OHPg induced autophagy in MCF-7 cells. TEM analysis was conducted in MCF-7 cells transfected with NS siRNA **A-E.** or with Beclin-1 siRNA **F-H.** treated with vehicle (-) A, B. or 10 nM OHPg C-H. for 24 h. Black arrows D, E. indicate the autophagic bodies. Figure shows the results of one representative out of three independent experiments. Images magnification: a 6300X, b 31500X, c 6300X, d 25000X, e 31500X, f 10000X, g 10000X, h 31500X.

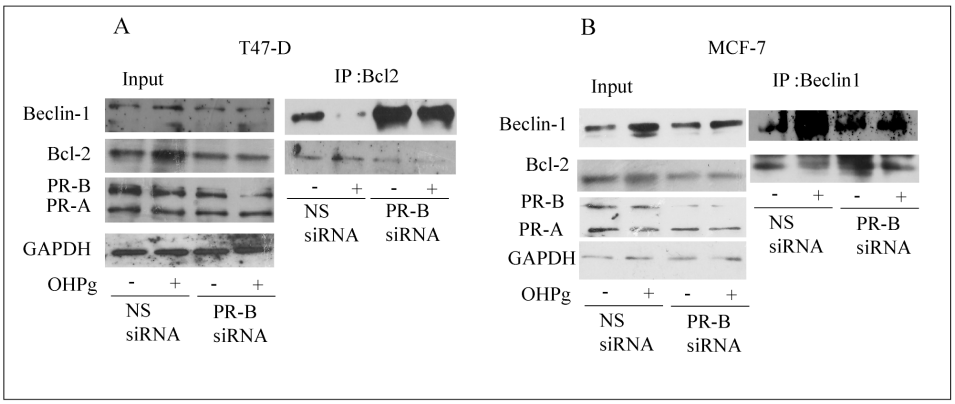

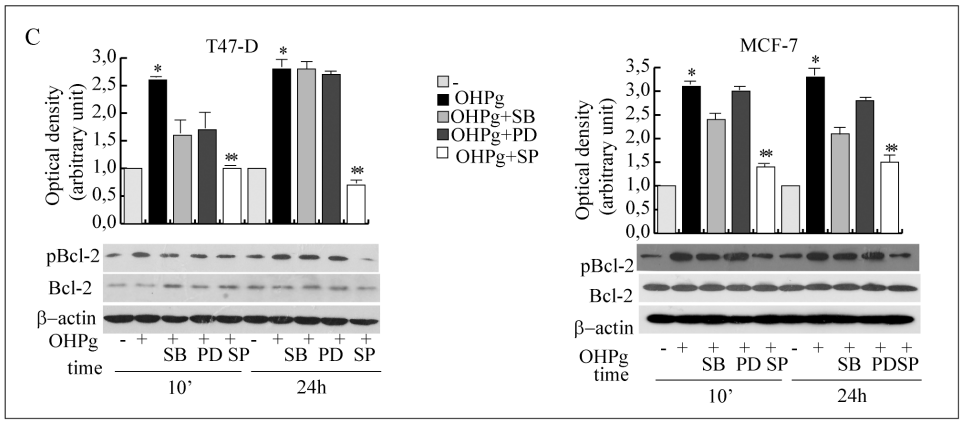

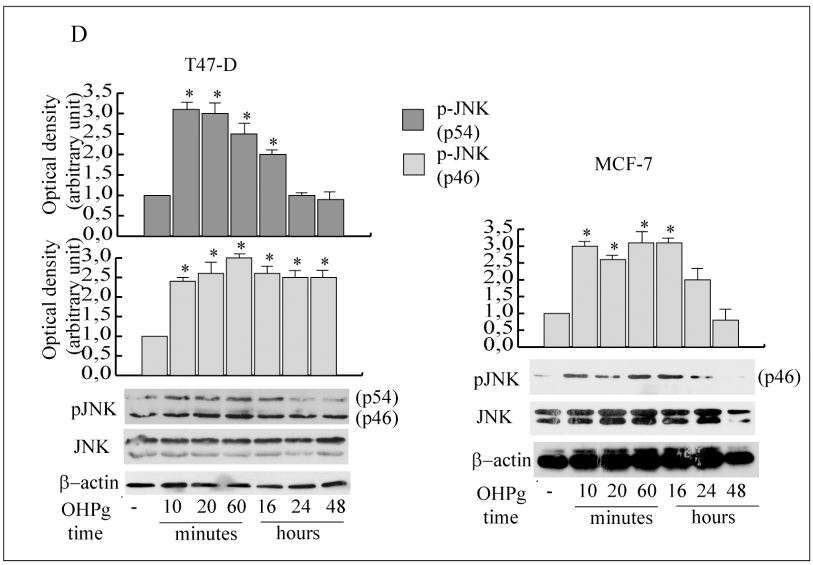

Figure 5: OHPg via JNK activation phosphorylates Bcl-2 and reduces Beclin-1/Bcl-2 interaction. A, B. Co-immunoprecipitation analysis. Total extracts from T47-D (A) and MCF-7 cells (B) transfected with non specific (NS) or targeted against PR-B siRNA treated with vehicle (-) or 10 nM OHPg for 24h, were used for input, or for immunoprecipitation by using specific anti-Bcl-2 or anti-Beclin-1 antibody as indicated. Filters were blotted with anti-Bcl-2 or Beclin-1 or PR or GAPDH antibody **C.** Western blotting analysis of p-Bcl-2 and Bcl-2. T47-D and MCF-7 cells were treated with 10 nM OHPg, 10 μM SB 203580, 1 μM PD 98059, 20 μM SP 600125 as indicated. B-actin was used as loading control. Autoradiographs show the results of one representative experiment out of three. Columns, are mean of three independent experiments in which band intensities were evaluated in terms of optical density arbitrary units and expressed as fold over vehicle, which was assumed to be 1; bars, SD. * $p \leq 0.05$ vs vehicle treated cells. ** $p \leq 0.05$ vs OHPg. **D.** Western blotting analysis of p-JNK/JNK. T47-D and MCF-7 cells were treated with 10 nM OHPg as indicated. B-actin was used as loading control. Autoradiographs show the results of one representative experiment. * $p \leq 0.05$ vs vehicle treated cells.

although total levels of JNK were equivalent, while p-p38 and p-MAPKs were weakly altered by OHPg (Supplementary Figure 1). Accordingly, pretreatment with 10 μM SB203580 (p38 inhibitor) or 1 μM PD98059 (MAPKs inhibitor) did not modified pBcl-2 levels, instead pretreatment with 20 μM SP600125 (JNK inhibitor) greatly counteracted the Bcl-2 phopshorylation induced by 24h of OHPg stimulation (Figure 5C) supporting the l role of JNK activation in the latter event.

Autophagy may represent: a) multistep pathway along which primarily long-lived proteins are degraded or b) a death-induced mechanism [12, 13, 19].

TUNEL assay results indicated that prolonged OHPg stimulus did not produce evidence of apoptosis (data not shown). Surprisingly, in the same experimental conditions we observed the accumulation of p62, a marker of degradation via the lysosomes [29] in T47-D as well as in MCF-7 cells (Figure 6A), suggesting a deficient autophagic clearance of damaged proteins.

OHPg/PR-B induce irreversible G1 arrest in breast cancer cells

Recent acquisitions sustain that the increase of impaired proteins may contribute to cellular senescence [30], described as an irreversible cell cycle arrest [31].

FACS analyses (Figure 6B) of T47-D cells show that after 72h of OHPg treatment an approximately 83% of cells accumulated in G1 phase as compared to ~69% of control, with a concomitant ~2-fold reduction of the population in the S-phase. The G1 arrest was persistent throughout 96h of OHPg treatment. To analyze whether the cell cycle block was reversible, OHPg was removed after 96h, by washing the cells and fresh medium was added for further 2 days. Percentage of T47-D cells in the G1/G0 phase of cell cycle remains unchanged (data not shown). Similar results were obtained in MCF-7 cells (Figure 6B).

Recent acquisitions suggest that cell cycle progression may be inhibited by Bcl-2 itself, *via* p27 KIP1 (p27) upregulation. [32, 33]. Accordingly, we observed an increase in the amount of p27 starting from 24h of OHPg treatment and sustained until 72h, in T47-D and MCF-7 cells (Figure 6A).

These effects were greatly counteracted in the presence of specific PR-B or Bcl-2 siRNA (Figure 6C) addressing the crucial role in the regulation of p27 levels.

OHPg/PR-B via Bcl-2 drive the transition from autophagy to senescence

The capability of OHPg/PR-B to promote the senescence process was demonstrated by the senescence-associated β-galactosidase (SAβGal) staining [34]. T47-D and MCF-7 cells exposed to 10 nM OHPg for 96h evidenced 40-60% SAβGal positivity relative to minimal SAβGal (10-15%) in vehicle-treated cells (Figure 7A, 7B). Worthy of note, specific silencing of PR-B, Beclin-1 or Bcl-2 greatly decreased the OHPg induced SAβGal positivity. This supports the idea that OHPg *via* PR-B/Bcl-2 axis drives breast cancer cellular senescence which follows an early autophagy mediated by Beclin-1.

Senescence is accompanied by a number of characteristic changes in gene expression [35]. Among these, the modulation of the p53/p21Cip1/Waf1 (p21) and p14ARF or p16Ink4a (p16) appears to be functionally relevant for the establishment and maintenance of the senescent state.

Protein content for p21 and p53 were scarcely influenced by OHPg treatment (Figure 7C) while, as expected, a dephosphorylation of Rb was evidenced especially after 48h of treatment, which was sustained until 96h in T47-D cells. In line with this, we observed the up-regulation of p16 mRNA levels starting from 48h until 96h (Figure 7D), while p14ARF remained unaltered by OHPg treatment. Similar results were obtained in MCF-7 cells (data not shown). These data indicate that the p16-pRb signaling is influenced by OHPg, suggesting this could be a pathway implicated by OHPg-mediated cellular senescence.

DISCUSSION

Autophagy is largely considered a catabolic process by which cellular components are recruited to lysosomes for their degradation. The insufficient remodeling of damaged proteins and organelles can led to the efficient transition to a senescent phenotype characterized by an irreversible growth arrest [31].

Actually there is an increasing evidence for autophagic inhibition of cancer cell survival by novel cancer drugs and the mechanisms involved in the different paradigms are very diverse and complex. A draft scenario of the key molecular targets involved is emerging and in this concern our recent acquisition underlines a functional interplay between OHPg/PR-B and PTEN stimulating autophagy initiation in breast cancer cells, further supporting a protective role of OHPg/PR-B in breast cancer [36]. Herein, we demonstrate for the first time that OHPg/PR-B induced autophagy drives to senescence in breast cancer cell models, as evidenced by several featuring markers.

We define the molecular mechanisms by which PR-B specific ligand OHPg determines autophagy initiation, through the up-regulation of the master regulator Beclin-1. OHPg action occurs at transcriptional level as demonstrated by functional studies. Interestingly, we identified the presence of a canonical 1/2PRE site, crucial for Beclin-1 promoter induction by OHPg. We evidenced that the binding of PR-B to the identified OHPg-responsive sequence favors the recruitment of the SRC-2 coactivator and RNA Pol II to the promoter.

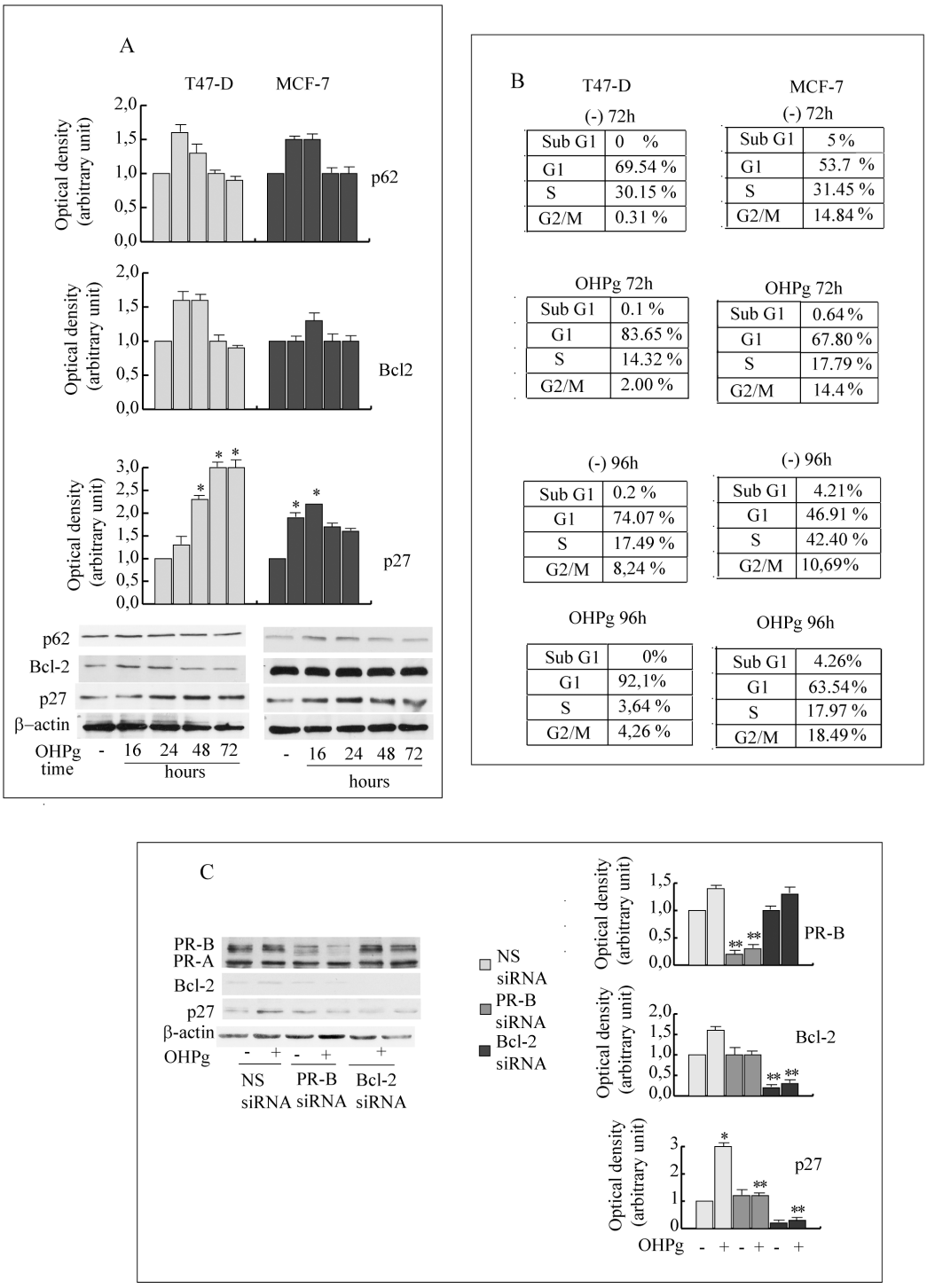

Figure 6: OHPg/PR-B induce irreversible G1 arrest in breast cancer cells. A. Western blot analysis of p62, Bcl-2 and p27 expression in T47-D and MCF-7 cells treated with 10 nM OHPg as indicated. β-actin was used as loading control. Autoradiographs show the results of one representative experiment. Columns, are mean of three independent experiments in which band intensities were evaluated in terms of optical density arbitrary units and expressed as fold over vehicle, which was assumed to be 1; bars, SD * $p \leq 0.05$ vs vehicle treated cells. **B.** FACS analysis. Cells were exposed to vehicle (-), 10 nM OHPgM as indicated. Data are representative of three independent experiments. **C.** Western blot analysis of PR-B, p27 and Bcl-2 expression in T47-D cells transfected with non specific (NS) or targeted against PR-B or Bcl-2 siRNA treated with vehicle (-) or 10 nM OHPg for 72h. Autoradiographs show the results of one representative experiment. Columns, are mean of three independent experiments in which band intensities were evaluated in terms of optical density arbitrary units and expressed as fold over vehicle, which was assumed to be 1; bars, SD * $p \leq 0.05$ vs vehicle treated cells. ** $p \leq 0.05$ vs NS siRNA.

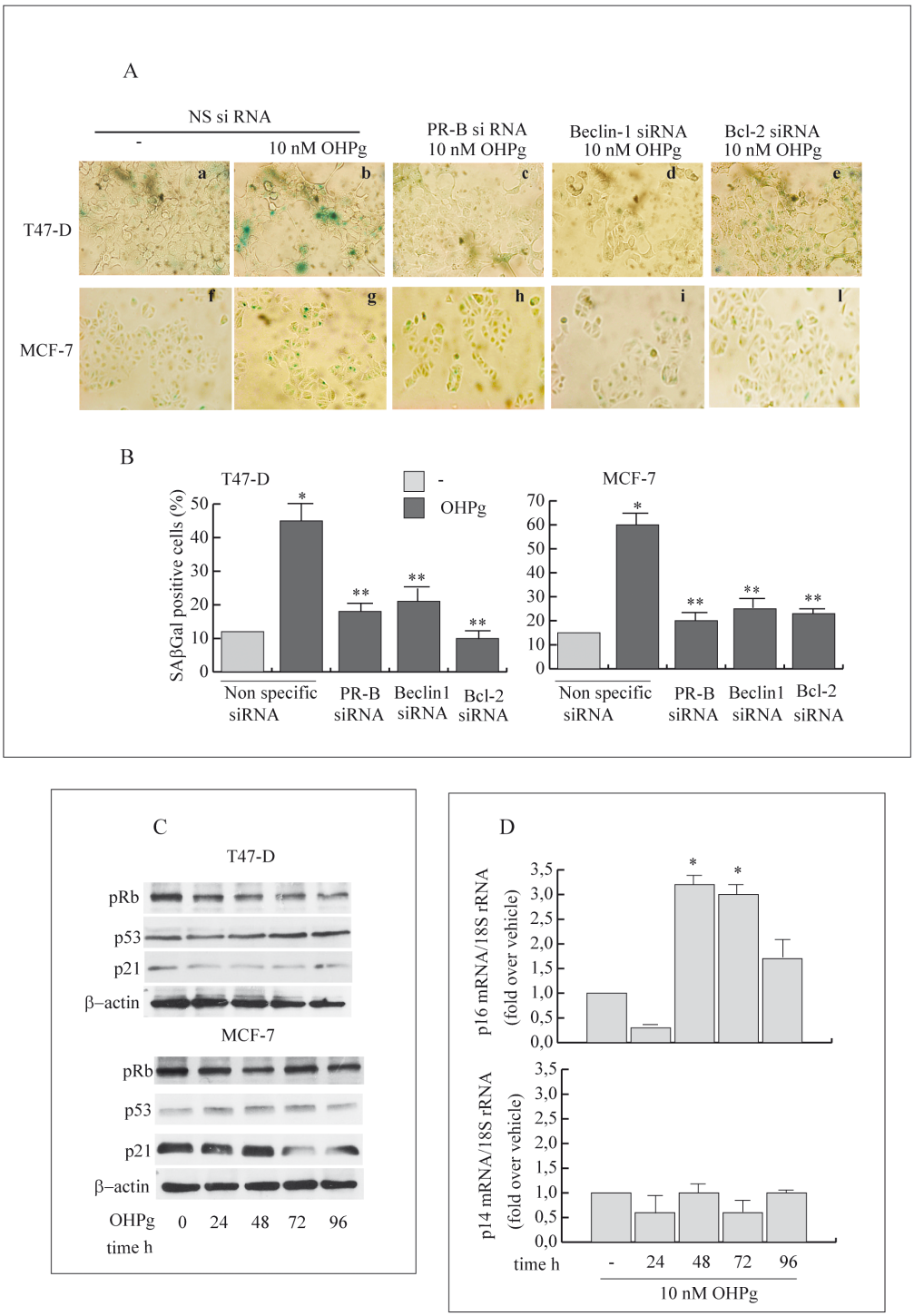

Figure 7: OHPg/PR-B induce cellular senescence and influence p16-pRb pathway in breast cancer cells. A. Representative staining for SAβGal activity of T47-D (A-E) and MCF-7 cells (F-L) transfected with non specific or targeted against PR-B, Beclin-1 or Bcl-2 siRNA treated with vehicle (-) or 10 nM OHPg for 96h. (magnification = 400×). Images are representative of three independent experiments. DAPI staining not shown **B.** Percentage of positive SAβGal cells was determined from quantitating three fields at 200× magnification. Values were normalized to total nuclei present in each field from DAPI staining *p ≤ 0.05 vs vehicle; ** p ≤0.05 vs NS siRNA 10 nM OHPg **C.** Western blot analysis of pRb, p53 and p21 expression in T47-D and MCF-7 cells treated with 10 nM OHPg as indicated. β actin was used as loading control. Autoradiographs show the results of one representative experiment out of three. **D.** Real-time PCR assay of p16 and p14 mRNA expression. T47-D cells were treated with vehicle (-) or 10 nM OHPg as indicated. 18S rRNA was determined as control. Columns are the mean of three independent experiments each in triplicate; bars, SD; * p ≤0.05 vs vehicle treated cells.

Beclin-1 induces autophagy by participating both in the biogenesis and degradation of autophagosomes *via* its interaction with different molecular complexes. Among Beclin-1-binding proteins, Bcl-2 is an important inhibitor for autophagy [31, 33]. The dissociation of Beclin-1 from Bcl-2 is regulated by many proteins and signal pathways and is necessary for autophagy induction.

An important finding in this paper is the significant increase of the functional Beclin-1 amount, resulting from the cooperation of two separate mechanisms stimulated by OHPg/PR-B : a) the increase of Beclin-1 expression b) the release of Beclin-1 from the inhibitory Bcl-2 interaction. The latter event is due to Bcl-2 phosphorylation, crucially determined by rapid and sustained JNK activation, thus enhancing the extent of Beclin-1 useful for autophagosomes assembly.

From our studies it emerges that the functional release of Beclin-1 from Bcl-2 however did not produce the efficient autophagic flux. Indeed p62 levels were not substantially reduced after OHPg stimulus [29, 37, 38]. We retain that the impaired autophagy could facilitate the irreversible growth arrest of breast cancer cells, induced by Bcl-2 *via* p27. Thus, the functional release of Bcl-2 from Beclin-1 interaction may represent the molecular bridge connecting autophagy to an irreversible G1 arrest, thus determining breast cancer cell fate decision.

For instance together with its well-established function in governing cell survival [39], Bcl-2 has been found to influence the cell cycle [32, 40]. Elevated Bcl-2 levels are associated with decreased proliferation and sometimes also a favorable prognosis in diverse malignancies, including breast [41]. Bcl-2 can both accelerate withdrawal from the cycle [42] and retard reentry [43] by increasing p27 [33] which inhibits G1-S progression [44]. Our study shows that OHPg/PR-B *via* Bcl-2 determine the induction of p27 and the cellular senescent phenotype. It is worth to mention that the specific silencing of Bcl-2 and PR-B reverse the effects produced by OHPg on p27 expression as well as the staining for SAβGal activity, marker of cellular senescence.

Thus, the most convincing interpretation of our results is that OHPg, by enhancing the levels of functional Beclin-1, causes the establishment of an early but incomplete autophagic process, linked to the release of Bcl-2 causing the induction of p27, which in turn leads to the irreversible inhibition of cell cycle progression (Figure 8). Indeed Beclin-1 depletion, which greatly attenuated the activation of autophagy by OHP as evidenced by TEM, also counteracted the establishment of senescence features. In other words the present paper highlights how OHPg triggering autophagy as early event, may create the susceptibility to cellular senescence.

In summary, we have demonstrated a significant role for OHPg/PR-B for Beclin-1 induction and function beginning from the autophagy initiation in breast cancer cells. Our findings thus indicate that an important tumor-suppressive pathway through Beclin-1 is target of OHPg *via* its own receptor, actually proposing a distinctive protecting action against breast cancer. Future studies may lead to additional strategies for the current therapy of breast cancer patients.

MATERIALS AND METHODS

Reagents

17-Hydroxyprogesterone (OHPg), aprotinin, leupeptin, phenylmethylsulfonyl fluoride (PMFS), sodium orthovanadate, NaCl, MgCl2, EGTA, glycerol,

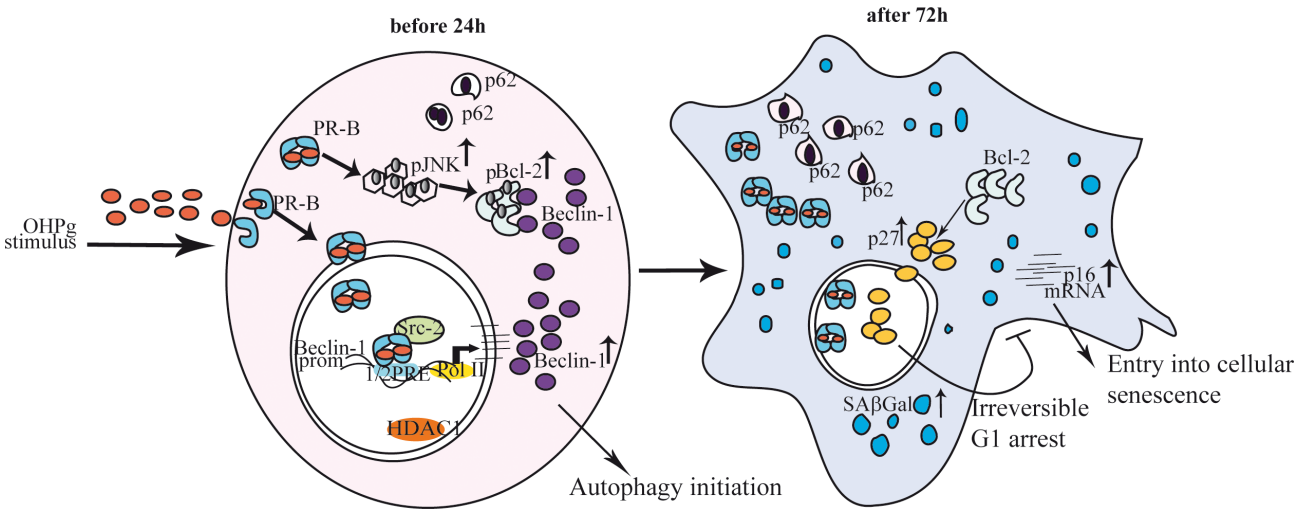

Figure 8: Proposed model for OHPg/PR-B-induced autophagy-senescence transition in ER+ breast cancer cells. See text for details.

Triton X-100, Fetal Calf Serum (FCS), Fetal bovine serum (FBS), HEPES were from Sigma-Aldrich (Milan-Italy). Antibodies against human PR, β-actin, p27, Bcl-2, p21, p53, RNA Pol II, SRC-2, p-JNK, p-MAPK (ERK1, ERK2), JNK, MAPKs (ERK1, ERK2) and Protein A/G PLUS-Agarose were from Santa Cruz Biotechnology (Santa Cruz, CA). Antibodies to p-p38, p-38, p62, p-pRb and Beclin-1 were from Cell Signaling (Beverly, MA). RU 486, SB203580, PD98059, SP600125 were from Calbiochem.

Plasmids

The firefly luciferase reporter plasmid containing the full-length of the Beclin1 promoter region [p-644 (-644/+197)] and the different deletion constructs [p-277 (-277/+197), p-58 (-58/+197)] gifts from Dr. Mujun Zhao (Institute of Biochem & Cell Biology, Chinese Academy of Sciences, China) [21]. The full-length PR-B consisting of the full-length PR-B cDNA fused with the SV40 early promoter and expressed in the pSG5 vector gift from Dr. D. Picard, (University of Geneva, Switzerland); the full length PR-A provided by Prof. Paul Kastener (Laboratary of Moleculare Genetic, CNRS, Strasbourg, France) [45]. PR DNA-binding mutant C587A (mDBD PR) was provided by Dr. C. Lange (University of Minnesota Cancer Center, Minneapolis, MN) [46] The Renilla luciferase expression vector pRL-TK (Promega) was used as a transfection standard.

Cell culture

T47-D, MCF-7 and MDA-MB-231 human breast cancer cells were obtained from the American Type Culture Collection (ATCC). MCF-7 were maintained in DMEM/F-12 medium containing 5% FCS, 1% L-glutamine, 1% Eagle's nonessential amino acids, and 1 mg/ml penicillin/streptomycin in a 5% CO2 humidified atmosphere. T47-D cells were routinely maintained in RPMI 1640 supplemented with 5% FCS, 1μg/ml insulin (Sigma, Milan, Italy), 1 mg/ml penicillin/streptomycin (Sigma, Milan, Italy). MDA-MB-231 were maintained in DMEM/F-12 medium containing 5% FBS. Hormone stimulation was performed in medium containing 5% charcoal-treated FCS to reduce the endogenous steroid concentration [47].

Transmission electron microscopy (TEM)

Transmission Electron Microscopy was conducted as previously described [9]. Briefly, cells treated as indicated were fixed in 3% glutaraldehyde (Sigma-Aldrich, Milan-Italy) solution in 0.1 M phosphate buffer (pH. 7.4) for 2h. Then the samples were post-fixed in osmium tetroxide (3%), dehydrated in graded acetone, and embedded in Araldite (Sigma-Aldrich, Milan-Italy). Ultrathin sections were collected on copper grids and contrasted using both lead citrate and uranyl acetate. The grids were examined in a "Zeiss EM 10" electron microscope.

Total RNA extraction, reverse transcription polymerase PCR and real-time RT-PCR assay

Total RNA was extracted from T47D and MCF-7 cells using TRIzol reagent and cDNA was synthesized by reverse transcription-polymerase chain reaction (PCR) method using a RETROscript kit. The expression of selected genes was quantified by real-time PCR using iCycler iQ Detection System (Bio-Rad, Hercules, CA).

Five microliters of diluted (1:4) cDNA was analyzed using SYBR Green Universal PCR Master Mix, following the manufacturer's recommendations. The primers all from Invitrogen were: 5'-CCTGGAGGCGGCGAGAAC-3' (p14 forward), 5'-CAGCACGAGGGCCACAGC-3' (p14 reverse), 5'-CTTGCCTGGAAAGATACCG-3' (p16 forward), 5'-CCCTCCTCTTTCTTCCTCC-3' (p16 reverse),. (Beclin-1 forward) 5'-AGCTGCCGTTATACTGTTCTG-3'; (Beclin-1 reverse) 5'-ACTGCCTCCTGTGTCTTCAATCTT-3' [48]. PCRs were performed in the iCycler iQ Detection System (Bio-Rad), using 0.1μM each primer in a total volume of 30 μL of reaction mixture following the manufacturer's recommendations. Each sample was normalized on the basis of its 18S ribosomal RNA content. The 18S quantification was performed using a TaqMan Ribosomal RNA Reagent kit (Applied Biosystems) following the method provided in the TaqMan Ribosomal RNA Control Reagent kit. The relative gene expression levels were normalized to a calibrator that was chosen to be the basal, untreated sample. Final results were expressed as n-fold differences in gene expression relative to 18S ribosomal RNA and calibrator, calculated following the ΔΔThreshold cycle (Ct) method, as published previously [49]. Assays were performed in triplicate.

Western blotting and immunoprecipitation

Cells were grown in 10 cm dishes exposed to treatments for different times as indicated and lysed. Total extracts were prepared and subjected to SDS-PAGE as previously described [50].

For Immunoprecipitation, 500 μg of protein lysates were incubated overnight with the specific antibody and 500 μL of HNTG buffer [50 mmol/L HEPES (pH 7.4), 50 mmol/L NaCl, 0.1% Triton X-100, 10% glycerol, 1 mmol/L phenylmethylsulfonyl fluoride, 10 Ag/mL leupeptin, 10 Ag/mL aprotinin]. Immunocomplexes were recovered by incubation with protein A/G-agarose. The beads containing bound proteins were washed by centrifugation in immunoprecipitation buffer, then

denatured by boiling in Laemmli sample buffer and analyzed by Western blot. The images were acquired by using an Epson Perfection scanner (Epson, Japan) using Photoshop software (Adobe). The optical densities of the spots were analyzed by using ImageJ software (NIH; http://rsb.info.nih.gov/IJ).

Transfections and luciferase assays

Transfections were done as described [51] using Fugene 6 reagent (Roche Diagnostics, Milan, Italy). Luciferase activity was measured with the Dual Luciferase kit (Promega, Milan, Italy).

Site-directed mutagenesis

Mutagenesis was performed on pGL3-644 of the Beclin-1 promoter by PCR. The sequence for the sense primer was:

5′-ATATAGATCTCCTTTTGTTGTTGCTGTT GT*TACCCT*GAGATGGAGCCTTGCCCTGT-3′. The amplified DNA fragment was digested and ligated into pGL3-basic vector. Mutation was confirmed by DNA sequencing.

Lipid-mediated transfection of siRNA duplexes

Cells were transfected with 4 functionally verified siRNA directed against human PR-B, Beclin1 or Bcl-2 or with a control siRNA (Qiagen, Mi, Italy) that does not match with any human mRNA used as a control for non-sequence specific effects. Cells were transfected using Lipofectamine 2000 reagent (Invitrogen, Paisley, UK) and then treated as indicated.

Chromatin immunoprecipitation (ChIP) assays and realtime ChIP

Cells were treated as indicated before harvesting for the assay performed as described [52].

The immuno-cleared chromatin was precipitated with antibodies as indicated. Immunoprecipitated DNA was analyzed in triplicates by real-time PCR by using 5 µl of the diluted (1 : 3) template DNA or PCR. The following primers, corresponding to the region between -629 bp to -514 bp, used for PCR: forward 5' ATTTTGGCCAGGCTGGTCT 3' and reverse 5' GCACGCCTATAATCCCAGCT 3' were used (Invitrogen, Paisley, UK). Real-time PCR data were normalized with respect to unprocessed lysates (input DNA). Inputs DNA quantification was performed by using 5 µl of the diluted (1/50) template DNA. The relative antibody bound fractions were normalized to a calibrator that was chosen to be the basal, untreated sample. Final results were expressed as percent to the relative inputs as previously described [53].

Flow cytometry

T47-D and MCF-7 cells, treated with OHPg 10 nM for different times as indicated were collected for cell cycle analysis. Cells were washed with PBS and fixed for 1h in ice-cold 70% ethanol. The samples were then washed once with PBS and suspended in 1ml of staining solution (10 mg/ml RNasi A, 10 mg/ml propidium iodide in PBS) and then incubated at room temperature in the dark for at least 30 min. FACS analysis was performed using ModFit LT software (Becton Dickinson, NJ). At least $2x10^4$ cells/sample were measured.

Senescence associated-β-galactosidase (SAβGal) activity assays

T47-D and MCF-7 cells were continuously treated in the presence or absence of 10 nM OHPg for 96h. Cells were washed, fixed and stained for SAβGal activity according to manufacturer's instructions using the Senescence β-Galactosidase Staining Kit (Cell Signaling Technology, #9860).

Statistical analysis

Data were analyzed by Student's t test using the GraphPad Prism 4 software program. and results were presented as mean ± SD. A value of $P \leq 0.05$ was considered to be significant.

CONFLICTS OF INTEREST

Authors declare that they have no competing financial interests in relation to the work.

GRANT SUPPORT

This work was supported by Ministero Istruzione Università e Ricerca (ex60% 2014), Associazione Italiana Ricerca sul Cancro (AIRC) (grant number IG11595 and IG15738).

REFERENCES

1. Siegel R, Naishadham D, Jemal A. Cancer statistics. CA Cancer J Clin. 2012; 62: 10–29. doi: 10.3322/caac.20138.
2. Skibinski A, Kuperwasser C. The origin of breast tumor heterogeneity. Oncogene. 2015; 34: 5309-16. doi: 10.1038/onc.2014.475.
3. Kim HJ, Cui X, Hilsenbeck SG, Lee AV. Progesterone receptor loss correlates with human epidermal growth factor receptor 2 overexpression in estrogen receptor-positive breast cancer. Clin Cancer Res. 2006; 12: 1013s–1018s.
4. Knutson TP, Daniel AR, Fan D, Silverstein KA, Covington KR, Fuqua SA, Lange CA. Phosphorylated

and sumoylation-deficient progesterone receptors drive proliferative gene signatures during breast cancer progression. Breast Cancer Res. 2012; 14: R95.

5. Scarpin KM, Graham JD, Mote PA, Clarke CL. Progesterone action in human tissues: regulation by progesterone receptor (PR) isoform expression, nuclear positioning and coregulator expression. Nucl Recept Signal. 2009; 31: 7:e009. doi: 10.1621/nrs.07009.
6. Wiebe JP, Rivas MA, Mercogliano MF, Elizalde PV, Schillaci R. Progesterone-induced stimulation of mammary tumorigenesis is due to the progesterone metabolite, 5α-dihydroprogesterone (5αP) and can be suppressed by the 5α-reductase inhibitor, finasteride. J Steroid Biochem Mol Biol. 2015; 149: 27-34. doi: 10.1016/j.jsbmb.2015.01.004.
7. Montazeri H, Bouzari S, Azadmanesh K, Ostad SN, Ghahremani MH. Divergent behavior of cyclin E and its low molecular weight isoforms to progesterone-induced growth inhibition in MCF-7 cells. Adv Biomed Res. 2015; 6: 4-16. doi: 10.4103/2277-9175.148299.
8. De Amicis F, Zupo S, Panno ML, Malivindi R, Giordano F, Barone I, Mauro L, Fuqua SA, Andò S. Progesterone receptor B recruits a repressor complex to a half-PRE site of the estrogen receptor alpha gene promoter. Mol Endocrinol. 2009; 23: 454-65. doi: 10.1210/me.2008-0267.
9. De Amicis F, Guido C, Santoro M, Lanzino M, Panza S, Avena P, Panno ML, Perrotta I, Aquila S, Andò S. A novel functional interplay between Progesterone Receptor-B and PTEN, via AKT, modulates autophagy in breast cancer cells. J Cell Mol Med. 2014; 18: 2252-65. doi: 10.1111/jcmm.12363.
10. Maycotte P, Thorburn A. Targeting autophagy in breast cancer. World J Clin Oncol. 2014; 10: 224-40. doi: 10.5306/wjco.v5.i3.224.
11. Kondo Y, Kanzawa T, Sawaya R, Kondo S. The role of autophagy in cancer development and response to therapy. Nature Reviews Cancer. 2005; 5: 726-734.
12. Gozuacik D, Kimchi A. Autophagy as a cell death and tumor suppressor mechanism. Oncogene. 2004; 23: 2891–2906.
13. Narita M, Young AR, Narita M. Autophagy facilitates oncogene-induced senescence. Autophagy. 2009; 5: 1046-1047.
14. Aguilera MO, Berón W, Colombo MI. The actin cytoskeleton participates in the early events of autophagosome formation upon starvation induced autophagy. Autophagy. 2012; 8: 1590-603. doi: 10.4161/auto.21459.
15. Dai JP, Zhao XF, Zeng J, Wan QY, Yang JC, Li WZ, Chen XX, Wang GF, Li KS. Drug screening for autophagy inhibitors based on the dissociation of Beclin1-Bcl2 complex using BiFC technique and mechanism of eugenol on anti-influenza A virus activity. PLoS One. 2013; 8: e61026. doi: 10.1371/journal.pone.0061026.
16. Oh S, Xiaofei E, Ni D, Pirooz SD, Lee JY, Lee D, Zhao Z, Lee S, Lee H, Ku B, Kowalik T, Martin SE, Oh BH, Jung JU, Liang C. Downregulation of autophagy by Bcl-2 promotes MCF7 breast cancer cell growth independent of its inhibition of apoptosis. Cell Death Differ. 2011; 18: 452-64. doi: 10.1038/cdd.2010.116.
17. Bassik MC1, Scorrano L, Oakes SA, Pozzan T, Korsmeyer SJ. Phosphorylation of BCL-2 regulates ER Ca2+ homeostasis and apoptosis. EMBO J. 2004; 23: 1207-16.
18. Maundrell K, Antonsson B, Magnenat E, Camps M, Muda M, Chabert C, Gillieron C, Boschert U, Vial-Knecht E, Martinou JC, Arkinstall S. Bcl-2 undergoes phosphorylation by c-Jun N-terminal kinase/stress-activated protein kinases in the presence of the constitutively active GTP-binding protein Rac1. J Biol Chem. 1997; 272: 25238-42.
19. Young AR, Narita M, Ferreira M, Kirschner K, Sadaie M, Darot JF, Tavaré S, Arakawa S, Shimizu S, Watt FM, Narita M. Autophagy mediates the mitotic senescence transition. Genes Dev. 2009; 23: 798-803. doi: 10.1101/gad.519709.
20. Huang YH, Yang PM, Chuah QY, Lee YJ, Hsieh YF, Peng CW, Chiu SJ. Autophagy promotes radiation-induced senescence but inhibits bystander effects in human breast cancer cells. Autophagy. 2014; 10: 1212-28. doi: 10.4161/auto.28772.
21. Dong Y, Yin S, Jiang C, Luo X, Guo X, Zhao C, Fan L, Meng Y, Lu J, Song X, Zhang X, Chen N, Hu H. Involvement of autophagy induction in penta-1,2,3,4,6-O-galloyl-β-D-glucose-induced senescence-like growth arrest in human cancer cells. Autophagy. 2014; 10: 296-310. doi: 10.4161/auto.27210.
22. Diep CH, Charles NJ, Gilks CB, Kalloger SE, Argenta PA, Lange CA. Progesterone receptors induce FOXO1-dependent senescence in ovarian cancer cells. Cell Cycle. 2013; 12: 1433-49. doi: 10.4161/cc.24550.
23. Tang H, Da L, Mao Y, Li Y, Li D, Xu Z, Li F, Wang Y, Tiollais P, Li T, Zhao M. Hepatitis B virus X protein sensitizes cells to starvation-induced autophagy via up-regulation of beclin 1 expression. Hepatology. 2009; 49: 60-71. doi: 10.1002/hep.22581.
24. Kihara A, Kabeya.Y, Ohsumi Y, Yoshimori T. Beclin–phosphatidylinositol3-kinase complex functions at the trans-Golgi network. EMBO Rep. 2001; 2: 330–335.
25. Shortle B, Dyrenfurth I, Ferin M. Effects of an antiprogesterone agent, RU-486, on the menstrual cycle of the rhesus monkey. J Clin Endocrinol Metab. 1985; 60: 731-5.
26. Johnson AB, O'Malley BW. Steroid receptor coactivators 1, 2, and 3: critical regulators of nuclear receptor activity and steroid receptor modulator (SRM)-based cancer therapy. Mol Cell Endocrinol. 2012; 348: 430-9. doi: 10.1016/j.mce.2011.04.021.
27. Mukherjee A, Soyal SM, Fernandez-Valdivia R, Gehin M, Chambon P, Demayo FJ, Lydon JP, O'Malley BW. Steroid receptor coactivator 2 is critical for progesterone-dependent uterine function and mammary morphogenesis in the mouse. Mol Cell Biol. 2006; 26: 6571-83.

28. De Chiara G, Marcocci ME, Torcia M, Lucibello M, Rosini P, Bonini P, Higashimoto Y, Damonte G, Armirotti A, Amodei S, Palamara AT, Russo T, Garaci E, Cozzolino F. Bcl-2 Phosphorylation by p38 MAPK: identifyication of target sites and biologic consequences. J Biol Chem. 2006; 281: 21353-61.
29. Jiang P, Mizushima N. LC3- and p62-based biochemical methods for the analysis of autophagy progression in mammalian cells. Methods. 2015; 75: 13-8. doi: 10.1016/j.ymeth.2014.11.021.
30. White E, Lowe SW. Eating to exit: autophagy-enabled senescence revealed. Genes Dev. 2009; 23: 784-7. doi: 10.1101/gad.1795309.
31. Blagosklonny MV. Geroconversion: irreversible step to cellular senescence. Cell Cycle. 2014; 13: 3628-35. doi: 10.4161/15384101.2014.985507.
32. Huang DC, O'Reilly LA, Strasser A, Cory S. The anti-apoptosis function of Bcl-2 can be genetically separated from its inhibitory effect on cell cycle entry. EMBO J. 1997; 16: 4628-38.
33. Vairo G, Soos TJ, Upton TM, Zalvide J, DeCaprio JA, Ewen ME, Koff A, Adams JM. Bcl-2 retards cell cycle entry through p27(Kip1), pRB relative p130, and altered E2F regulation. Mol Cell Biol. 2000; 20: 4745-53.
34. Dimri GP, Lee X, Basile G, Acosta M, Scott G, Roskelley C, Medrano E E, Linskens M, Rubelj I, Pereira-Smith O. A biomarker that identifies senescent human cells in culture and in aging skin in vivo. Proc Natl Acad Sci USA. 1995; 92: 9363–7.
35. J. Campisi. Senescent cells, tumor suppression, and organismal aging: good citizens, bad neighbors. Cell. 2005; 120: 513–522.
36. Shyamala G, Yang X, Cardiff RD, Dale E. Impact of progesterone receptor on cell-fate decisions during mammary gland development. Proc Natl Acad Sci USA. 2000; 97: 3044–3049.
37. Karantza-Wadsworth V, Patel S, Kravchuk O, Chen G, Mathew R, Jin S, White E. Autophagy mitigates metabolic stress and genome damage in mammary tumorigenesis. Genes Dev. 2007; 21: 1621–1635.
38. Mathew R, Karp CM, Beaudoin B, Vuong N, Chen G, Chen HY Bray K, Reddy A, Bhanot G, Gelinas C, Dipaola RS, Karantza-Wadsworth V, White E. Autophagy suppresses tumorigenesis through elimination of p62. Cell. 2009; 137: 1062–1075.
39. Adams J M, Cory S. The Bcl-2 protein family: arbiters of cell survival. Science. 1998; 281: 1322–1326.
40. Aster JC. Longtine JA. Detection of BCL2 Rearrangements in Follicular Lymphoma. Am J Pathol. 2002; 160: 759–763.
41. Knowlton K, Mancini M, Creason S, Morales C, Hockenbery D, Anderson B O. Bcl-2 slows in vitro breast cancer growth despite its antiapoptotic effect. J Surg Res. 1998; 76: 22–26.
42. Vairo G, Innes K M, Adams J M. Bcl-2 has a cell cycle inhibitory function separable from its enhancement of cell survival. Oncogene. 1996; 13: 1511–1519.
43. O'Reilly LA, Huang DC, Strasser A. The cell death inhibitor Bcl-2 and its homologues influence control of cell cycle entry. EMBO J. 1996; 15: 6979-90.
44. Slingerland J. p27 Regulation by Estrogen and Src Signaling in Human Breast Cancer. Hormonal Control of Cell Cycle. 2008, 89-97.
45. Kastner P, Krust A, Turcotte B, Stropp U, Tora L, Gronemeyer H, Chambon P. Two distinct estrogen-regulated promoters generate transcripts encoding the two functionally different human progesterone receptor forms A and B. EMBO J. 1990; 9: 1603–14.
46. Faivre EJ, Lange CA. Progesterone receptors upregulate Wnt-1 to induce epidermal growth factor receptor transactivation and c-Src-dependent sustained activation of Erk1/2 mitogen-activated protein kinase in breast cancer cells. Mol Cell Biol. 2007; 27: 466–480.
47. Lanzino M, De Amicis F, McPhaul MJ, Marsico S, Panno ML, Andò S. Endogenous coactivator ARA70 interacts with estrogen receptor alpha (ERalpha) and modulates the functional ERalpha/androgen receptor interplay in MCF-7 cells. J Biol Chem. 2005; 280: 20421–30.
48. Wang J, Pan XL, Ding LJ, Liu DY, Da-Peng Lei, Jin T. Aberrant expression of Beclin-1 and LC3 correlates with poor prognosis of human hypopharyngeal squamous cell carcinoma. PLoS One. 2013; 8: e69038. doi: 10.1371/journal.pone.0069038.
49. Maris P, Campana A, Barone I, Giordano C, Morelli C, Malivindi R, Sisci D, Aquila S, Rago V, Bonofiglio D, Catalano S, Lanzino M, Andò S. Androgens inhibit aromatase expression through DAX-1: insights into the molecular link between hormone balance and Leydig cancer development. Endocrinology. 2015; 156: 1251-62. doi: 10.1210/en.2014-1654.
50. Mauro L, Pellegrino M, Giordano F, Ricchio E, Rizza P, De Amicis F, Catalano S, Bonofiglio D, Panno ML, Andò S. Estrogen receptor-α drives adiponectin effects on cyclin D1 expression in breast cancer cells. FASEB J. 2015; 29: 2150-60. doi: 10.1096/fj.14-262808.
51. De Amicis F, Aquila S, Morelli C, Guido C, Santoro M, Perrotta I, Mauro L, Giordano F, Nigro A, Andò S, Panno ML. Bergapten drives autophagy through the up-regulation of PTEN expression in breast cancer cells. Mol Cancer. 2015; 14:130. doi: 10.1186/s12943-015-0403-4.
52. De Amicis F, Russo A, Avena P, Santoro M, Vivacqua A, Bonofiglio D, Mauro L, Aquila S, Tramontano D, Fuqua SA, Andò S. In vitro mechanism for downregulation of ER-α expression by epigallocatechin gallate in ER+/PR+ human breast cancer cells. Mol Nutr Food Res. 2013; 57: 840-53. doi: 10.1002/mnfr.201200560.
53. Bittencourt D, Dutertre M, Sanchez G, Barbier J, Gratadou L, Auboeuf D. Cotranscriptional splicing potentiates the mRNA production from a subset of estradiol-stimulated genes. Mol Cell Biol. 2008; 28: 5811-24. doi: 10.1128/MCB.02231-07.

Androgens downregulate miR-21 expression in breast cancer cells underlining the protective role of androgen receptor

Ivan Casaburi[1,*], Maria Grazia Cesario[1,*], Ada Donà[1], Pietro Rizza[1], Saveria Aquila[1], Paola Avena[1], Marilena Lanzino[1], Michele Pellegrino[1], Adele Vivacqua[1], Paola Tucci[1], Catia Morelli[1,], Sebastiano Andò[1] and Diego Sisci[1,**]**

[1] Department of Pharmacy and Health and Nutritional Sciences, University of Calabria, Arcavacata di Rende (CS), Italy

[*] These authors have contributed equally to this work

[**] These authors are joint senior authors

Correspondence to: *Diego Sisci*, ***email***: *diego.sisci@unical.it*

Keywords: androgen receptor, breast cancer, miR-21, androgens

Received: *November 24, 2015* ***Accepted***: *January 25, 2016* ***Published***: *February 05, 2016*

ABSTRACT

Although the protective role of androgen receptor (AR) in breast cancer (BC) is well established, the mechanisms involved remains largely unexplored. MicroRNAs play fundamental roles in many biological processes, including tumor cell development and metastasis. Herein, we report that androgens reduce BC cells proliferation acting as a negative modulator of the onco-miRNA-21.

The synthetic androgen miboleron (Mib) decreases BC cell proliferation induced by miR-21 over-expression and AR knockdown evidenced the requirement of AR in the down-regulation of miR-21 expression. These effects seem to be a general mechanism occurring in BC tissues.

Chromatin immune-precipitation (ChIP) analysis disclosed the binding of AR to a specific ARE sequence in miR-21 proximal promoter and recognizes the recruitment of HDAC3 as component for AR-mediated transcriptional repression. Such event is associated to a significantly reduced PolII binding in Mib treated extracts confirming that activated AR is a transcriptional repressor of miR-21 expression, providing further insight into the protective role of androgens in breast cancer cells.

Collectively, our data and the widespread AR expression in primary and metastatic breast tumours, suggest a careful examination of the therapeutic potential of androgens also in potentiating the effectiveness of anti-oestrogen adjuvant therapies.

INTRODUCTION

The importance of androgens in the treatment of breast cancer (BC) has been reported in many studies, but the role of androgen receptor (AR) remains not completely elucidated. AR is expressed in the majority of primary tumors [1] and in many of the metastatic lesions [2]. Although estrogen receptor α (ER) plays a pivotal role in driving BC growth, AR is the most commonly expressed hormone receptor in "*in situ*", invasive and metastatic BC. It is well known that BCs are classified based on ER, progesterone receptor and HER2neu expression but, as a consequence of the importance of AR activity a reclassification of BCs into three subtypes based on the expression of ER and AR has been proposed [3]: luminal (ER+, AR+), basal (ER-, AR-) and molecular apocrine (ER-, AR+). AR expression was found to be a favorable prognostic indicator of disease outcome by the majority of studies investigating the relationship between AR levels and the clinical-pathological characteristics in BCs (reviewed in [4]). Moreover, AR content was reported to correlate with a better response to chemotherapy and hormonal therapy [5]. All these effects have been strictly related to ER expression. Recently, the overall survival and the disease-free survival that are directly correlated to AR expression have been reported to be irrespective to ER co-expression [6]. Many "*in vitro*" studies have investigated the clinical significance of AR expression and the effects of androgens on BC cell lines, demonstrating the inhibitory role of AR signaling on BC cells proliferation [7-9]. Some of the mechanisms involved in the inhibition of BC cells proliferation have

been already elucidated. Specifically, androgens-activated AR inhibits endogenous cyclin D1 expression [10], and down-regulates C-MYC and K-RAS protein expression by up-regulating the miRNA let-7a [11].

MicroRNAs (miRs) are a class of short non-coding RNA genes that act post-transcriptionally as negative regulators of gene expression. A large body of research shows that animal miRs play fundamental roles in many biological processes, including tumor cell development and metastasis [12]. Many are the miRs regulated by androgens in various tissues, such as miR-32 and others in prostate cancer [13], let-7a in breast cancer [11] and miR-21 in prostate cancer [14] and in hepatocellular carcinoma [15]. Among these, miR-21 is considered a key onco-miRNA in carcinogenesis since its expression is consistently high in a wide range of cancers including BCs [16]. Furthermore, miR-21 is the most abundant in breast tumor tissue as compared to matched normal tissue [17], and its expression is higher in invasive and malignant breast tumors [18]. Several potential miR-21 targets have been identified including some tumor suppressor genes such as phosphatase and tensin homolog (PTEN) [19], tropomyosin 1 (TPM1) [20] and programmed cell death 4 (PDCD4) [21].

Considering the oncogenic action of miR-21 in BC and the ability of androgens-activated-AR to bind directly to miR-21 promoter increasing its expression in prostate cancer [14], we evaluated the expression of miR-21 in response to androgen stimulation in BC cells where androgens exert a protective role [7-9].

Herein we demonstrated that, in response to androgens, AR contributes to the reduction of BC cell growth by inhibiting miR-21 expression through the recruitment of HADAC3 on miR-21 promoter.

RESULTS

Mibolerone inhibits miR-21 induced breast cancer cells growth

It is well established that miR-21 expression promotes proliferation and invasiveness of breast cancer cells [16]. The oncogenic potential of miR-21 was also evidenced in other cancer cell types, including prostate cancer cells [14], where its expression has been reported to be clearly induced by androgens [14]. Considering

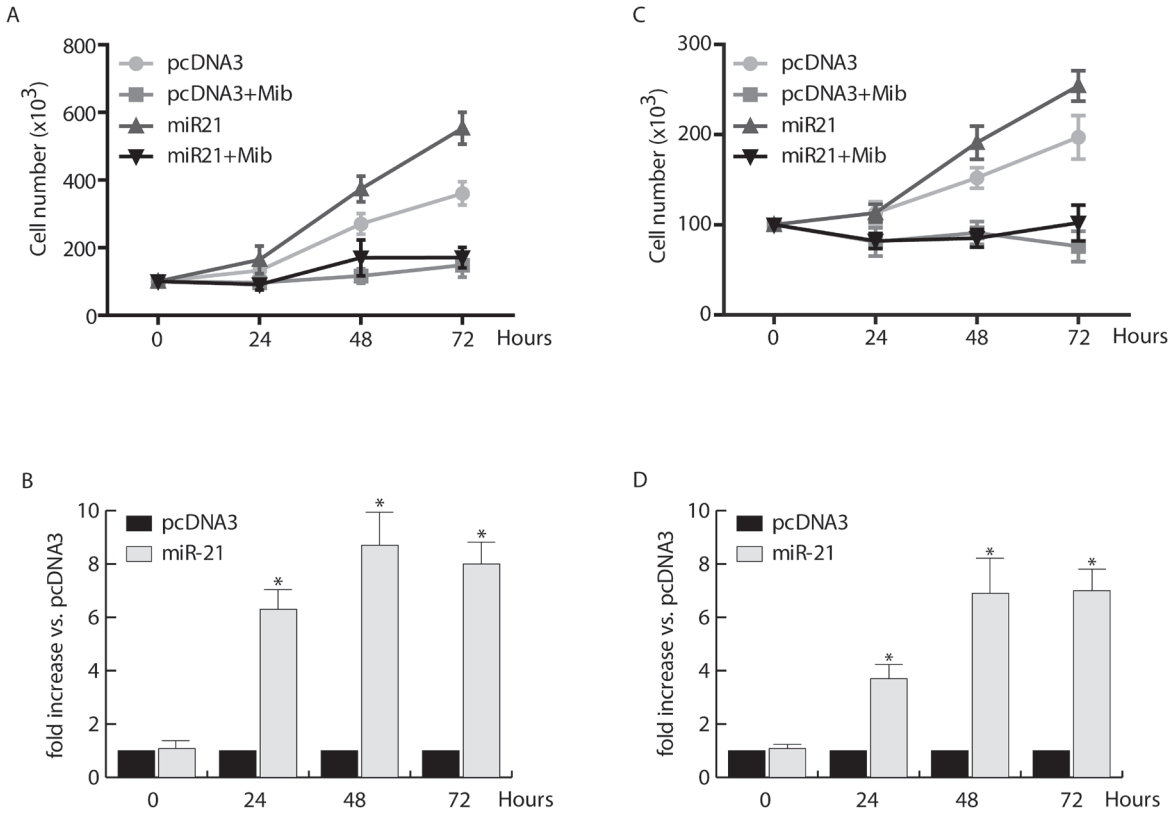

Figure 1: Proliferative effects of miR-21 on human breast cancer cells. MCF-7 **A.** and ZR-75-1 **C.** cells were transfected with pcDNA3/pre-miRNA-21 or pcDNA3, allowed to recover overnight, and then incubated in the presence or absence of 10 nM Mib for 24, 48, and 72 hours. Cell proliferation was quantified by trypan blue exclusion. miR-21 expression was evaluated by qRT-PCR on total RNA extracted from transfected MCF-7 **B.** and ZR-75-1 **D.** cells as reported in *materials and methods*. All the qRT-PCR results were normalized to RNU6B and expressed as fold increase *versus* pcDNA3 samples. All the data represent Mean ± SD of three different experiments analyzed in triplicate.

that we, and others, demonstrated the existence of some mechanisms by which androgens inhibit BC cell proliferation [10], we investigated if they are able to inhibit BC cell growth also in response to miR-21 overexpression.

To this aim, MCF-7 cells were transfected with pcDNA3/pre-miRNA-21 and pcDNA3 (control vector) (Figure 1B), synchronized in serum free medium (PRF) for 24 hours (h) and treated with Mib 10 nM in PRF-CT for 24, 48, and 72 h. As expected, Mib inhibited dramatically MCF-7 cell proliferation, while miR-21 overexpression induced about 3 fold increase of cell proliferation (Figure 1A). Interestingly, Mib was able to counteract miR-21 induced MCF-7 cell proliferation. These effects are not related to the cell type but to the tissue since, under the same experimental conditions (Figure 1D), comparable results were obtained in other BC cell lines such as ZR-75-1 (Figure 1C) and SKBR3 (data not shown).

Mibolerone inhibits basal expression of miR-21 in MCF-7 breast cancer cells

Based on proliferation results we questioned if androgens were able to counteract miR-21 action by regulating miR-21 expression in BC cells. To this aim, serum starved MCF-7 cells were left untreated or treated with increasing amount of Mib for 24 h (Figure 2A). The results indicate a significative reduction (60 %) in mature miR-21 content in response to 10 nM Mib. Interestingly, a 10 fold higher concentration of Mib did not exert additional decrease in miR-21 expression.

Since 10 nM Mib were able to strongly reduce the expression of miR-21, we used this concentration to evaluate miR-21 expression in time course experiments (Figure 2B). A marked reduction of miR-21 expression was observed after 24 and 48 h of treatment (60 % and 80 % respectively). These results were also confirmed

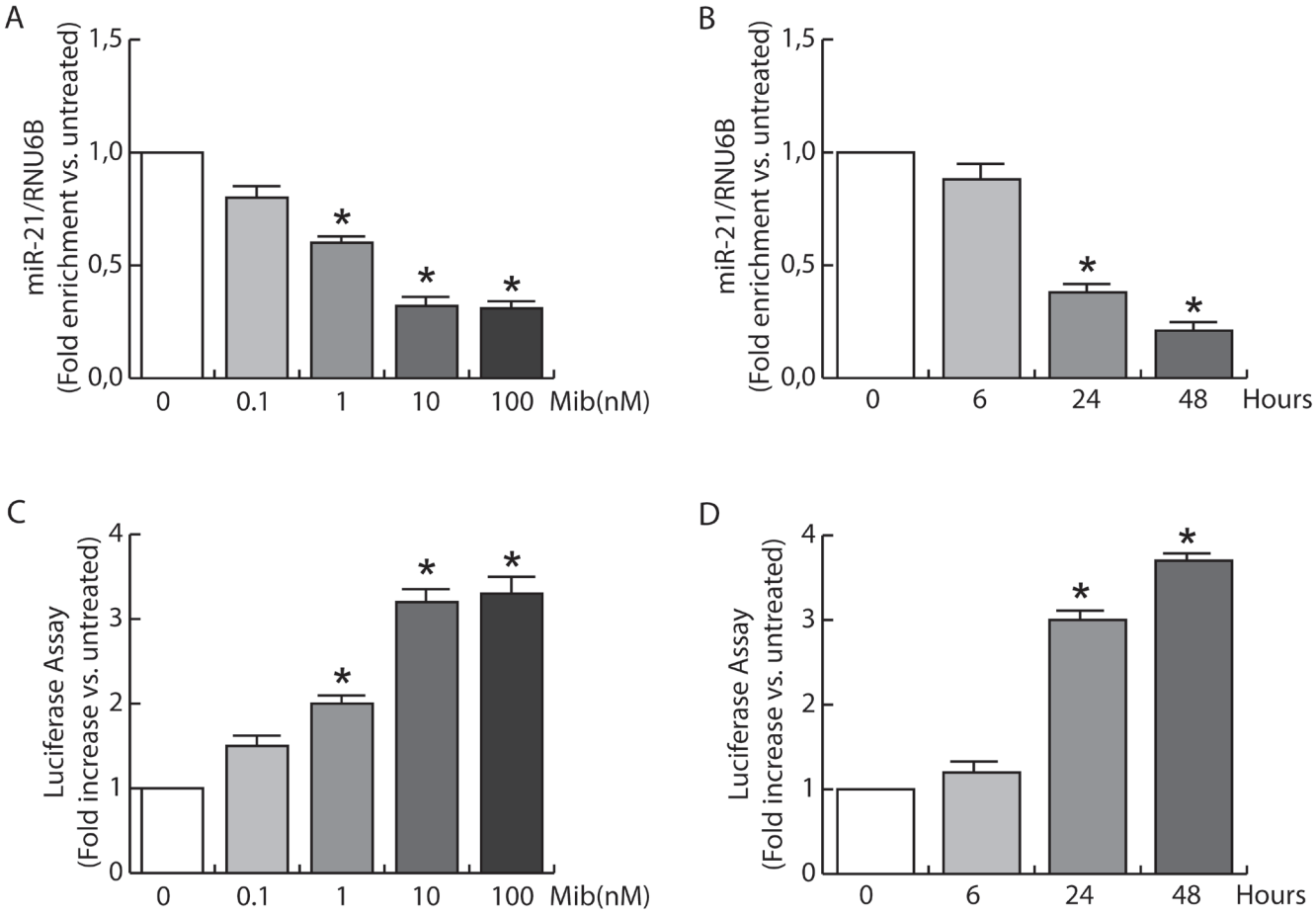

Figure 2: miR-21 expression is inhibited by androgens in breast cancer cells. A. Total RNA from MCF-7 cells treated with increasing amount of Mib (0, 0.1, 1, 10, and 100 nM) was extracted and miR-21 content was quantified by qRT-PCR. The y-axis represents log fold enrichment after miR-21 pull down, relative to input RNA. **B.** Total RNA from MCF-7 cells treated with Mib (10 nM) was collected after 6, 24, and 48 hours of incubation. miR-21 expression was quantified by qRT-PCR. All the qRT-PCR results were normalized to RNU6B. The regulation of miR-21 expression was evaluated also by transfecting MCF-7 cells with the plasmid Luc-miR-21. MCF-7 cells were treated as reported in A for **C.** and as reported in B for **D.** At the end, cells were subjected to luciferase assay. Renilla tk was used as control of transfection. Data represent fold enrichment with respect to untreated (A, C) or time 0 (B, D) samples, and are reported as Mean ± s.d. derived from three independent measurements *$P < 0.05$.

by evaluating the effect of Mib on miR-21 target gene reporter activity in MCF-7 cells. Starved MCF-7 cells were transfected with pGL3-miR-21-Luciferase and pRL-tk plasmids and then treated with increasing amount of Mib for 24 h (Figure 2C) or subjected to a time course study with 10 nM Mib (Figure 2D). The results revealed an increase of luciferase protein expression, showing that Mib reduces miR-21 expression.

Androgens reduce miR-21 expression through androgen receptor

Having confirmed the ability of androgens to counteract miR-21 induced breast cancer cell growth by reducing miR-21 expression, we evaluated if AR was involved in the down regulation of miR-21. MCF-7 cells were transfected with Vector (pcDNA3) and an AR expression plasmid or with Vector (psiRNA) and psiAR (shAR) to evaluate the involvement of AR overexpression or its knock down on the regulation of miR-21 expression. Treatment with Mib leads to a 50 % reduction of miR-21 expression within the vector transfected group (Figure 3A). Interestingly, AR overexpression was sufficient to reduce miR-21 expression reaching a value comparable to Mib treated vector samples. An additional reduction of miR-21 expression was obtained in AR overexpressing cells exposed to Mib. AR knock-down (Figure 3B) was associated to an increased miR-21 expression even in response to Mib treatment. Overlapping results were observed by treating MCF-7 cells with 5α-Dihydrotestosterone (DHT), an AR natural ligand, indicating that such a reduction was not an artifact of the treatment used. Further, by using Hydroxyflutamide, an AR antagonist (Figure 3C), we confirmed that the inhibitory effect on miR-21 expression is mediated by AR activation (Figure 3C). These results were further strengthened by expressing AR in the AR negative MDA-MB-231 cell line (Figure 4A) or knocking down it in the AR positive ZR-75-1 cells (Figure 4B).

Since previous studies have shown that miR-21 is an AR-regulated miRNA in prostate cancer [14] where it promotes cell growth, we questioned if the inhibitory effect observed in MCF-7 is exclusively related to the cell system used or it is a normal response of the mammary epithelium. To exclude the influence of specific factors present in MCF-7 cells, we measured miR-21 expression in other two AR positive breast cancer cells, SK-BR-3 and ZR-75-1, evaluating the ability to repress luciferase expression when the miR is expressed. To this aim, cells were transfected with MiR-21-Luc reporter vector and luciferase expression was evaluated in response to Mib treatment both in Scrambled and shAR cells (Figure 5D and 5E). Also in these cell models, treatment with Mib led to an increase of luciferase activity in Vector transfected cells (Figure 5B, 5D and 5E), that resulted repressed knocking down AR. Moreover, the expression of AR in MDA-MB-231 cell line (Figure 5C) reproduced the same response observed in MCF-7 (Figure 5A). Altogether, these results indicate that AR is required to down regulate miR-21 expression and that it is a general mechanism

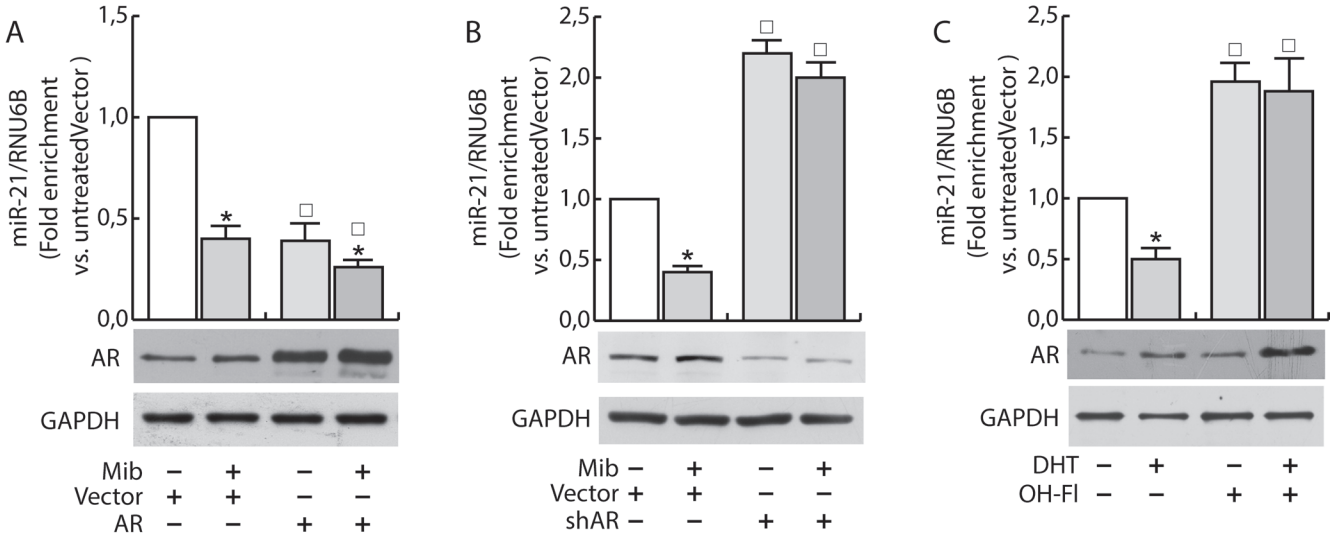

Figure 3: Androgens regulate miR-21 expression in breast cancer cells. MCF-7 cells were transfected with Vector (pcDNA3) and the AR expression plasmid (pcDNA2-AR) **A.** or with Vector (psiRNA) and psiAR (shAR) **B.** and treated with Mib (10nM) for 24 h. In addition, synchronized MCF-7 cells were treated with DHT 10 nM and OH-Fl 100 nM for 24 h C). Total RNA was extracted after the treatment and analyzed by qRT-PCR to evaluate miR-21 content. All the qRT-PCR results were normalized to RNU6B. AR expression was determined by western blotting using 30 mg of protein lysates. GAPDH expression was assessed as protein loading control. Data represent fold enrichment with respect to the correspondent untreated Vector sample and are reported as Mean ± s.d. derived from three independent measurements. Statistical analysis was performed applying Student's *t* test: $*P < 0.05$ is referred to the correspondent untreated sample; □ to the correspondent Vector samples ($p < 0.05$).

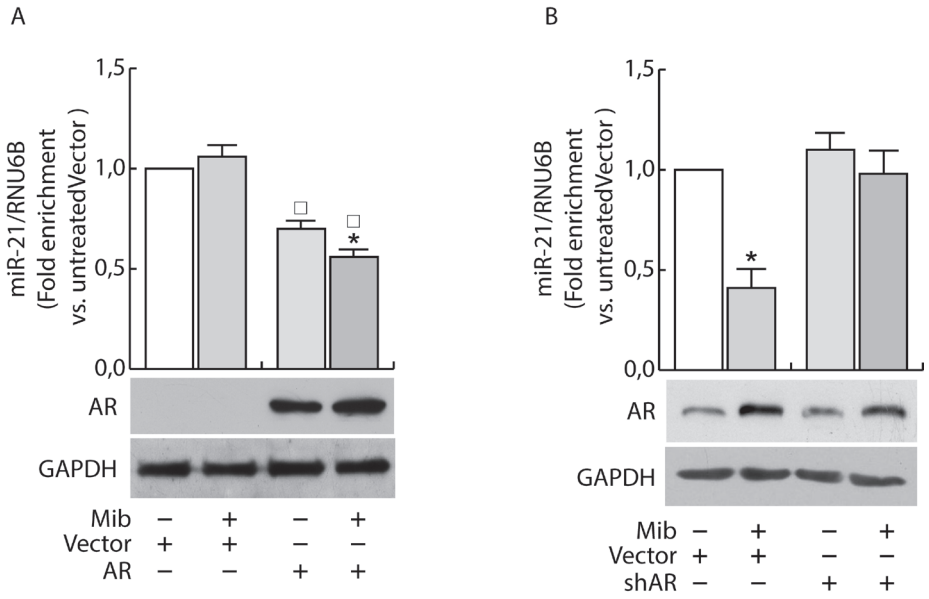

Figure 4: AR regulates miR-21 expression in breast cancer cells. MDA-MB-231 cells were transfected with Vector (pcDNA3) and AR expression plasmid (pcDNA3-AR) (AR). After 24 h, cells were treated with Mib (10nM) **A.** for 24 h. ZR-75-1 cells were transfected with psiCon a scrambled shRNA (Vector) or psiAR (shAR) and treated as described before **B.**. At the end of the treatment, total RNA was extracted and analyzed by qRT-PCR to evaluate miR-21 content. All the qRT-PCR results were normalized to RNU6B. Data represent fold enrichment with respect to the correspondent untreated Vector sample and are reported as Mean ± s.d. derived from three independent measurements. Statistical analysis was performed applying Student's t test: **P* < 0.05 is referred to the correspondent untreated sample; □ to the correspondent Vector samples ($p < 0.05$).

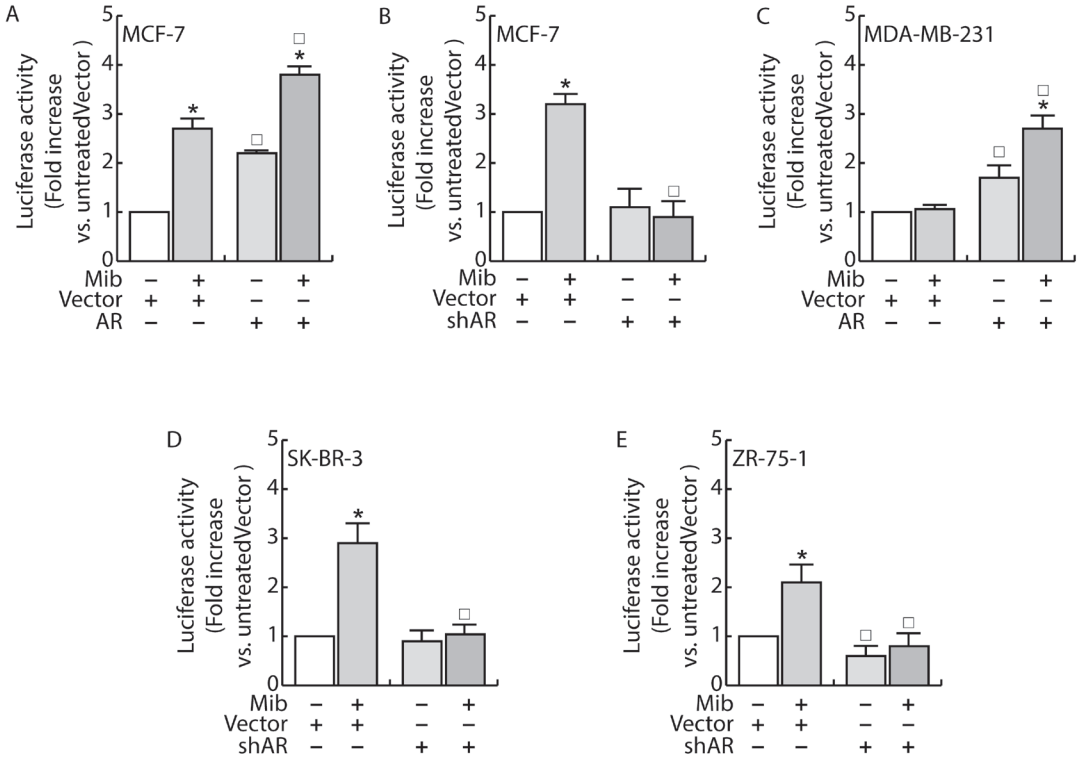

Figure 5: AR regulates miR-21 expression in breast cancer cells. MCF-7 **A.** and MDA-MB-231 **C.** cells were transfected with Vector (pcDNA3) and the AR expression plasmid (pcDNA3-AR). MCF-7 **B.**, SKBR3 **D.** and ZR-75 **E.** cells were transfected with Vector (psiRNA) or psiAR (shAR) **B.**. All the cell lines were concomitantly transfected with with Luc-miR-21 and PRL-tk. 24 h after, cells were treated with Mib 10nM for 24 h and, at the end, luciferase content was evaluated as reported in "*Materials and Methods"*. Data represent fold enrichment with respect to the correspondent untreated Vector sample and are reported as Mean ± s.d. derived from three independent measurements. Statistical analysis was performed applying Student's t test: **P* < 0.05 is referred to the correspondent untreated sample; □ to the correspondent Vector samples ($p < 0.05$).

occurring in breast cancer tissue. In addition, it is also independent from other steroid receptors expression since the effect was observed in MDA-MB-231 cells that are estrogen and progesterone receptor negative.

Miboleron increased the recruitment of HDAC3 on the miR-21 promoter in MCF-7 cells

To clarify the mechanism through which androgens down-regulate miR-21 expression in breast cancer cells, we verified the binding of AR on the ARE sequence within the miR-21 promoter.

Considering that an ARE sequence involved in the direct transcriptional regulation of miR-21 induced by AR binding to the miR-21 promoter has been previously reported by Ribas et al. in prostate [14], we questioned if the same responsive element may be still involved in the negative regulation of miR-21 expression in breast cancer cells (Figure 6A). Chromatin immune-precipitation (ChIP) analysis was performed in nuclear extracts from MCF-7 and LNCap cells. There was no recruitment of AR to the negative control region (see "*Materials and methods*") and no amplification of PCR products in ChIP reactions using IgG. By contrast, a significant recruitment of AR on the region containing the ARE sequence was observed in

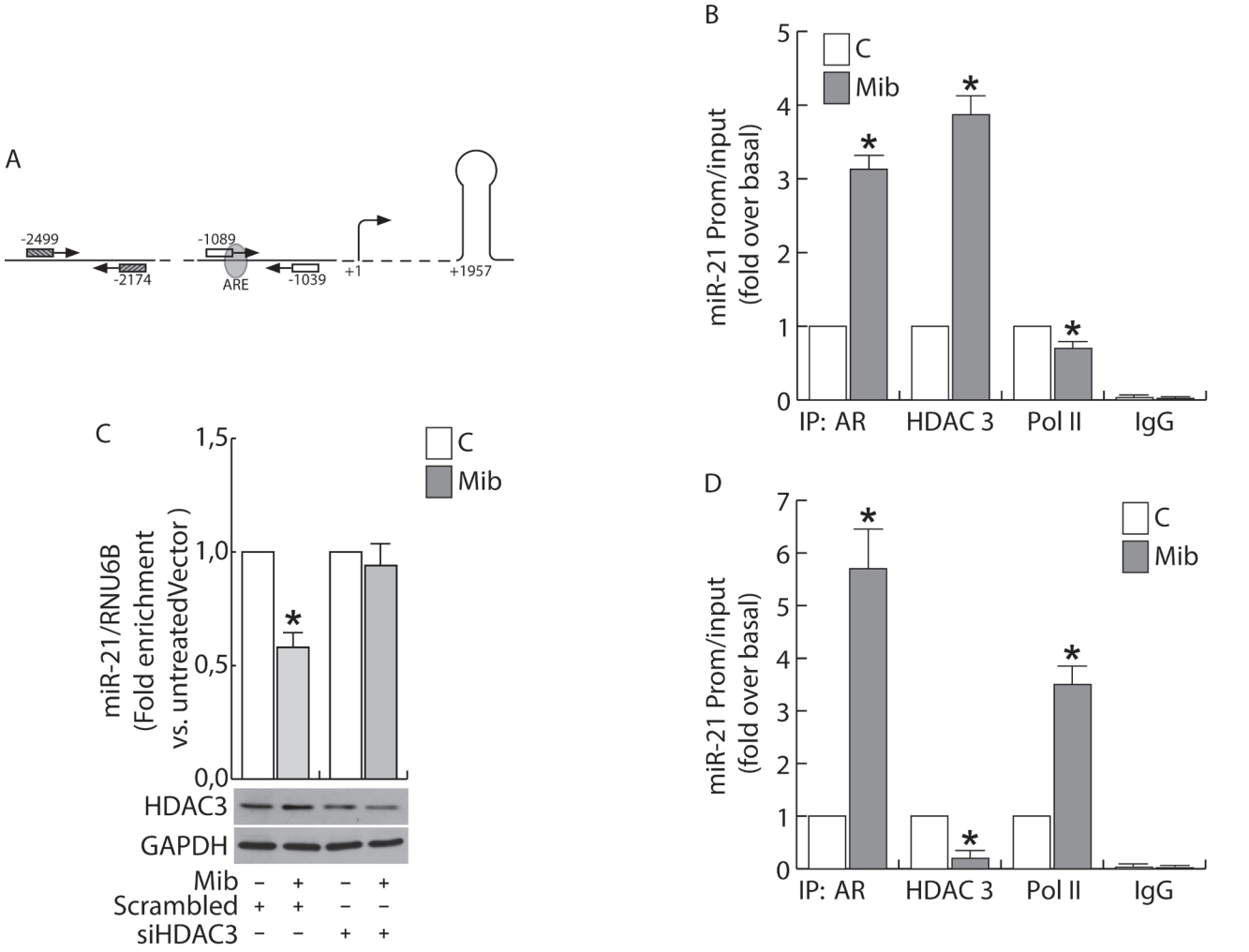

Figure 6: Androgens regulate miR-21 expression by binding to miR-21 promoter in breast cancer cells. ChIP analysis was performed on nuclear extracts from sub-confluent MCF-7 **B.** and LNCap **D.** cells, switched to PRF-CT. 24h later cells were left untreated or treated for 45 min with 10 nM Mib. The ARE-containing miR21 promoter region **A.**, was precipitated with either anti-AR, anti-HDAC3 or anti-Pol II Abs and amplified using a specific pair of primers reported in "*Materials and Methods*". Mib-treated samples were also precipitated with normal rabbit IgG that was used as negative control. In addition, a 325 bp fragment located at -2051/-1726 was amplified on the same precipitated samples as qualitative control. HDAC3 expression was knock down by transfecting siRNA recognizing HDAC3 mRNA (siHDAC3) or a Scrambled siRNA in MCF-7 cells **C.** as reported in *"Materials and Methods*". After 24 h, cells were treated with Mib (10nM) for 24 h. At the end of the treatment, total RNA was extracted and analyzed by qRT-PCR to evaluate miR-21 content. HDAC3 expression was determined by WB using 30 mg of protein lysates. GAPDH expression was assessed as protein loading control. Data represent the mean ± s.d. of three independent experiments. Statistical analysis was performed applying Student's *t* test: * $p < 0.05$ *vs*. untreated.

response to Mib exposure (Figure 6B). Interestingly, the increased recruitment of AR was not paralleled by PolII binding that resulted significantly reduced in Mib treated extracts (Figure 6B). To explain the different response to androgen stimulation observed in BC cells with respect to prostate cancer cells, we focused our attention to fast mechanisms that may alter the transcriptional response to a stimulus. The same samples were precipitated with HDAC3 whose binding to the promoter resulted strongly increased in response to Mib (Figure 6B). The involvement of HDAC3 in the regulation of miR-21 expression by AR was confirmed by knocking down HDAC3 in BC cells (Figure 6C). Interestingly, HDAC3 is not recruited on miR-21 promoter in LNCap cells in response to Mib treatment (Figure 6D). All together, these results may evidence the involvement of an epigenetic mechanism in determining an opposite response of prostate and BC cells to Mib treatment.

DISCUSSION

The interest on androgens as factors involved in BC progression was intuited several years ago through the "hyperandrogenic" theory on the basis of which an increased androgenic activity is present in BC [22]. Although androgens were successfully used to treat BC [23, 24], the role of AR and its signaling in breast carcinogenesis are not yet elucidated and are very often controversial [4]. AR expression in BC tissue samples has been associated with a better prognosis [25, 26] and the lack of AR expression correlates with transformation from "*in situ*" to invasive basal subtype ductal breast carcinoma [27]. In addition, loss of AR in triple-negative breast cancers is associated with a worse prognosis, including those with basal-like features [28]. Conversely, some reports suggest that AR may participate to the development of invasive ductal carcinoma by repressing E-cadherin expression [29]. It is worth noting that, most of these results have been obtained stimulating the cells with enzymatically metabolizable androgens, such as testosterone and DHT, while non-metabolizable AR agonists are now used for the treatment of breast cancer. Some of the mechanisms by which AR inhibits breast cancer cell growth have been explained, for example through the down regulation of cyclin D1 [10], by increasing DAX 1 expression that causes an inhibition of aromatase content [30], by up-regulating ER-beta gene expression [31], by down-regulating CMYC and KRAS expression in response to let-7a increased expression [11], and more. Here we demonstrated that AR inhibits breast cancer cell growth by down-regulating miR-21 expression.

The involvement of miR-21 in both carcinogenesis, by increasing the growth of breast cancer cells [16], and tumor progression and invasion [18] is well described. miR-21 expression is regulated in response to various stimuli, including androgens, as demonstrated by Ribas et al. in prostate cancer cells [14]. Interestingly, in prostate cancer cells androgens increase miR-21 expression by trans-activating miR-21 promoter. Our data provide evidence that in breast cancer cells activated AR is a transcriptional repressor of miR-21 expression. Analysis of the molecular events associated with the negative regulation of miR-21 transcription disclose the binding of AR to a specific ARE sequence in miR-21 proximal promoter, and recognizes the recruitment of HDAC3 as component for AR-mediated transcriptional repression. HDACs are well known to repress the transcription of genes regulated by multiple nuclear receptors [32]. In response to receptor antagonists HDACs are recruited at hormone receptor binding sites to block ligand-induced gene expression. Interestingly, AR promotes the recruitment of the repressor complex to the ARE binding site in miR-21 promoter previously indicated by Ribas et al. [14] as the AR permissive binding domain for miR-21 transcription in prostate cancer. These data indicate a specificity in AR functional response depending only by cell type that leads to the protective role of androgens in breast cancer cells. Paradoxically, HDACs are also required for the activation of a fraction of AR target genes of human prostate cancers [33]. These observations clearly indicate the different role played by AR in breast cancer with respect to other cancer, such as prostate [14] and liver [15].

A discrepancy appears considering the suppression of mir-21 expression at promoter level and the inhibition of proliferation induced by ectopic expression of miR-21 in response to androgens (Figure 1). Such a discrepancy may be explained taking into account the ability of androgens to inhibit Cyclin D1 expression in breast cancer cells [10], whose translation is accelerated by miR-21 [34].

Collectively, these data and the widespread expression of AR in primary and metastatic breast tumours, justify a careful examination of the therapeutic potential of androgens also in potentiating the effectiveness of anti-oestrogen adjuvant therapies.

MATERIALS AND METHODS

Cell culture, conditions, and treatments

Authenticated human BC epithelial cell lines MCF-7, ZR-75-1, MDA-MB-231, SKBR3 and LNCap were purchased from Interlab Cell Line Collection, Italy. Cells were stored according to supplier's instructions and used within 4 months after frozen aliquots resuscitations (less than 30 passages). Every 4 months, cells were authenticated by short tandem repeat analysis (AmpFLSTR Profiler Plus PCR Amplification Kit, Applied Biosystems) at our Sequencing Core; morphology, doubling times, estrogen sensitivity, and mycoplasma

negativity (MycoAlert, Mycoplasma Detection kit, Lonza) were tested.

MCF-7 and ZR-75-1 were maintained in DMEM/Ham F-12 medium (1:1) (DMEM/F-12) supplemented with 5 % Fetal Bovine Serum (FBS). MDA-MB-231 were cultured in 10 % FBS DMEM, LNCaP were grown in RPMI 1640 supplemented with 10 % FBS. Additionally, culture media were supplemented with 100 IU/ml penicillin, 100 ng/ml streptomycin, and 0.2 mM L-glutamine. For experimental purposes, cells were synchronized in phenol red-free (PRF) and serum-free media (SFM) for 24 hours (h) and then switched to PRF-media containing 5% charcoal-treated FBS (PRF-CT) in the presence or absence of Mibolerone (Mib, from Perkin Elmer), 5α-Dihydrotestosterone (DHT, Sigma) and hydroxyflutamide (OH-Fl, from Sigma Aldrich). All media were purchased from Invitrogen, Italy.

Plasmids and transfections assays

The following plasmids were used: pcDNA3 empty vector (Life technologies); pcDNA3-miR21, for the expression of pre-miR-21 (provided by Joshua Mendell, Addgene plasmid # 21114) [35]; the vector-based pSiAR plasmid (shAR), coding for a small interfering RNA targeting the 5'-untranslated region of AR mRNA, and the scrambled control construct pSiCon (Vector) [36]; pcDNA3-AR (AR) encoding full-length AR [10].

For transfections, MCF-7, SKBR3, ZR-75-1 and MDA-MB-231 were resuspended in PRF-growing medium (PRF-GM) and transfected with Lipofectamine 2000 (Life technologies), according to the manufacturer's instructions. Six hours after transfection cells were synchronized for 24 h and then switched to PRF-CT, in the presence or absence of Mib, for cell growth or RNA extraction purposes.

For luciferase assays, the following constructs were used: Luc-miR-21 [37], a reporter construct for miR activity containing the complementary sequences of mature miR-21 downstream to luciferase, in which Luciferase cDNA was modified in 3'UTR to complementary bind miR-21 (provided by Dr. Qihong Huang) and pRL-Tk (Promega).

Cell proliferation assays

Cell proliferation was evaluated by cell counting assay as previously described [38]. Briefly, BC cells were seeded on six-well plates ($2x10^5$cells/well) in 2.5% PRF-CT. After 24h, cells were exposed to Mib (10 nM) [30] or vehicle for 24, 48, and 72 h. The effects of Mib on cell proliferation were measured at each time point by counting cells using a hemocytometer, and cell viability was determined by Trypan blue dye exclusion test.

miR extraction and quantitative real-time PCR (qRT-PCR)

Total micro-RNAs were isolated from cells using the *mir*Vana miRNA Isolation Kit (Life technologies) according to the manufacturer's instructions. Total miR were reverse transcribed using a TaqMan MicroRNA Reverse transcription kit (Life technologies) and qRT-PCR was performed with TaqMan universal master mix by using specific primers for miR-21 (all from Life technologies). RNU6B (Life technologies) was used as internal control. Gene and miR expression was defined from the threshold cycle (Ct), and relative expression levels were calculated after normalization to a calibrator that was chosen to be the basal, untreated sample as previously described [39].

Western blotting assays

Proteins expression was assessed by Western blotting (WB) assay as previously described [40]. Briefly, cells were lysed in Triton lysis buffer, cleared by centrifugation and the protein content was determined by Bradford dye reagent (Bio-Rad). Cellular lysates (20 μg of protein/lane) were resolved by SDS-PAGE, transferred to nitrocellulose membranes and probed with specific polyclonal (p) or monoclonal (m) antibodies (Abs), recognized by peroxidase-coupled secondary Abs, and developed using the Amersham ECL start Western Blotting Detection Reagent (GE Healthcare).

The following Abs were used: anti-AR mAb (441), anti-GAPDH pAb (FL-335) and normal mouse immunoglobulin G (Ig) (all from Santa Cruz Biotechnology). Images were acquired by using an Epson Perfection scanner (Epson).

Chromatin immunoprecipitation (ChIP)

ChIP assay was performed as previously described [39]. Chromatin extracts were precipitated with anti-AR mAb (441), anti HDAC III (H-99) and anti-Polymerase II (N-20) pAbs (all from Santa Cruz Biotechnology). Normal rabbit IgG (Santa Cruz Biotechnology) was used instead of primary Abs as negative control. Immuno-precipitated DNA was analyzed by qRT-PCR, and the miR-21 promoter sequence containing the Androgen Responsive Element (ARE) was amplified using the following pairs of primers: forward 5′-TCCCAATCATCTCAGAACAAGCT-3' and reverse 5′-TGCACAGAAACTCCAGTACATTAGTAAC-3' (50 bp) (Figure 5A) [14]. A sequence upstream of the considered ARE was amplified as control (Figure 5A) forward 5′-CCAGAAGTTAGGGATATGTTAGCA-3' and reverse 5′-TACCTCCAGGGTTCAAGTGATTCT-3' (325 bp).

Data were normalized with respect to unprocessed lysates (input DNA). Input DNA quantification was performed by using 5 µl of diluted (1/50) template DNA. The relative antibody-bound fractions were normalized as described in "miR extraction and quantitative real-time PCR (qRT-PCR)". The results were expressed as fold differences with respect to the relative inputs.

Luciferase assays

MCF-7 were seeded in culture medium on 24-well plates, serum starved for 24 h, co-transfected in PRF-CT with Luc-miR-21 and pRL-Tk, in the presence of pcDNA3, pcDNA3-AR, pSiCon and pSiAR vectors. After 6 h, Mib (10 nM) was added to the medium, where opportune, and the next day cells were harvested, and luciferase activity was measured using dual luciferase assay System (Promega), normalized to renilla luciferase activity (pRL-Tk) and expressed as relative luciferase units.

HDAC3 silencing

MCF-7 cells were transfected with RNA duplex of stealth siRNA targeted for human HDAC3 (SI03057901), or with AllStars Negative Control siRNA (SI03650318) (both from Qiagen, Milan, Italy). Cells were transfected using RNAiFect Transfection Reagent (Qiagen) as recommended by the manufacturer with minor modifications. After 5 h the transfection medium was changed with SFM, and then the cells were exposed to treatments.

Statistical analysis

All data were expressed as the mean ± S.D. of at least 3 independent experiments. Statistical significances were evaluated using Student's *t*-test. Statistical significance was accepted as $p \leq 0.05$.

CONFLICTS OF INTEREST

No potential conflicts of interest were disclosed.

GRANT SUPPORT

This study was supported by Grant IG 15738/2014 from Associazione Italiana Ricerca sul Cancro (AIRC), and MIUR EX 60%.

Editorial note

This paper has been accepted based in part on peer-review conducted by another journal and the authors' response and revisions as well as expedited peer-review in Oncotarget.

REFERENCES

1. Park S, Koo J, Park HS, Kim JH, Choi SY, Lee JH, Park BW and Lee KS. Expression of androgen receptors in primary breast cancer. Annals of oncology. 2010; 21: 488-492.
2. Gucalp A, Tolaney S, Isakoff SJ, Ingle JN, Liu MC, Carey LA, Blackwell K, Rugo H, Nabell L, Forero A, Stearns V, Doane AS, Danso M, Moynahan ME, Momen LF, Gonzalez JM, et al. Phase II trial of bicalutamide in patients with androgen receptor-positive, estrogen receptor-negative metastatic Breast Cancer. Clinical cancer research. 2013; 19: 5505-5512.
3. Farmer P, Bonnefoi H, Becette V, Tubiana-Hulin M, Fumoleau P, Larsimont D, Macgrogan G, Bergh J, Cameron D, Goldstein D, Duss S, Nicoulaz AL, Brisken C, Fiche M, Delorenzi M and Iggo R. Identification of molecular apocrine breast tumours by microarray analysis. Oncogene. 2005; 24: 4660-4671.
4. Hickey TE, Robinson JL, Carroll JS and Tilley WD. Minireview: The androgen receptor in breast tissues: growth inhibitor, tumor suppressor, oncogene? Molecular endocrinology. 2012; 26: 1252-1267.
5. Loibl S, Muller BM, von Minckwitz G, Schwabe M, Roller M, Darb-Esfahani S, Ataseven B, du Bois A, Fissler-Eckhoff A, Gerber B, Kulmer U, Alles JU, Mehta K and Denkert C. Androgen receptor expression in primary breast cancer and its predictive and prognostic value in patients treated with neoadjuvant chemotherapy. Breast cancer research and treatment. 2011; 130: 477-487.
6. Vera-Badillo FE, Templeton AJ, de Gouveia P, Diaz-Padilla I, Bedard PL, Al-Mubarak M, Seruga B, Tannock IF, Ocana A and Amir E. Androgen receptor expression and outcomes in early breast cancer: a systematic review and meta-analysis. Journal of the National Cancer Institute. 2014; 106: djt319.
7. Lanzino M, Garofalo C, Morelli C, Le Pera M, Casaburi I, McPhaul MJ, Surmacz E, Ando S and Sisci D. Insulin receptor substrate 1 modulates the transcriptional activity and the stability of androgen receptor in breast cancer cells. Breast cancer research and treatment. 2009; 115: 297-306.
8. Labrie F, Luu-The V, Labrie C, Belanger A, Simard J, Lin SX and Pelletier G. Endocrine and intracrine sources of androgens in women: inhibition of breast cancer and other roles of androgens and their precursor dehydroepiandrosterone. Endocrine reviews. 2003; 24: 152-182.

9. Birrell SN, Bentel JM, Hickey TE, Ricciardelli C, Weger MA, Horsfall DJ and Tilley WD. Androgens induce divergent proliferative responses in human breast cancer cell lines. The Journal of steroid biochemistry and molecular biology. 1995; 52: 459-467.

10. Lanzino M, Sisci D, Morelli C, Garofalo C, Catalano S, Casaburi I, Capparelli C, Giordano C, Giordano F, Maggiolini M and Ando S. Inhibition of cyclin D1 expression by androgen receptor in breast cancer cells—identification of a novel androgen response element. Nucleic acids research. 2010; 38: 5351-5365.

11. Lyu S, Yu Q, Ying G, Wang S, Wang Y, Zhang J and Niu Y. Androgen receptor decreases CMYC and KRAS expression by upregulating let-7a expression in ER-, PR-, AR+ breast cancer. International journal of oncology. 2014; 44: 229-237.

12. Tucci P, Agostini M, Grespi F, Markert EK, Terrinoni A, Vousden KH, Muller PA, Dotsch V, Kehrloesser S, Sayan BS, Giaccone G, Lowe SW, Takahashi N, Vandenabeele P, Knight RA, Levine AJ, et al. Loss of p63 and its microRNA-205 target results in enhanced cell migration and metastasis in prostate cancer. Proceedings of the National Academy of Sciences of the United States of America. 2012; 109: 15312-15317.

13. Jalava SE, Urbanucci A, Latonen L, Waltering KK, Sahu B, Janne OA, Seppala J, Lahdesmaki H, Tammela TL and Visakorpi T. Androgen-regulated miR-32 targets BTG2 and is overexpressed in castration-resistant prostate cancer. Oncogene. 2012; 31: 4460-4471.

14. Ribas J, Ni X, Haffner M, Wentzel EA, Salmasi AH, Chowdhury WH, Kudrolli TA, Yegnasubramanian S, Luo J, Rodriguez R, Mendell JT and Lupold SE. miR-21: an androgen receptor-regulated microRNA that promotes hormone-dependent and hormone-independent prostate cancer growth. Cancer research. 2009; 69: 7165-7169.

15. Teng Y, Litchfield LM, Ivanova MM, Prough RA, Clark BJ and Klinge CM. Dehydroepiandrosterone-induces miR-21 transcription in HepG2 cells through estrogen receptor beta and androgen receptor. Molecular and cellular endocrinology. 2014; 392: 23-36.

16. Yan LX, Wu QN, Zhang Y, Li YY, Liao DZ, Hou JH, Fu J, Zeng MS, Yun JP, Wu QL, Zeng YX and Shao JY. Knockdown of miR-21 in human breast cancer cell lines inhibits proliferation, *in vitro* migration and *in vivo* tumor growth. Breast cancer research. 2011; 13: R2.

17. Si ML, Zhu S, Wu H, Lu Z, Wu F and Mo YY. miR-21-mediated tumor growth. Oncogene. 2007; 26: 2799-2803.

18. Petrovic N, Mandusic V, Stanojevic B, Lukic S, Todorovic L, Roganovic J and Dimitrijevic B. The difference in miR-21 expression levels between invasive and non-invasive breast cancers emphasizes its role in breast cancer invasion. Medical oncology. 2014; 31: 867.

19. Huang GL, Zhang XH, Guo GL, Huang KT, Yang KY, Shen X, You J and Hu XQ. Clinical significance of miR-21 expression in breast cancer: SYBR-Green I-based real-time RT-PCR study of invasive ductal carcinoma. Oncology reports. 2009; 21: 673-679.

20. Zhu S, Si ML, Wu H and Mo YY. MicroRNA-21 targets the tumor suppressor gene tropomyosin 1 (TPM1). The Journal of biological chemistry. 2007; 282: 14328-14336.

21. Frankel LB, Christoffersen NR, Jacobsen A, Lindow M, Krogh A and Lund AH. Programmed cell death 4 (PDCD4) is an important functional target of the microRNA miR-21 in breast cancer cells. The Journal of biological chemistry. 2008; 283: 1026-1033.

22. Grattarola R, Secreto G and Recchione C. Androgens in breast cancer. III. Breast cancer recurrences years after mastectomy and increased androgenic activity. American journal of obstetrics and gynecology. 1975; 121: 169-172.

23. Goldenberg IS. Testosterone Propionate Therapy in Breast Cancer. Jama. 1964; 188: 1069-1072.

24. Goldenberg IS, Sedransk N, Volk H, Segaloff A, Kelley RM and Haines CR. Combined androgen and antimetabolite therapy of advanced female breast cancer. A report of the cooperative breast cancer group. Cancer. 1975; 36: 308-310.

25. Ogawa Y, Hai E, Matsumoto K, Ikeda K, Tokunaga S, Nagahara H, Sakurai K, Inoue T and Nishiguchi Y. Androgen receptor expression in breast cancer: relationship with clinicopathological factors and biomarkers. International journal of clinical oncology. 2008; 13: 431-435.

26. Sauter ER, Tichansky DS, Chervoneva I and Diamandis EP. Circulating testosterone and prostate-specific antigen in nipple aspirate fluid and tissue are associated with breast cancer. Environmental health perspectives. 2002; 110: 241-246.

27. Hanley K, Wang J, Bourne P, Yang Q, Gao AC, Lyman G and Tang P. Lack of expression of androgen receptor may play a critical role in transformation from *in situ* to invasive basal subtype of high-grade ductal carcinoma of the breast. Human pathology. 2008; 39: 386-392.

28. Thike AA, Yong-Zheng Chong L, Cheok PY, Li HH, Wai-Cheong Yip G, Huat Bay B, Tse GM, Iqbal J and Tan PH. Loss of androgen receptor expression predicts early recurrence in triple-negative and basal-like breast cancer. Modern pathology. 2014; 27: 352-360.

29. Liu YN, Liu Y, Lee HJ, Hsu YH and Chen JH. Activated androgen receptor downregulates E-cadherin gene expression and promotes tumor metastasis. Molecular and cellular biology. 2008; 28: 7096-7108.

30. Lanzino M, Maris P, Sirianni R, Barone I, Casaburi I, Chimento A, Giordano C, Morelli C, Sisci D, Rizza P, Bonofiglio D, Catalano S and Ando S. DAX-1, as an androgen-target gene, inhibits aromatase expression: a novel mechanism blocking estrogen-dependent breast cancer cell proliferation. Cell death & disease. 2013; 4: e724.

31. Rizza P, Barone I, Zito D, Giordano F, Lanzino M, De

Amicis F, Mauro L, Sisci D, Catalano S, Wright KD, Gustafsson JA and Ando S. Estrogen receptor beta as a novel target of androgen receptor action in breast cancer cell lines. Breast cancer research. 2014; 16: R21.

32. Karagianni P and Wong J. HDAC3: taking the SMRT-N-CoRrect road to repression. Oncogene. 2007; 26: 5439-5449.

33. Welsbie DS, Xu J, Chen Y, Borsu L, Scher HI, Rosen N and Sawyers CL. Histone deacetylases are required for androgen receptor function in hormone-sensitive and castrate-resistant prostate cancer. Cancer research. 2009; 69: 958-966.

34. Ng R, Song G, Roll GR, Frandsen NM and Willenbring H. A microRNA-21 surge facilitates rapid cyclin D1 translation and cell cycle progression in mouse liver regeneration. The Journal of clinical investigation. 2012; 122: 1097-1108.

35. Hwang HW, Wentzel EA and Mendell JT. Cell-cell contact globally activates microRNA biogenesis. Proceedings of the National Academy of Sciences of the United States of America. 2009; 106: 7016-7021.

36. Recchia AG, Musti AM, Lanzino M, Panno ML, Turano E, Zumpano R, Belfiore A, Ando S and Maggiolini M. A cross-talk between the androgen receptor and the epidermal growth factor receptor leads to p38MAPK-dependent activation of mTOR and cyclinD1 expression in prostate and lung cancer cells. The international journal of biochemistry & cell biology. 2009; 41: 603-614.

37. Gumireddy K, Young DD, Xiong X, Hogenesch JB, Huang Q and Deiters A. Small-molecule inhibitors of microrna miR-21 function. Angewandte Chemie. 2008; 47: 7482-7484.

38. Morelli C, Lanzino M, Garofalo C, Maris P, Brunelli E, Casaburi I, Catalano S, Bruno R, Sisci D and Ando S. Akt2 inhibition enables the forkhead transcription factor FoxO3a to have a repressive role in estrogen receptor alpha transcriptional activity in breast cancer cells. Molecular and cellular biology. 2010; 30: 857-870.

39. Sisci D, Maris P, Cesario MG, Anselmo W, Coroniti R, Trombino GE, Romeo F, Ferraro A, Lanzino M, Aquila S, Maggiolini M, Mauro L, Morelli C and Ando S. The estrogen receptor alpha is the key regulator of the bifunctional role of FoxO3a transcription factor in breast cancer motility and invasiveness. Cell cycle. 2013; 12: 3405-3420.

40. Sisci D, Aquila S, Middea E, Gentile M, Maggiolini M, Mastroianni F, Montanaro D and Ando S. Fibronectin and type IV collagen activate ERalpha AF-1 by c-Src pathway: effect on breast cancer cell motility. Oncogene. 2004; 23: 8920-8930.

Bergapten induces metabolic reprogramming in breast cancer cells

MARTA SANTORO[1-3], CARMELA GUIDO[1-3], FRANCESCA DE AMICIS[1,3], DIEGO SISCI[1,3], ERIKA CIONE[3], DOLCE VINCENZA[3], ADA DONÀ[1,3], MARIA LUISA PANNO[3*] and SAVERIA AQUILA[1,3*]

[1]Centro Sanitario, [2]Post-Graduate School Clinical Pathology, [3]Department of Pharmacy and Science of Health and Nutrition, University of Calabria, I-87030 Arcavacata di Rende (CS), Italy

Received March 13, 2015; Accepted August 4, 2015

DOI: 10.3892/or.2015.4327

Abstract. Alterations in cellular metabolism are among the most consistent hallmarks of cancer. Herein, after a comprehensive metabolic phenotype characterization of MCF7 and ZR75 breast cancer cells, we investigated the activity of bergapten (Bg), a plant-derived compound, against breast cancer. The study of different biochemical pathways involved in cell metabolism revealed that the two cell lines have different bioenergetic phenotypes: MCF7 cells express a glycolytic phenotype only partially oxidative, while ZR75 cells mainly have an oxidative phenotype. In both cell lines, Bg blocked glycolysis and significantly decreased glucose-6-phosphate dehydrogenase (G6PDH) activity promoting glucose accumulation; modulated bioenergetic requirements altering the expression of oxidative phosphorylation (OXPHOS) complexes and ATP production; and induced a lipid-lowering effect since an increased lipase activity concomitantly to a reduction in triglyceride levels was observed. Quantitative data of different metabolites and enzymatic activities were presented. Treatment with Bg resulted in an alteration in different metabolic pathways inducing death in the cells. We report a novel action of the natural product Bg on breast cancer, since it induced metabolic reprogramming by disrupting the interconnected network of different metabolic mechanisms. Bg can be used in combination with other forms of targeted chemotherapy to improve cancer treatment outcomes.

Correspondence to: Professor Saveria Aquila, Department of Pharmacy and Science of Health and Nutrition, University of Calabria, I-87036 Arcavacata di Rende (CS), Italy
E-mail: saveria.aquila@libero.it; mamissina@yahoo.it

*Joint senior authorship

Abbreviations: Bg, bergapten; LDH, lactate dehydrogenase; G6PDH, glucose-6-phosphate dehydrogenase; OXPHOS, oxidative phosphorylation

Key words: cancer metabolism, lactate dehydrogenase, lipase activity, glucose-6-phosphate dehydrogenase activity, OXPHOS, methoxypsoralen

Introduction

Recently, energy metabolism has been considered an attractive target for antitumoral therapies, since metabolic changes are a common feature of cancerous tissues. Multiple molecular mechanisms, both intrinsic and extrinsic, converge to alter cellular metabolism. The best characterized metabolic phenotype observed in tumor cells is the Warburg effect, which involves ATP generation through glycolysis instead of oxidative phosphorylation (OXPHOS), even under normal oxygen concentrations (1). However, metabolic adaptation in tumors extends beyond the Warburg effect. In fact, the classical theory on the metabolism of cancer cells (increased glycolytic activity and downregulation of OXPHOS) is still under investigation since different studies have shown that cancer cells can live in a wide spectrum of states ranging from the predominance of the glycolytic phenotype to a phosphorylative phenotype (2). Complete catabolism of pyruvate to CO_2 may be counterproductive in a dividing cell as it may limit the availability of precursors necessary for cell replication, e.g., sugars for nucleotide biosynthesis.

In normal cells, glucose is catabolized to pyruvate, which can be later converted to acetyl-CoA to fuel the tricarboxylic acid cycle. On the other hand, the manner by which tumor cells process pyruvate, the end product of glycolysis, is also different from normal cells, since pyruvate-to-lactate is a preferred reaction in tumor cells (3). Therefore, in cancer cells, the glycolytic flux may be blocked at pyruvate production by pyruvate kinase. In this case, pyruvate is no longer oxidized in mitochondria and is metabolized by cytosolic lactate dehydrogenase. Neverthess, a portion of pyruvate is imported into mitochondria and it still might be metabolized through a mitochondrial oxidative phosphorylative pathway (OXPHOS), creating the partial OXPHOS phenotype.

Differences in OXPHOS status originate from variability of metabolic reprogramming among cancer cells and from the relative contributions of different oncogenes, tumor environment, and mitochondrial function. Disruption of cancer cell metabolism represents an elegant approach to induce tumoral cell death; indeed cell death and metabolic alteration are closely related. The strategy to target tumor metabolism requires an integrated vision of this process since it is not a single metabolic step that is altered; but the entire energetic metabolism working in a pattern is profoundly affected with respect to normal cells. In addition, the metabolic alterations

and adaptations of cancer cells create a particular phenotype essential for tumor cell growth and survival that is particular for each type of cancer. Therefore, it may help to understand how, step by step, the metabolic pathways are arranged in comparison with normal metabolism to characterize a cancer metabolic phenotype.

Several drugs could be referred to as mitocans, metabocans, or aberrocans and many are being developed at present (4). Recently, several studies have documented the ability of chemopreventive phytochemicals to increase the sensitivity of tumoral cells to anticancer drugs (5,6). Bergapten (5-methoxypsoralen, Bg) is a psoralen or taxol (also known as furocoumarins) found in bergamot essential oil and in other citrus essential oils. It belongs to the flavonoid class, which has been found to exhibit a variety of biological activities, usually associated with low toxicity. Flavonoids have attracted considerable interest because of their diverse pharmacological properties. Bg activity against different types of tumor including prostate, ovarian, lung cancer and breast cancer has been observed (7).

It is generally believed that the antitumor effect of Bg is due to its interference with the normal function of microtubule-inducing arrest of the cell cycle (7). However, studies have shown that taxol-induced cell death is via multiple signaling pathways (8-11). For example, taxol-induced apoptosis in breast cancer cells requires downregulation of IκBα, which in turn activates NF-κB (10). Activation of MAPK pathways by taxol in HeLa cells was found to lead to a time-dependent increase in poly(ADP-ribose) polymerase cleavage and apoptosis (11). A study of differential gene expression in mouse cells treated with taxol identified a number of genes that modulate apoptosis (9). We previously demonstrated that in breast cancer cells, bergapten (Bg) treatment affects the PI3K/AKT survival pathway, inducing apoptosis and lowering cell proliferation (12). In addition, we found that Bg enhanced p53 gene expression inducing apoptosis in breast cancer cells (13).

Herein, we report a new anticancer effect of Bg on human breast cancer, since it was able to interfere in cancer reprogrammed metabolism. We characterized the basal metabolic profile of MCF7 and ZR75 cells and evaluated the effect of Bg on different metabolic pathways. Moreover, we present various quantitative aspects of human breast cancer cell metabolism which are limited by the lack of available data at the level of metabolite amounts and enzymatic activities. The quantification can yield multiple insights into the organization of the cancer metabolic network.

Materials and methods

Materials. Methoxypsoralen or Bg, aprotinin, leupeptin, phenylmethylsulfonyl fluoride (PMFS), sodium orthovanadate, Tris-Cl, $MnCl_2$, $NADP^+$, isocitrate and malate were obtained from Sigma-Aldrich (Milan, Italy). Antibodies used in this study were from Santa Cruz Biotechnology (Santa Cruz, CA, USA). MitoProfile® Total OXPHOS WB Antibody Cocktail was from Abcam (Milan, Italy). Triglycerides, lipase activity, glucose-6-phosphate dehydrogenase (G6PDH) activity, LDH activity and glucose assay kits were from Inter-Medical (Biogemina Italia Srl, Catania, Italy). Molecular Probes' ATP Determination kit (A22066) was from Invitrogen (Milan, Italy). Bg was dissolved in ethanol (0.02% final concentration) which was used as a solvent control and did not induce any positive results in all *in vitro* assays (data not shown).

Cell culture. Human breast cancer MCF7 and ZR75-1 (ZR75) cells (American Type Culture Collection, ATCC) were stored according to supplier's instructions. Every 4 months, cells were authenticated by single tandem repeat analysis at our Sequencing Core; morphology, doubling times, estrogen sensitivity, and mycoplasma negativity were tested (MycoAlert; Lonza). Both cell lines were maintained in DMEM/F-12 medium containing 5% fetal calf serum (FCS), 1% L-glutamine, 1% Eagle's non-essential amino acids and 1 mg/ml penicillin/streptomycin in a 5% CO_2 humidified atmosphere. Cells cultured in phenol red and serum-free medium for 24 h, were treated with Bg in medium containing 5% charcoal-treated FCS. The Bg concentrations were chosen on the basis of our previous studies (12,13). In addition, we found that Bg induces apoptosis at 24 h, therefore we hypothesized that a metabolic disruption may occur in a shorter time period, thus we treated the cells for 6 and 16 h (12).

Western blotting. Total protein extracts were obtained as previously described (14). Proteins were resolved on a 10% sodium dodecyl sulfate-polyacrylamide gel, transferred to a nitrocellulose membrane, and probed overnight at 4˚C with the indicated antibodies. β-actin was used as loading control.

Glucose assay. Glucose oxidase catalyzes the oxidation of glucose to gluconic acid. The formed hydrogen peroxide is detected by a chromogenic oxygen acceptor, phenol, 4-aminophenazone in the presence of peroxidase. The intensity of the color formed is proportional to the glucose concentration in the sample (14). Data are presented as nM/mg protein.

LDH assay. LDH catalyzes the interconversion of pyruvate and lactate with concomitant interconversion of NADH and NAD^+. After the treatments, LDH assay was performed on cell lysates as previously described (13). Data are presented as absorbance change at 340 nm.

Triglyceride assay. Triglycerides were measured in duplicate by a GPO-POD enzymatic colorimetric method according to the manufacturer's instructions in cell lysates and as previously described (16). Data are presented as nM/mg protein.

Lipase activity assay. Lipase activity was evaluated by the method of Panteghini *et al* (17) based on the use of 1,2-o-dilauryl-rac-glycero-3-glutaric acid-(6'-methylresorufin) ester as substrate, as previously described (18). Data are presented as nM/min/mg protein.

Assay of the G6PDH activity. The conversion of $NADP^+$ to NADPH, catalyzed by G6PDH, was measured by the increase in absorbance at 340 nm as previously described (16,18). Data are presented as nM/min/mg protein.

ATP assay. A bioluminescence assay for quantitative determination of ATP with recombinant firefly luciferase and its substrate D-luciferin (light emission at 560 nm at pH 7.8), was

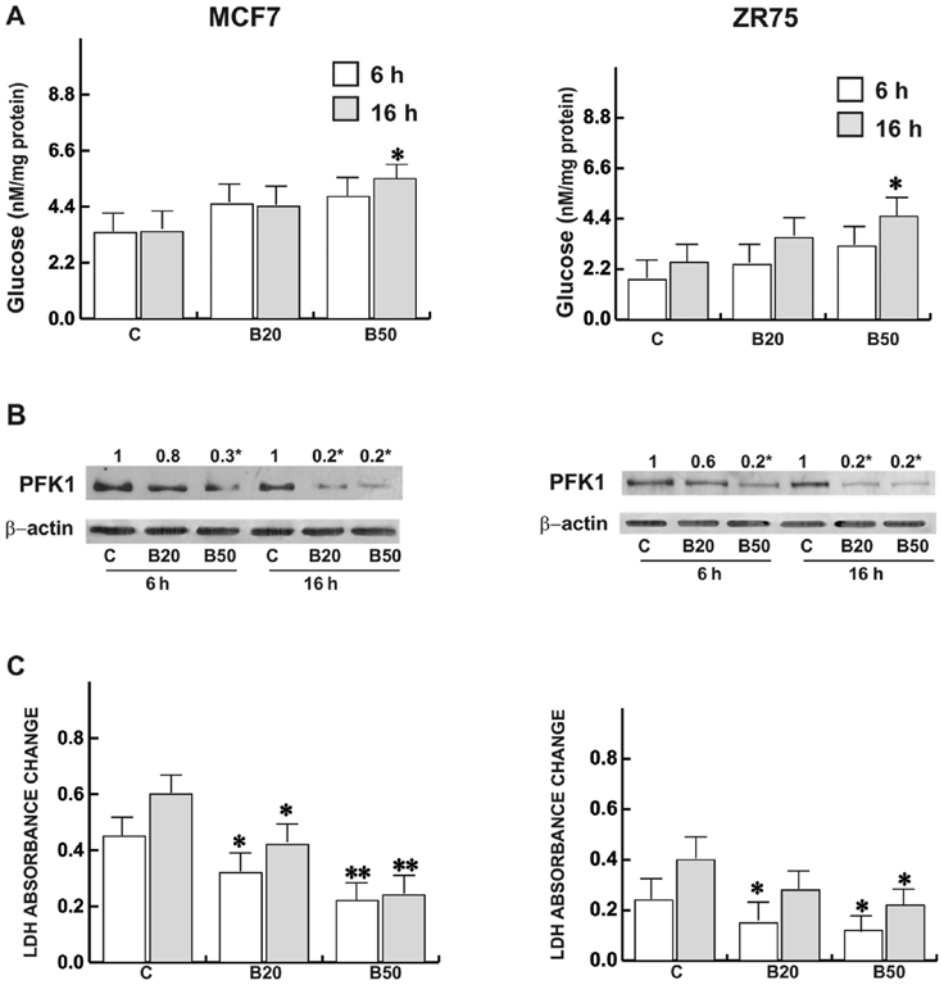

Figure 1. Bg disrupts glycolysis in breast cancer cells. (A) Glucose content was assessed as reported in Materials and methods and in both cell lines in the absence (C) or with increasing Bg concentrations (B20 μM and B50 μM) at the indicated times. Columns represent the mean ± SEM of 20 independent experiments performed in duplicate. *P<0.05 vs. control. (B) Western blot assay of PFK1 in both cell lines in the absence (C) or with increasing Bg concentrations (B20 μM and B50 μM) at the indicated times. β-actin was used as control. The autoradiographs show the results of one representative experiment, and the numbers on the top of the blot, are the mean of three independent experiments in which band intensities were evaluated in terms of optical density arbitrary units and expressed as the fold over each control (C), which was assumed to be 1. *P<0.01 vs. the control (C) at the same time. (C) LDH activity was assessed as reported in Materials and methods. Columns represent the mean ±SEM of 20 independent experiments performed in duplicate. *P<0.05; **P<0.02 vs. control (C) at the same time. Bg, bergapten; LDH, lactate dehydrogenase.

performed as previously described (19). Data are presented as nM/mg protein.

Isocitrate dehydrogenase (ICD) activity assay. ICD activity was measured as in Gnoni and Paglialonga (20). The reaction was performed on the cell lysate using a final 1-ml reaction volume containing 0.2 mg protein, 50 mM Tris-Cl pH 7.4, 5 mM $MnCl_2$, 0.25 mM $NADP^+$ and 0.25 mM isocitrate, at 37˚C. Reaction progress was monitored at 340 nm for 2 min; the NADPH production was calculated using an NADPH extinction coefficient of 6.26103 M^{-1} cm^{-1}. Data are presented as nM/min/mg protein.

Malic enzyme (ME) activity assay. ME activity was measured in the cell lysates as in Gnoni and Paglialonga (20). The reaction was performed using a final 1-ml reaction volume containing 0.3 mg protein, 50 mM Tris-HCl pH 7.4, 5 mM $MnCl_2$, 0.1 mM $NADP^+$ and 5 mM malate, at room temperature. Reaction progress was monitored at 340 nm for 2 min; the NADPH production was calculated using an NADPH extinction coefficient of 6.26103 M^{-1} cm^{-1}. Data are presented as nM/min/mg protein.

Trypan blue assay. Cells were treated as indicated and the loss of survival was assessed by the trypan blue assay as previously described (14).

Statistical analysis. Each datum point represents the mean ± SEM of the experimental values as indicated in the figure legends. Data were analyzed by the Student's t-test using the GraphPad Prism 4 software program. P<0.05 was considered to indicate a statistically significant result.

Results

Bg interferes with the glycolysis in MCF7 and ZR75 cells. To characterize the basal metabolic phenotype of both breast cancer cell lines as well as following Bg treatment, we first

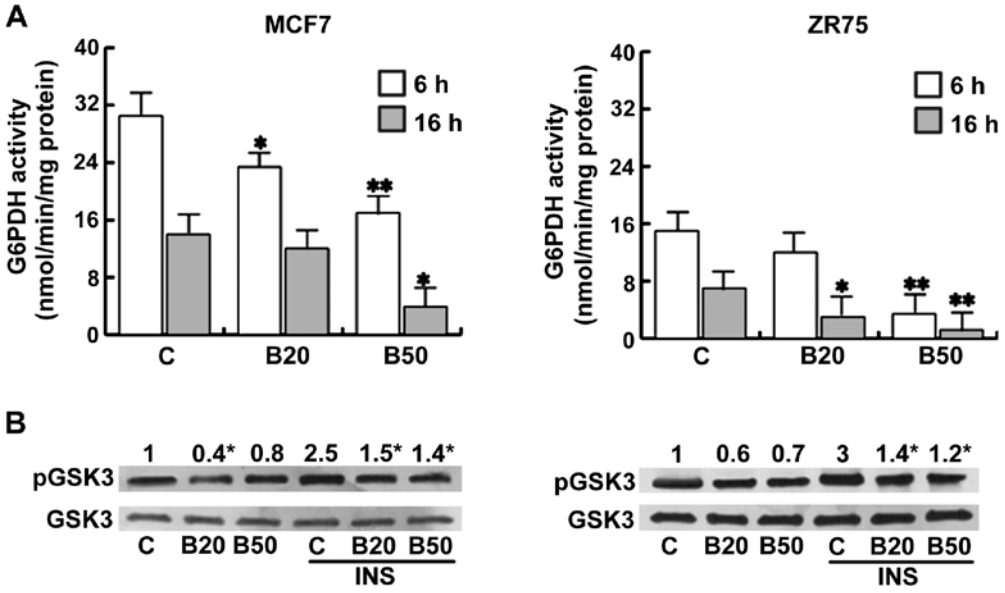

Figure 2. Bg modifies glucose utilization in breast cancer cells. (A) G6PDH activity was performed as reported in Materials and methods and in both cell lines in the absence (C) or with increasing Bg concentrations (B20 μM and B50 μM) at the indicated times. Columns represent the mean ± SEM of 20 independent experiments performed in duplicate. *P<0.05, **P<0.01 vs. the control (C) at the same time. (B) Western blot analysis of pGSK3S9 and GSK3 in MCF7 and ZR75 cells cultured as indicated. INS, insulin 100 nM. The autoradiographs show the results of one representative experiment, and the numbers on the top of the blot are the mean of 3 independent experiments in which band intensities were evaluated in terms of optical density arbitrary units and expressed as the fold over control (C), which was assumed to be 1. *P<0.05 vs. the control (C) at the same time. Bg, bergapten.

determined the glucose content and analyzed various key enzymes involved in the carbohydrate metabolism: 6-phosphofructo-1-kinase (PFK1) expression and the LDH activity. Bg produced a slight glucose accumulation although it was significant following treatment with Bg at 50 μM at 16 h in both cell types (Fig. 1A). The cells had decreased glucose utilization after 16 h, and this commensurated with inhibition of cell viability as reported in previous studies (12,13); while a drastic reduction in the glycolytic enzyme PFK1 was observed following treatment with Bg at 20 and 50 μM (Fig. 1B). In the same experimental conditions, lactate production significantly decreased (Fig. 1C), both at 6 and 16 h. Noteworthy, ZR75 cells possessed lower basal LDH activity as well as glucose content with respect to the MCF7 cells.

Effects of Bg on biosynthetic contributions in MCF7 and ZR75 cells. Another manner of glucose utilization is via the pentose phosphate cycle (PPP), through G6PDH activity. Bg treatment induced a significant reduction in the enzymatic activity (Fig. 2A), indicating how the decrease in G6PDH in treated cells contributes to the decrease in glucose utilization. Interestingly, ZR75 cells possessed a lower basal G6PDH activity with respect to the MCF7 cells. Glycogen represents an alternative energy source in tumors expressing active glycogen synthase (20). Phosphorylation of glycogen synthase by GSK3 phosphorylated on Ser9 inhibits glycogen synthesis. In the present study, Bg was able to reduce this GSK3 phosphorylation, implying a blockade on the glycogen synthase activity. GSK3 has been initially identified as a key regulator of insulin-dependent glycogen synthesis and we found that Bg antagonized the upregulatory effect elicited by insulin on this enzyme (Fig. 2B).

Therefore, we decided to further investigate the effect of Bg on the bioenergetic balance of breast cancer cells. Two enzymes involved in the production of NADPH other than PPP, ME and ICDH, were studied. In MCF7 cells, (Fig. 3A and B), treatment of Bg at 20 μM was able to induce the activities of both enzymes, while treatment with Bg at 50 μM reduced ME activity although not significantly; the extension of treatment with Bg at 50 μM for up to 16 h induced a significant reduction in ICDH activity. A similar pattern of response was obtained in ZR75 cells upon treatment of Bg at 20 μM; however, following treatment with Bg at 50 μM, the enzymatic activities were close to that of the controls. Notably, ZR75 cells possessed lower basal enzymatic activities with respect to the MCF7 cells.

Bg modulates bioenergetic requirements in MCF7 and ZR75 cells. Successively, we focused our investigation on OXPHOS, by analyzing the mitochondrial OXPHOS components, the ATP content and the AMP-activated protein kinase (AMPK) expression.

Some of the OXPHOS components were not affected by Bg treatment in the MCF7 cells, except for Complex (C) IV that resulted in its upregulation, while CI was reduced particularly at 16 h (Fig. 4A and B). These data, as expected, resulted in a decrease in ATP production (Fig. 4C). Concerning ZR75 cells, the OXPHOS protein pattern at basal conditions and under Bg was expressed to a greater extent with respect to the MCF7 cells, although starting from the same protein loading. Even when the CIV component was poorly expressed with respect to the other components in ZR75 cells, it ensured the flow of electrons along the other components, that were overexpressed (including the CII) maintaining a high ATP synthesis, as shown in Fig. 4C. The CIV component of the mitochondrial respiratory chain was expressed to a lesser extent in the ZR75 cells with respect to the MCF7 cells.

AMPK is activated by metabolic stresses that interfere with ATP production (2). In basal conditions the levels of ATP

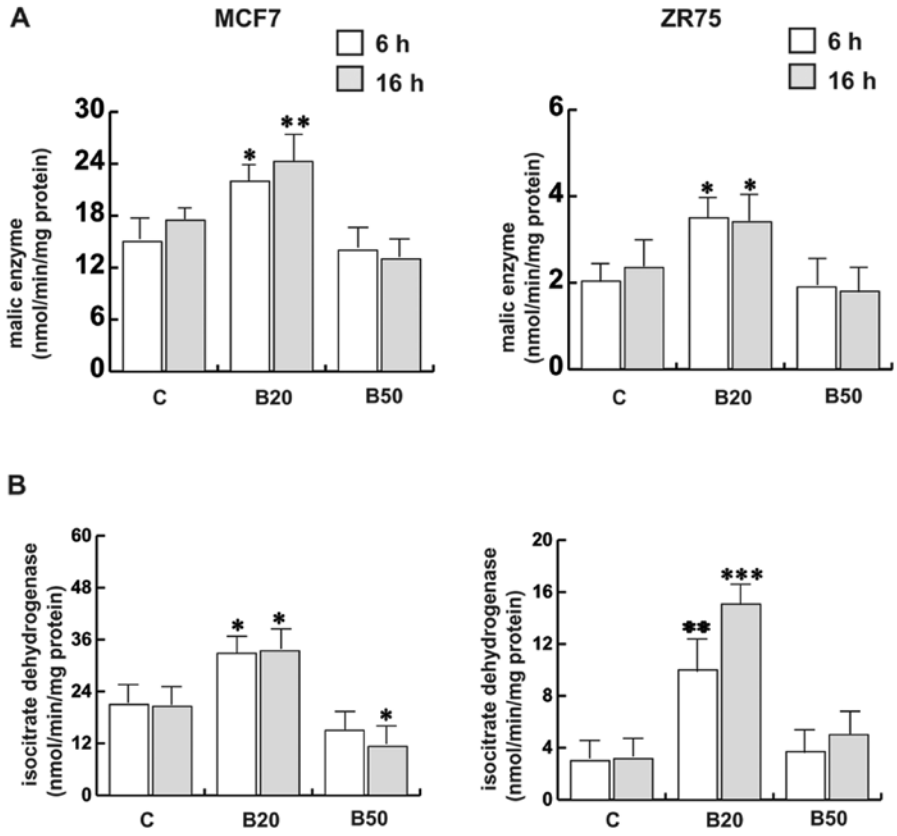

Figure 3. Bg influences the reducing potential in breast cancer cells (A) Malic enzyme assay was performed as reported in Materials and methods and in both cell lines in the absence (C) or with increasing Bg concentrations (B20 μM and B50 μM) at the indicated times. Columns represent the mean ± SEM of 20 independent experiments performed in duplicate. *P<0.05, **P<0.02 vs. the control (C) at the same time. (B) Isocitrate dehydrogenase activity was performed as reported in Materials and methods. Columns represent the mean ± SEM of 20 independent experiments performed in duplicate. *P<0.05, **P<0.02. ***P<0.01 vs. the control (C) at the same time. Bg, bergapten.

appeared to be higher in the ZR75 cells, although not significantly different from that observed in the MCF7 cells Fig. 4D. Following treatment with Bg, our data correlated well with the increased AMPK expression in the MCF7 cells accordingly to the reduced ATP production, while AMPK expression was unchanged in the ZR75 cells, that produced a major amount of ATP.

Bg promotes a lipid-lowering effect in breast cancer cells. The bioenergetic and biosynthetic requirements of cancer cells are balanced by regulating the flux of pathways that metabolize fatty acids other than glucose. Increased fatty acid synthesis has been linked to poor prognosis in breast cancer (22). Bg-treated cells exhibited a reduced triglyceride level compared to the untreated cells, accordingly to the increased lipase activity observed in both cell lines in a time- and concentration-dependent manner (Fig. 5A and B).

Bg-induced metabolic reprogramming produces cell death in breast cancer. As shown in Fig. 6 both MCF7 and ZR75 cells exposed to Bg exhibited a loss of cell survival, although the effect was higher in the MCF7 than that in the ZR75 cells.

Discussion

It has now been clearly established that cancer cells depend on an altered cellular metabolism (23). Cancers are extremely heterogeneous diseases and each cancer has its individual metabolic features. The literature indicates that the Warburg phenotype is not exclusive and that a decrease in mitochondrial function is not a general feature of cancer cells. In fact, even in glycolytic tumors, OXPHOS is not completely shut down. Herein, we characterized the metabolic profile of MCF7 and ZR75 cells evaluating various features of tumor metabolism. We found that Bg, a natural product, alters both glucose and lipid metabolism in a way and extent that cannot be counterbalanced by breast cancer cells as they die.

Energy metabolism represents an additional hallmark of cancer cells and a new promising target for its treatment. Multiple molecular mechanisms converge to alter core cellular metabolism. Malignant cells have the ability to adopt an altered metabolic profile that fulfills biosynthetic and bioenergetic requirements for rapid and uncontrolled growth. Thus, its disruption may then resolve the malignant process, independently of its origin.

In the present study, detailed attention was given to evaluate the effect of Bg on breast cancer metabolism. Glycolysis is the metabolic program of choice for cells that are actively engaged in cell growth and mitogenesis. Because of this fact, we first analyzed the glucose content and utilization in both MCF7 and ZR75 cells. The basal glucose content was higher in MCF7 than in ZR75 cells and it increased upon Bg treatment in both cell lines, while the PFK1 expression and the lactate production rates were strongly decreased.

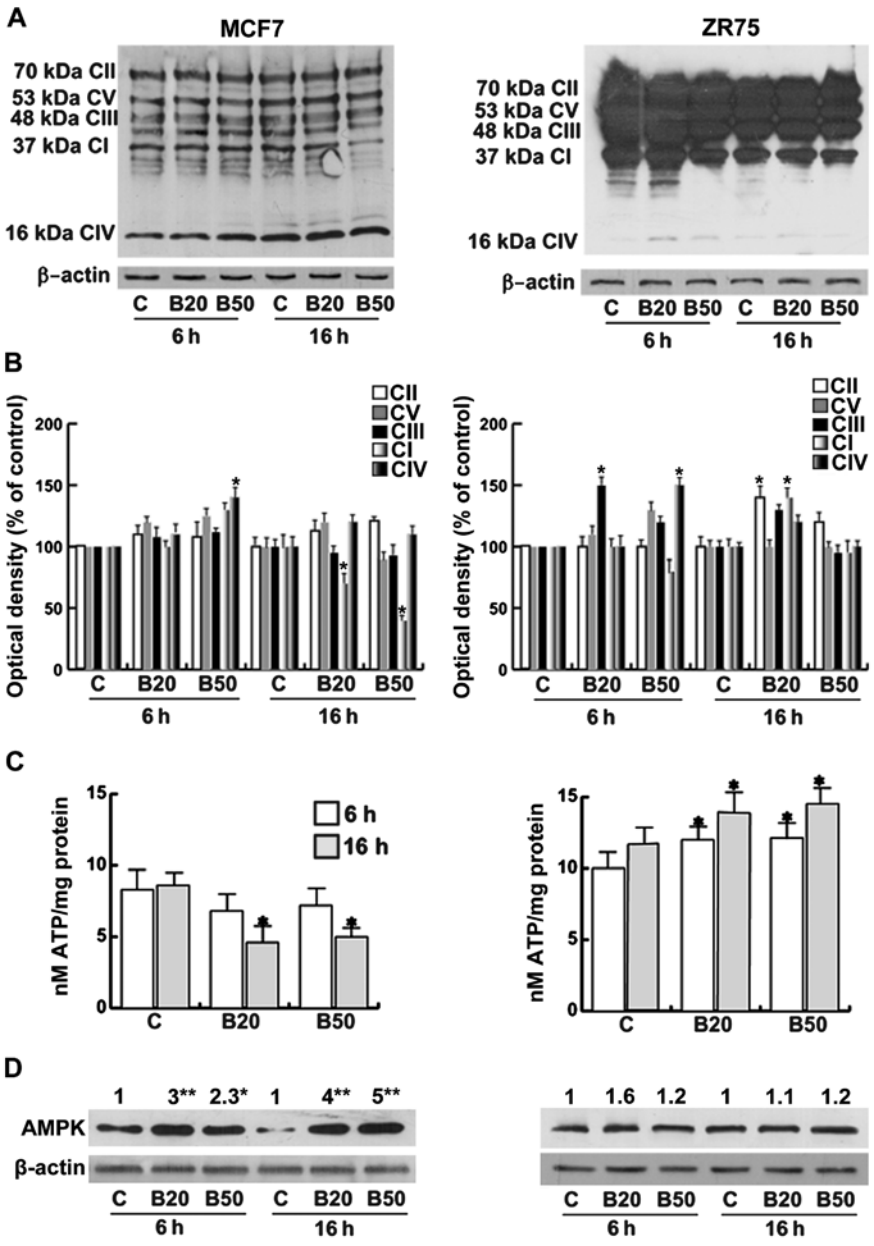

Figure 4. Bg alters the bioenergetics in breast cancer cells. (A) Western blot assay of OXPHOS in both cell lines in the absence (C) or with increasing Bg concentrations (B20 μM and B50 μM) at 6 and 16 h. The autoradiographs show the results of one representative experiment repeated at least 3 times. β-actin was used as a control. (B) Quantitative representation after densitometry of the OXPHOS components. The columns are the mean of three independent experiments in which band intensities were evaluated in terms of optical density arbitrary units and expressed as a percentage with respect to the respective time controls, which were assumed to be 100%. *P=0.05, *P<0.02. CIV, CI, CIII, CV, CII indicate OXPHOS components. (C) ATP content was assessed as reported in Materials and methods. Columns represent the mean ± SEM of 20 independent experiments performed in duplicate. *P<0.05 vs. the control (C) at the same time; 6 and 16 h.. (D) Western blot assay of AMPK in both cell lines in the absence (C) or with increasing Bg concentrations (B20 μM and B50 μM) at the indicated times. β-actin was used as a control. The autoradiographs show the results of one representative experiment, and the numbers on the top of the blot are mean of 3 independent experiments in which band intensities were evaluated in terms of optical density arbitrary units and expressed as the fold over each control (C), which was assumed to be 1. *P<0.02, **P<0.01 vs. the control (C) at the same time. Bg, bergapten.

Elevated production of lactate has been previously correlated with the activation of PFK1, the major regulatory glycolytic enzyme (24). It has been proposed that inhibition of LDH and PFK1 may represent alternative strategies toward the development of anti-glycolytic-based therapies for cancer and in this scenario, the data obtained upon Bg treatment was well-fit. The LDH activity may be reduced since PFK1 was in turn lowered, however it was not a rate-limiting step in our breast tumor cell lines. It is known that inhibition of PFK-1 results in the accumulation of fructose-6-phosphate, which is then isomerized to glucose-6-phosphate and in turn is diverted into PPP, an important pathway of glucose catabolism representing another feature of the cancer metabolic phenotype. PPP is the primary cellular source of NADPH, the principal intracellular reductant and crucial to fatty acid and amino acid biosynthesis. It has been reported that the enhanced activation of PPP has a number of pro-oncogenic effects (1) and it is known to be hyperactive in cancer (25,26). In this respect, our data showed that Bg was able to affect the PPP pathway reducing G6PDH activity. The Bg-induced lowering of LDH and G6PDH

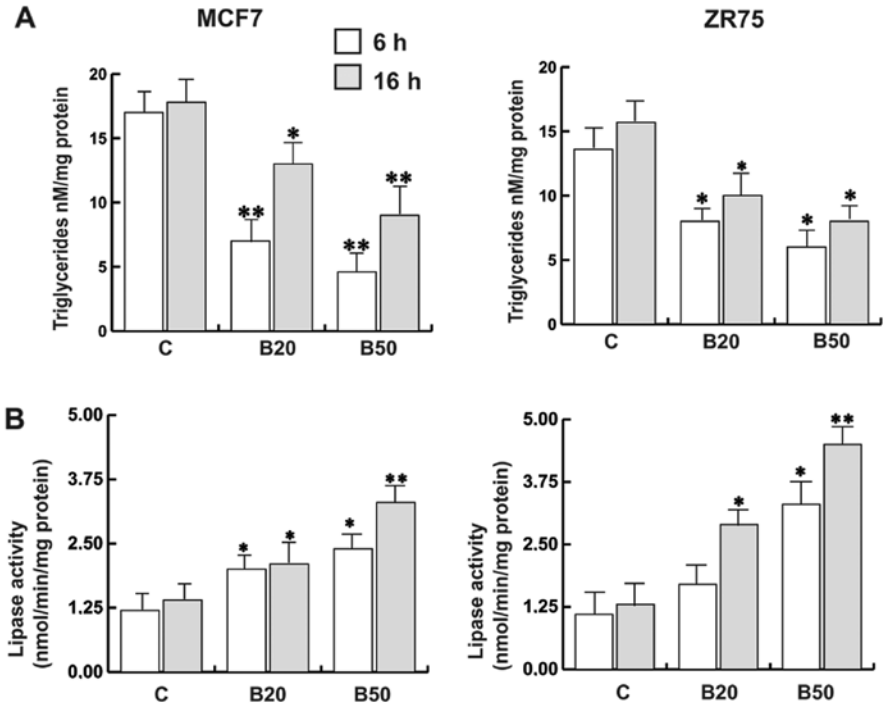

Figure 5. Bg has a lipid-lowering effect in breast cancer cells. (A) Triglyceride assay was performed as reported in Materials and methods and in both cell lines in the absence (C) or with increasing Bg concentrations (B20 μM and B50 μM) at the indicated times. Columns represent the mean ± SEM of 20 independent experiments performed in duplicate. *P<0.05, **P<0.01 vs. the control (C) at the same time. (B) Lipase activity was performed as reported in Materials and methods. Columns represent the mean ± SEM of 20 independent experiments performed in duplicate. *P<0.05, **P<0.01 vs. the control (C) at the same time; 6 and 16 h. Bg, bergapten.

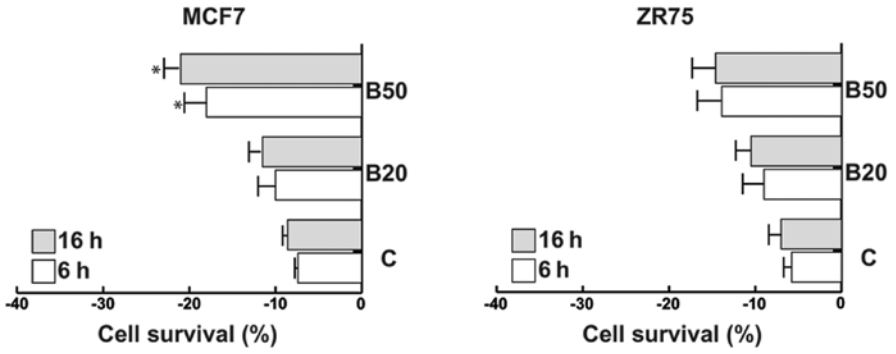

Figure 6. Bg induces cell death in breast cancer cells. (A) Increasing Bg concentrations (B20 μM and B50 μM) produce loss of cell survival in the MCF7 and ZR75 cells, as assessed by the Trypan blue assay as described in Materials and methods. Columns are the mean ± SEM of 20 independent experiments performed in duplicate. *P<0.05 vs. untreated cells; 6 and 16 h. Bg, bergapten.

activities may explain the higher glucose levels upon treatment as were obtained. The basal levels of G6PDH activity were lower at 16 h, which may be due to the longer absence of growth factor in the medium used (27). The different LDH and G6PDH basal activities between MCF7 and ZR75 cells that we found, may suggest that the MCF7 cells have a marked glycolytic phenotype when compared with the ZR75 cells. Moreover, the reduction in these enzymatic activities by Bg indicates that it is able to derange glucose metabolism in breast cancer cells. It appears that Bg shares similarities with other classes of molecules found in nature within polyphenols, that are widely known as enzyme inhibitors and particularly of glucose metabolism. The repression of the PI3K/Akt activity as we previously demonstrated (12), also impaired anabolic glucose metabolism supporting our new data. Furthermore, Bg also antagonized the upregulatory effect of insulin on pGSK3S9 expression, an essential control point in glycogen synthesis. It is clear that the absence of energetic reservoirs does not favors cancer cell survival.

Since oncogenic metabolic programs support bioenergetics, we focused our study on NAPDH production, oxidative mitochondrial activity as well as ATP content. Other than PPP, two enzymes are involved in the production of NADPH, ME and ICDH. Bg was able to affect both ME and ICDH activities, by inducing an increase at 20 μM, while at a higher dose after 16 h of incubation the level decreased significantly in the MCF7 cells. A similar pattern of response was obtained in ZR75 cells at 6 h; however, treatment with Bg at 50 μM was

not able to reduce both enzymatic activities. Of consequence, it appears that Bg acts on NADPH production without biasing these two metabolic steps. Furthermore, as observed for LDH and G6PDH activities, both basal ME and ICDH activities were higher in the MCF7 cells when compred with the activities in the ZR75 cells.

It is well known that oxidation of NADH mainly occurs via mitochondrial OXPHOS, where electron transport is coupled along 4 enzyme complexes (CI-CIV), and ATP is synthesized at CV (ATP synthase) (28,29). From our data, it is evident that treatment with Bg in MCF7 cells tended to reduce the expression of CI, and then the entrance of the electrons in the mitochondria, although levels of the other downstream components were maintained. This would translate into an internal imbalance that is unable to supply energy to the cells, accordingly to the minor amount of ATP produced. In contrast, in ZR75 cells, the amount of OXPHOS in untreated and Bg-treated cells was higher compared to that observed in the MCF7 cells. This finding supports the increased ATP production in ZR75 cells where a reduction in complex IV of the respiratory chain was noted. Deregulation of these processes is a major pathological consequence of cancer progression.

AMPK is a highly conserved sensor of increased levels of AMP and ADP originating from ATP depletion (30,31). It appears to be involved in cancer because of its ability to act as a tumor-suppressor. From our data, upon Bg treatment, the AMPK content increased in MCF7 cells acting as an energy sensor allowing the cells to meet the reduced energy supply, while in ZR75 cells its expression did not change, in agreement with the higher ATP levels obtained in these cells. Summarizing the role of Bg on glucose utilization and bioenergetics: in MCF7 cells, upon Bg treatment, glycolysis and PPP rates were significantly reduced, OXPHOS components were scarcely impaired and the ATP production was reduced. In ZR75 cells, the psoralen induced similar effects on glycolysis, while an increased OXPHOS as well as ATP content were observed. These data suggest that the two cell lines exhibit different bioenergetic phenotypes. MCF7 cells express prevalently a glycolytic phenotype only partially oxidative, while ZR75 cells mainly express an oxidative phenotype. This may explain why ZR75 cells are more resistant to B-induced cell death vs. MCF7 cells, as we previously reported (12). This assumption is supported by a recent finding demonstrating how ZR75 cells selectively use genes for energy, sugar metabolism and other pathways differently from MCF7 cells, imparting more aggressiveness to ZR75 cells (24).

The bioenergetic and biosynthetic requirements of cancer cells are balanced by regulating the flux of pathways that metabolize fatty acids other than glucose. Proliferating cells can synthesize fatty acids and cholesterol *de novo* from glucose and increased fatty acid synthesis has been linked to poor prognosis in breast cancer (32). The dependence of tumor cells on deregulated lipid metabolism suggests that pathways involved in this process are additional attractive targets for cancer treatment. In our study, Bg greatly impacted this feature of cancer cell metabolism since it induced a general lipid-lowering effect. Triglyceride levels decreased concomitantly with an increase in lipase activity. All together, the metabolic reprogramming by Bg was acutely efficacious to reduce cancer cell survival according to previously reported data.

We report, for the first time, that Bg treatment interferes with breast cancer cell metabolism disrupting different features of this process. The outcomes emerged from an extensive characterization of the different biochemical pathways involved in cell metabolism. On the basis of these and previous data, the activity of Bg against breast cancer cells is therefore orchestrated by several components rather than being the result of the effect on a single molecular target and/or signaling pathway.

Future clinical data describing the metabolic profiles of human tumors will be required to determine which metabolic alterations are most prevalent in specific tumor types. In conclusion, bergapten, on the basis of its metabolic targeting, can be used in combination with other forms of targeted chemotherapy to improve cancer treatment outcomes.

Acknowledgements

The present study was supported by MIUR Ex 60%-2014 and Associazione Italiana Ricerca sul Cancro (AIRC) (grant no. IG15738). Our special thanks to Dr Vincenzo Cunsolo (Biogemina Italia Srl, Catania, Italy); and Serena Gervasi and Maria Clelia Gervasi for the English language revision of the manuscript.

References

1. Barger JF and Plas DR: Balancing biosynthesis and bioenergetics: Metabolic programs in oncogenesis. Endocr Relat Cancer 17: R287-R304, 2010.
2. Smolková K, Plecitá-Hlavatá L, Bellance N, Benard G, Rossignol R and Ježek P: Waves of gene regulation suppress and then restore oxidative phosphorylation in cancer cells. Int J Biochem Cell Biol 43: 950-968, 2011.
3. Phan LM, Yeung S-C and Lee M-H: Cancer metabolic reprogramming: importance, main features, and potentials for precise targeted anti-cancer therapies. Cancer Biol Med 11: 1-19, 2014.
4. Vamecq J, Colet JM, Vanden Eynde JJ, Briand G, Porchet N and Rocchi S: PPARs: Interference with Warburg' effect and clinical anticancer trials. PPAR Res 2012: 304760, 2012.
5. Nabekura T: Overcoming multidrug resistance in human cancer cells by natural compounds. Toxins (Basel) 2: 1207-1224, 2010.
6. da Rocha AB, Lopes RM and Schwartsmann G: Natural products in anticancer therapy. Curr Opin Pharmacol 1: 364-369, 2001.
7. Rowinsky EK: Paclitaxel pharmacology and other tumor types. Semin Oncol 2: S19-1-S19-12, 1997.
8. Jordan MA, Toso RJ, Thrower D and Wilson L: Mechanism of mitotic block and inhibition of cell proliferation by Taxol at low concentrations. Proc Natl Acad Sci USA 90: 9552-9556, 1993.
9. Moos PJ and Fitzpatrick FA: Taxanes propagate apoptosis via two cell populations with distinctive cytological and molecular traits. Cell Growth Differ 9: 687-697, 1998.
10. Huang Y, Johnson KR, Norris JS and Fan W: Nuclear factor-kappaB/IkappaB signaling pathway may contribute to the mediation of paclitaxel-induced apoptosis in solid tumor cells. Cancer Res 60: 4426-4432, 2000.
11. McDaid HM and Horwitz SB: Selective potentiation of paclitaxel (Taxol)-induced cell death by mitogen-activated protein kinase kinase inhibition in human cancer cell lines. Mol Pharmacol 60: 290-301, 2001.
12. Panno ML, Giordano F, Mastroianni F, Palma MG, Bartella V, Carpino A, Aquila S and Andò S: Breast cancer cell survival signal is affected by bergapten combined with an ultraviolet irradiation. FEBS Lett 584: 2321-2326, 2010.
13. Panno ML, Giordano F, Palma MG, Bartella V, Rago V, Maggiolini M, Sisci D, Lanzino M, De Amicis F and Andò S: Evidence that bergapten, independently of its photoactivation, enhances p53 gene expression and induces apoptosis in human breast cancer cells. Curr Cancer Drug Targets 9: 469-481, 2009.

14. Guido C, Panza S, Santoro M, Avena P, Panno ML, Perrotta I, Giordano F, Casaburi I, Catalano S, De Amicis F, *et al*: Estrogen receptor beta (ERβ) produces autophagy and necroptosis in human seminoma cell line through the binding of the Sp1 on the phosphatase and tensin homolog deleted from chromosome 10 (PTEN) promoter gene. Cell Cycle 11: 2911-2921, 2012.
15. Saifer A and Gerstenfeld S: The photometric microdetermination of blood glucose with glucose oxidase. J Lab Clin Med 51: 448-460, 1958.
16. Guido C, Perrotta I, Panza S, Middea E, Avena P, Santoro M, Marsico S, Imbrogno P, Andò S and Aquila S: Human sperm physiology: Estrogen receptor alpha (ERα) and estrogen receptor beta (ERβ) influence sperm metabolism and may be involved in the pathophysiology of varicocele-associated male infertility. J Cell Physiol 226: 3403-3412, 2011.
17. Panteghini M, Bonora R and Pagani F: Measurement of pancreatic lipase activity in serum by a kinetic colorimetric assay using a new chromogenic substrate. Ann Clin Biochem 38: 365-370, 2001.
18. Aquila S, Bonofiglio D, Gentile M, Middea E, Gabriele S, Belmonte M, Catalano S, Pellegrino M and Andò S: Peroxisome proliferator-activated receptor (PPAR)gamma is expressed by human spermatozoa: Its potential role on the sperm physiology. J Cell Physiol 209: 977-986, 2006.
19. Pingitore A, Cione E, Senatore V and Genchi G: Adrenal glands and testes as steroidogenic tissue are affected by retinoylation reaction. J Bioenerg Biomembr 41: 215-221, 2009.
20. Gnoni GV and Paglialonga G: Resveratrol inhibits fatty acid and triacylglycerol synthesis in rat hepatocytes. Eur J Clin Invest 39: 211-218, 2009.
21. Luo J: Glycogen synthase kinase 3beta (GSK3beta) in tumorigenesis and cancer chemotherapy. Cancer Lett 273: 194-200, 2009.
22. Zhang F and Du G: Dysregulated lipid metabolism in cancer. World J Biol Chem 3: 167-174, 2012.
23. Phan LM, Yeung SC and Lee MH: Cancer metabolic reprogramming: Importance, main features, and potentials for precise targeted anti-cancer therapies. Cancer Biol Med 11: 1-19, 2014.
24. Mandal S and Davie JR: An integrated analysis of genes and pathways exhibiting metabolic differences between estrogen receptor positive breast cancer cells. BMC Cancer 7: 181, 2007.
25. Richardson AD, Yang C, Osterman A and Smith JW: Central carbon metabolism in the progression of mammary carcinoma. Breast Cancer Res Treat 110: 297-307, 2008.
26. Meadows AL, Kong B, Berdichevsky M, Roy S, Rosiva R, Blanch HW and Clark DS: Metabolic and morphological differences between rapidly proliferating cancerous and normal breast epithelial cells. Biotechnol Prog 24: 334-341, 2008.
27. Tian WN, Braunstein LD, Pang J, Stuhlmeier KM, Xi QC, Tian X and Stanton RC: Importance of glucose-6-phosphate dehydrogenase activity for cell growth. J Biol Chem 273: 10609-10617, 1998.
28. Sun X, Wang JF, Tseng M and Young LT: Downregulation in components of the mitochondrial electron transport chain in the postmortem frontal cortex of subjects with bipolar disorder. J Psychiatry Neurosci 31: 189-196, 2006.
29. Reinecke F, Smeitink JA and van der Westhuizen FH: OXPHOS gene expression and control in mitochondrial disorders. Biochim Biophys Acta 1792: 1113-1121, 2009.
30. Hardie DG: AMP-activated protein kinase: An energy sensor that regulates all aspects of cell function. Genes Dev 25: 1895-1908, 2011.
31. Mihaylova MM and Shaw RJ: The AMPK signalling pathway coordinates cell growth, autophagy and metabolism. Nat Cell Biol 13: 1016-1023, 2011.
32. Shurbaji MS, Kalbfleisch JH and Thurmond TS: Immunohistochemical detection of a fatty acid synthase (OA-519) as a predictor of progression of prostate cancer. Hum Pathol 27: 917-921, 1996.